Doctoral theses at NTNU, 2012:279

Nurul Huda Mahmood

Interference Analysis and Management with Applications in Heterogeneous Small-cell Cognitive Radio Networks

Doctoral Thesis

Nurul Huda Mahmood

NTNU
Norwegian University of Science and Technology
Thesis for the degree of Philosophiae Doctor
Faculty of Information Technology, Mathematics and Electrical Engineering
Department of Electronics and Telecommunications

Doctoral theses at NTNU, 2012:279

NTNU – Trondheim
Norwegian University of Science and Technology

NTNU

NTNU – Trondheim
Norwegian University of Science and Technology

ISBN 978-82-471-3872-4 (printed version)
ISBN 978-82-471-3871-7 (electronic version)
ISSN 1503-8181

Nurul Huda Mahmood

Interference Analysis and Management with Applications in Heterogeneous Small-cell Cognitive Radio Networks

Thesis for the degree of Philosophiae Doctor

Trondheim, December 2012

Norwegian University of Science and Technology
Faculty of Information Technology,
Mathematics and Electrical Engineering
Department of Electronics and
Telecommunications

NTNU – Trondheim
Norwegian University of
Science and Technology

NTNU
Norwegian University of Science and Technology

Thesis for the degree of Philosophiae Doctor

Faculty of Information Technology,
Mathematics and Electrical Engineering
Department of Electronics and
Telecommunications

ISBN 978-82-471-3872-4 (printed version)
ISBN 978-82-471-3871-7 (electronic version)
ISSN 1503-8181

Doctoral theses at NTNU, 2012:279

Printed by Skipnes Kommunikasjon as

Abstract

This thesis examines interference modeling and management in small cell cognitive radio networks.

A generalized unified statistical model is presented for the interference from a heterogeneous next generation network at a target receiver located at the centre of a cell. The derived model is then applied in devising a simple distributed power allocation algorithm for the next generation network nodes, and in the various performance analyses of the the coexisting systems.

Cooperative communication improves the outage performance and coverage of wireless links under certain channel conditions, but is not spectrally efficient when channel conditions are favorable. A hybrid cooperation technique that can reap the diversity benefits of cooperative communication without sacrificing the multiplexing gain is proposed, and the performance of an interference temperature constrained cognitive radio network employing the proposed cooperation technique is analyzed.

Next, a formulation of the power allocation problem in the cognitive interference channel is presented whereby the interference margin at the primary receivers are seen as resources to be shared optimally. A relative rate utility based power allocation algorithm that is shown to achieve favorable sum throughput is then proposed.

Finally, the thesis investigates various interference coordination techniques for multi antenna cognitive radio users coexisting with multiple primary users under a restricted interference temperature constraint. Knowledge of the zero forcing beamforming techniques and the interference alignment schemes are applied to satisfy the restricted interference temperature constraint at the primary receivers while supporting significant sum rate at the secondary system.

Preface

This thesis is submitted in partial fulfillment of the requirements of the degree of philosophiae doctor (PhD) at the Norwegian University of Science and Technology (NTNU).

This doctoral work has been performed at the Department of Electronics and Telecommunications (IET) of the Faculty of Information Technology, Mathematics and Electrical Engineering (IME-fakultet), NTNU, Trondheim, with Professor Geir Egil Øien as main supervisor and with co-supervisors Professor Ralf Müller and Associate Professor Torbjörn Ekman.

The PhD study was conducted during the period June 2008 to September 2012 under the Nordic project titled "Cross-Layer Optimization in Short-Range Wireless Sensor Networks, part 2" (CROPS2). The research was supported by the Research Council of Norway (NFR) under the NORDITE/VERDIKT program, Project CROPS2 (Grant 181530/S10).

Acknowledgements

In the name of Allah, the Most Merciful, the Most Beneficient

As I write these final few words of my PhD thesis, I humbly remember the many 'chance events' that have marvelously come together to enable my journey thus far. Despite coming from one of the poorest countries in the world, I am extremely lucky to have been born into a family that has the passion, as well as the ability, to support my education. The enthusiasm and the capability in myself to pursue an education at this level is a further blessing. Without any of the above, and numerous other similar 'chance events', this PhD study would have remained a dream; to say the least. Statistically speaking, it is amazing to realize how all these independent 'good fortunes' have spectacularly come together to result in such an outcome. As a matter of fact, these are all gifts from Allah Almighty - the Creator, which He has bestowed upon myself without any effort from my end. Thus I say, *"All praises are for Allah alone, the Lord of all that exist"*. *"Glory to You (O Allah): of knowledge we have none, save that what You have taught us: truly, You who are the perfect in knowledge and wisdom"*.

Like most other PhD students, I had experienced a phase in my studies when the road seemed only bleak and all uphill. Most probably I would not have made it through had I not had Prof. Geir Egil Øien as my supervisor. He is invariably a wise mentor, a caring teacher and most importantly an wonderful person. He has always been very kind and friendly, and constantly provided me with encouragement, support and motivation through thick and thin.

Sincere thanks also to Professor Mohamed-Slim Alouini and Dr. Ferkan Yilmaz (Abi) for their sincere co-operation during my stay at the King Abdullah University of Science and Technology (KAUST), Saudi Arabia. Through their feedback, advice and patience, they have made a significantly positive difference to this work. I would also like to sincerely thank Professor David Gesbert, who hosted me at the Institute Eurécom. It was there that my PhD studies truly began. Special thanks are further due to all the co-authors for their suggestions and contributing guidelines, and to Associate Professor Kimmo Kansanen and John Flåm for proof-reading the thesis.

The administrative and technical staff at the department and the faculty have always been very helpful during my studies here, and I would like to give great thanks to all of them. Ms Kirsten Ekseth, our 'big sister', deserves special mention. She has an amazing ability to solve all sorts of problems with a heart melting smile. I am also grateful for the wonderful colleagues and friends at the signal processing group, and the lovely and lively

coffee room; and all my friends from MSAT, BCO, Trondheim and elsewhere.

Last but most importantly, I am inexpressibly thankful to my wonderful family for everything. My work performance before and after my wedding explicitly proves that this thesis would have remained a distant dream, had it not been for the unconditional love and support of my dearest wife Tamrina; and to her do I dedicate this thesis. Heartfelt gratefulness also goes to my parents, Dr. Rafique and Mrs. Saqeba; parents in law, Mr. Muzahid and Mrs. Tamanna, and to my immediate and in laws' family. You all make me who I am.

Contents

List of Included Publications

- PAPER A:
  N. H. Mahmood, F. Yilmaz, M.-S. Alouini and G. E. Øien, *Interference Modeling for Heterogeneous Next Generation Wireless Networks - and its Applications*, Submitted to Wiley International Journal on Wireless Communications and Mobile Computing, August 2012.

- PAPER B:
  N. H. Mahmood, F. Yilmaz, G. E. Øien and M.-S. Alouini, *On Hybrid Cooperation in Underlay Cognitive Radio Networks*, Submitted to IEEE Transaction on Wireless Communication, September 2012.

- PAPER C:
  N. H. Mahmood, G. E. Øien, L. Lundheim and U. Salim, *A Relative Rate Utility based Distributed Power Allocation Algorithm for Cognitive Radio Networks*, In Proceedings of the 2012 International WDN Workshop on Cooperative and Heterogeneous Cellular Networks (WDN-CN2012) held in conjunction with the 23^{rd} IEEE International Symposium on Personal, Indoor and Mobile Radio Communications (PIMRC 2012), Sydney, Australia, September, 2012.

- PAPER D:
  N. H. Mahmood and G. E. Øien, *Generalized Hierarchical Spectrum Usage under Spatio-orthogonal Co-existence Policy*, Submitted for possible publications to the IEEE Wireless Communication and Networking Conference (IEEE-WCNC) 2013.

List of Tables

List of Figures

List of Acronyms

AF	Amplify-and-Forward
ASE	Area Spectral Efficiency
AWGN	Additive White Gaussian Noise
BC	Broadcast Channel
BER	bit error rate
BPP	Binomial Point Process
BPSK	Binary Phase Shift Keying
CBP	Coexistence Beacon Protocol
C-CRN	cooperative cognitive radio networks
CDF	Cumulative Distribution Function
CR	Cognitive Radio
CRN	Cognitive Radio Network
CSI	Channel State Information
DF	decode-and-forward
DoF	Degree of Freedom
DPC	Dirty Paper Coding
DSA	Dynamic Spectrum Access
EGC	Equal Gain Combining
FCC	Federal Communications Commission
FDD	Frequency-Division Duplex
FDM	Frequency-Division Multiplexed
IA	Interference Alignment
IRC	Interference Rejection Combining
KPI	Key Performance Indicator

MAC Medium Access Channel

Mbps Mega bits per second

MGF Moment Generating Function

MIMO Multiple-Input Multiple-Output

MISO Multiple-Input Single-Output

MPSK M-ary Phase Shift Keying

MRC Maximum Ratio Combining

MSE mean squared error

NGwN Next Generation wireless Network

OFDMA Orthogonal Frequency Division Multiple Access

OIA Opportunistic Interference Alignment

OT Opportunistic Transmitter

PDF Probability Density Function

PLE Path Loss Exponent

PPP Poisson Point Process

PR Primary Receiver

PT Primary Transmitter

PU Primary User

QAM Quadrature Amplitude Modulation

QoS Quality of Service

QPSK Quaternary Phase Shift Keying

RKRL Radio Knowledge Representation Language

RV Random Variable

SBS Secondary Base Station

SDR Software Defined Radio

SER Symbol Error Rate

SINR Signal-to-Interference-plus-Noise Ratio

SNR Signal-to-Noise Ratio

SR Secondary Receiver

ST Secondary Transmitter

SU Secondary User

TDD Time-Division Duplex

TS Time slot

WLAN Wireless Local Area Network

WRAN Wireless Regional Area Network

ZMSW zero mean spatially white

Introduction

Chapter 1

Introduction

1.1 Introduction to Cognitive Radio

Approximately 50% of the global internet data traffic in 2011 was caused by mobile devices. According to a forecast by Cisco Systems [1], mobile internet data traffic will continue to increase dramatically in the years to come. Driving such a significant increase are the growing number of wireless (particularly mobile) devices and faster mobile network connections [1]. The forecasted number of mobile interconnected devices is expected to exceed 10 billion by the year 2015 [1], of which more than 2 billion are foreseen to be Wireless Local Area Network (WLAN) capable electronic devices [2]. Similarly, the mobile network access speed is also projected to increase nine-fold from 2011 to 2016 [1]. In order to meet these expectations and given that the radio spectrum is a scarce resource, radio systems have to fundamentally change to accommodate disruptive technology innovation [3].

The Federal Communications Commission (FCC) proposed CR as the most promising technology in this regard. Briefly CR is a Software Defined Radio (SDR) with the capabilities of Dynamic Spectrum Access (DSA) techniques. SDRs were first introduced by J. Mitola in the early 1990s to allude to the shift in radio technology from the digital radio in which most radio functionalities are embedded in the hardware, to software defined digital radios which are almost completely programmable, including radio frequency (RF) band, channel access mode, and channel modulation [4]. This adaptability in the RF front end as well as the networking protocols will enable adaptive wireless networks that can dynamically adapt to the changing operational requirement, thus enabling higher spectrum efficiency and performance gains [3].

Due to its tremendous societal value, the radio spectrum has traditionally been carefully managed at the national and international levels through static and long-term licensing [3]. Although such static leasing can be managed easily, studies have shown that it leads to inefficient utilization of spectrum in many cases [5], and indicated that a dynamic usage of the spectrum would lead to increased efficiency. This dynamic spectrum exploitation is known as DSA. Due to the technological, regulatory and economical challenges, full incorporation of DSA is a complex problem [6]. Nonetheless, its potential benefits are recognized by different initiatives such as the DARPA next generation (xG) program [7] based on intelligent CRs .

In communication theory, there are no single universally accepted definition of the term "Cognitive Radio". However, in a broad context, it is used to refer to 'intelligent' radio devices that can sense their external radio environment and adjust their operating regime accordingly. The term was first coined by J. Mitola III and G. Q. Maguire Jr. in late 1990s through the pioneering paper [8], where the authors have introduced the concept of cognitive radio and Radio Knowledge Representation Language (RKRL). In this paper, the authors further discussed the relationship between CR and SDR as well as the role of RKRL in implementing CRs and SDRs.

CR were initially envisioned as very smart devices with "advanced degree of *understanding*". The underlying motivation was comprehensive service (through the radio network) by understanding the user's goals, service context, the network condition, and other real-time information [8]. In his PhD dissertation, Mitola identified this novel approach to wireless communication as: "the point at which personal digital assistants (PDAs) have become maximally computationally intelligent about wireless services and related computer-to-computer communications" such that it can recognize the correct context of the communications needs, and facilitate the most appropriate services that can meet these needs [9]. A functional block diagram of a RKRL-capable CR, as proposed in [9], is illustrated in Figure 1.1.

Following the pioneering work of Mitola, CR caught the attention of the research community, and resulted in a flurry of research in this new direction. Soon the originally envisaged 'very smart device' vision of the CR became modified into more pragmatic, practical and able-to-be-implemented-soon agile radio devices. This is reflected in the definition of CR offered by Haykin in his seminal paper [10]:

"Cognitive radio is an intelligent wireless communication system that is aware of its surrounding environment (i.e., outside world), and uses the methodology of understanding-by-building to learn from the environment and adapt its internal states to statistical vari-

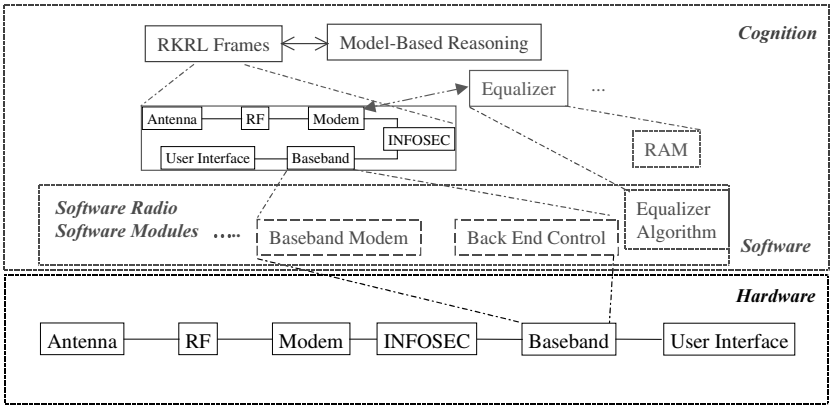

Figure 1.1: Mitola Cognitive Radio Framework [9]

ations in the incoming RF stimuli by making corresponding changes in certain operating parameters (e.g., transmit-power, carrier-frequency, and modulation strategy) in real-time, with two primary objectives in mind:

- *highly reliable communications whenever and wherever needed;*
- *efficient utilization of the radio spectrum."*

Another widely used definition of CR, which nicely captures all its key features of DSA, is the definition forwarded by Akyildiz et. al. in [6]

"More specifically, the cognitive radio technology will enable the users to (1) determine which portions of the spectrum is available and detect the presence of licensed users when a user operates in a licensed band (spectrum sensing), (2) select the best available channel (spectrum management), (3) coordinate access to this channel with other users (spectrum sharing), and (4) vacate the channel when a licensed user is detected (spectrum mobility)."

Taking the concept of CR further, the term 'cognitive' has also been used in the context of wireless networks to refer to networks with adaptive and distributed control and operation. However, in this case too, there are a multitude of different definitions. We present a few of them in this section. Ramming [11] presents a vision for the 'cognitive network' as a distributed network that can manage itself, is aware of the application context, can automatically balance resources and respond to complaints, and is capable of reinforcement learning to gradually improve and evolve itself over time.

Sifalakis et al. define the term "cognitive" when applied to networks as follows: "*The term "cognitive" refers to the intended capability of the network to adapt itself in response to conditions or events, based on reasoning and prior knowledge it has acquired*" [12]; and propose to implement a 'cognition layer' on top of the active network to enable cognition capabilities in the network. However, in order for a network to be truly cognitive as envisioned by them, simply adding a cognitive layer does not suffice. Rather an end-to-end approach has to be considered to satisfy all the goals of such a dynamic network [13].

At a workshop discussing the direction of the future trends in Cognitive Radio Network (CRN) research [3], a CRN was considered to be a DSA enabled network with certain additional functionalities. These functionalities are: (i) network with agile nodes that are able to 'decide' its operating frequency and operate in multiple frequency bands, and (ii) network-level capabilities to configure on-the-fly in order to realize various physical, link and network layer functions suited to the operation band and satisfying regulatory constraints that apply to those bands [3]. This definition of a CRN is adopted in this dissertation.

As we have indicated, there exists a multitude of definitions on CR. In one way or another, all of these involve capabilities for detecting changes in the radio environment, and adapting accordingly. This thesis does not make a hard decision about which definition to adopt. Instead, it focuses on some of the underlying technical challenges that must be addressed, regardless of which definition one prefers.

1.2 Different Models for Cognitive Radios

Following the discussion leading thus far, it is naturally observed that CRs seek to opportunistically coexist with the licensed (or primary users) in a given geo-spectral location. This brings about the question of the extent and the nature of the coexistence between the Primary User (PU) of the band and the CR (or secondary user). In a very broad sense, the SU can coexist with the PUs by overlaying, underlaying or interweaving its signal with respect to the PUs' signals, as explained further below.

Coexistence of primary-secondary signals raises the concern for a new way of quantifying and assessing the unpredictable appearance of new sources of interference at the PR due to the opportunistic nature of SUs' access of the primary band. As a solution to this problem, the FCC Spectrum Policy Task Force recommended a new metric called the interference temperature [5, 10].

1.2.1 Interference Temperature Metric

In 2003, the FCC proposed to define the interference temperature as $T_{int} = \frac{I+N}{kB}$, where $I+N$ is the power generated by undesired emitters plus noise sources, B is the bandwidth and k is the *Boltzman's constant*. More specifically, the interference temperature metric is the temperature equivalent of the noise power measured in units of "Kelvin per Hz" [14]. Moreover, the interference temperature metric can be used to calculate the received interference power at the a receiver, P_{int}, in watts, using the relation $P_{int} = kT_{int}B$ [10, 15]. An introductory analysis of the interference temperature metric is given in [15], wherein the author also discusses other alternative definitions of the said metric. Reference [16] provides a detailed survey on the general considerations for describing an interference constraint.

Note that, the *interference temperature* concept actually caused some controversy over the years after its introduction and was in fact abandoned as a working concept by the FCC in 2007. However, the concept is once again gaining attention and is making its way to being re-considered [17]. Such receiver centric radio rights may be the beginning of a paradigm shift in spectrum regulation from the rigid spectrum licensing policies of today, to spectrum allocation in time-frequency slots under possibly more stringent operating conditions in the future as envisioned in [18].

1.2.2 Underlay Cognitive Radio Model

In the underlay CR model, SUs are allowed to coexist simultaneously with the PUs, by guaranteeing that the interference perceived at the primary receivers is below a given threshold [19, 20]. This is possible by controlling the transmit power at the secondary transmitters [20], or by spreading the communication over a wide bandwidth as in ultra-wideband (UWB) or spread spectrum systems [19]. Due to the interference constraints associated with underlay systems, the underlay technique is only useful for short range communications. Note that, global Channel State Information (CSI) has been an underlying assumption in most earlier analyses of the underlay CR model. However, some recent works have investigated underlay CRNs with partial CSI (e.g. [21]).

Underlay CRs can be modeled as communication links with constraints placed on the channel output (in addition to the traditional constraints on the channel input signals). Thus the capacity for the underlay CR model under different channel models and a received power constraint at the PR can be characterized by translating the received power

constraints into a transmit power constraint at the STs [22]. In a Gaussian multiple access channel (MAC), this received power constraint translates to a weighted sum power constraint at the different STs [23]. Analyzing the capacity region is analytically intractable for the general case when there are multiple primary and secondary users, all interfering with each other and under a received power constraint at the PRs (and possibly a maximum transmit power constraint at the transmitters). However, some properties of the sum-rate maximizing power control problem can be derived by investigating the problem using game theory [23]. Multiple antennas can also be exploited at the STs to minimize the interference at PR, and hence facilitate secondary usage of the spectrum by beamforming the secondary transmission to steer the secondary message away from the direction of the PRs [24].

1.2.3 Overlay Cognitive Radio Model

The spectrum overlay approach also allows the primary and secondary systems to transmit concurrently, and is facilitated by the SUs' active participation in assisting the PUs transmissions. The SUs use part of their power budget to relay the PUs message in exchange of permission to use the PUs band. Thus, the interference experienced due to the SUs transmission can be compensated by the increase in a PU's SNR due to the assistance from the SU [19].

In the overlay model, the SU is assumed to have message side information, i.e. information about the primary channel gains, codebooks and possibly even the PU messages. In the absence of such information, this model reduces to the basic interference channel. On the other hand, when only the SU transmits (the messages intended for both the receivers), the overlay model reduces to the broadcast channel [23]. Due to its similarity with the interference channel and the broadcast channel, encoding techniques developed for either of these channels are suitable for analyzing the overlay CR channel. More specifically, the following encoding techniques are investigated in the literature: rate-splitting, Gel'fand-Pinsker (GP) binning for interference cancellation, and cooperation [23].

Similar to the interference channel, determining the capacity region for the overlay CR model is still an open problem in most cases, though the capacity can be achieved in special cases by applying any of the above mentioned encoding techniques [23]. In the strong interference regime where both the receivers (primary and secondary) can decode all messages with no rate penalty, the capacity can be achieved through cooperation [25]. On the contrary, in the weak interference regime, the ST can precode its message using GP

binning to eliminate the interference at the SR; and together with cooperation, the capacity can be achieved in certain cases (e.g. the Gaussian cognitive channel model [26]). For a general Gaussian cognitive interference channel, the capacity can be determined to within one bit/s/Hz and to within a factor of two bit/s/Hz regardless of the channel parameters by using techniques for analyzing the deterministic cognitive interference channel [27].

Note however that the overlay CR model assumes message side information at the ST, which is very difficult to obtain in practice unless the primary and secondary transmitters can communicate through a very good link between them (e.g. through a backhaul or when they are close to each other). The secondary interference at the PR can be avoided by designing the secondary system such that the SUs transmit only when there are no primary transmission in a given band. This is the interweave principle, which is discussed next.

1.2.4 The Interweave Cognitive Radio Model

The interweave model is the DSA model proposed by Mitola [8], where he used the terminology spectrum pooling to refer to the arrangement under which primary and secondary systems share the same spectrum band. In this access method, the SUs can access the licensed spectrum when there is a "spectrum hole", which results from the time during which the PU is inactive in a given space and frequency. Thus, a spectrum hole is defined in time, space and frequency [10]. Accessing the spectrum holes are not limited by any other constraints, such as the interference temperature discussed earlier. However, an SU has to constantly monitor the radio spectrum to detect possible spectrum holes; and the re-emergence of the PUs in order to evacuate the band when required. Such opportunistic access method is adopted by the DARPA xG program [7] and the first CR-based standard IEEE 802.22 [28].

Accurate sensing of the PU's presence is of central importance in the interweave approach, and becomes even more crucial in a sparsely populated network where all secondary nodes cannot sense all the primary terminals [29]. In such a scenario, the interweave approach corresponds to communication with partial side information [23]. By using queuing theory, an upper-bound performance analysis for a spectral agile cognitive radio networks is presented in [30], where the spectrum agility of the CR system is shown to facilitate significant improvement of spectral utilization.

It must however be noted that the terms for the above DSA methods are used differently by different authors. For example, the authors in [20] use the term 'overlay' to refer

to the above-described 'interweave' approach. In this dissertation, we have adopted the definitions as given in [23] and described above. A comparison of the different models is shown in Table 1.2.

Underlay	**Overlay**	**Interweave**
Channel Side Information: Cognitive (secondary) transmitter knows the channel strengths to noncognitive (primary) receiver(s).	Message Side Information: Cognitive nodes know channel gains, codebooks and possibly the messages of the noncognitive users.	Activity Side Information: Cognitive user knows the spectral holes in space, time, or frequency when the noncognitive user is not using these holes.
Cognitive user can transmit simultaneously with noncognitive user as long as interference caused is below an acceptable limit.	Cognitive user can transmit simultaneously with noncognitive user; the interference to noncognitive user can be offset by using part of the cognitive user's power to relay the noncognitive user's message.	Cognitive user transmits simultaneously with a noncognitive user only in the event of a false spectral hole detection.
Cognitive user's transmit power is limited by the interference constraint.	Cognitive user can transmit at any power, the interference to noncognitive users can be offset by relaying the noncognitive user's message.	Cognitive user's transmit power is limited by the range of its spectral hole sensing.

TABLE I: Comparison of underlay, overlay and interweave cognitive radio techniques.

Figure 1.2: Comparison of Underlay, Overlay and interweave CR technologies [23].

1.3 Coexistence Strategies for Cognitive Radios

Interference management is essential for coexistence between the primary and the secondary system in order to facilitate efficient opportunistic utilization of the spectrum. In this section, we present some of the interference management techniques proposed in the literature.

1.3.1 Interference Cancellation

In the underlay CR model, the SUs can opportunistically use the primary spectrum by canceling the interference at the PR. A general framework for interference cancellation at the PR based on beamforming and beam nulling for a multi-antenna CR system is discussed in [31]. Under the proposed method, STs use beamforming techniques to find antenna weights that place nulls at the PRs, by leveraging the pilot feedback from the primary receiver.

An alternate type of interference cancellation technique, that is cancellation of primary interference at the secondary receivers is proposed in [32], which is termed as opportunistic interference cancellation (OIC). The authors in [32] advocate that the SRs should decode the primary signal when the selected rate and the received power of the primary message

creates such an opportunity; and devise a method that can be applied by SU to achieve the maximal possible secondary rate. Therefore, the secondary rate should be adapted by first considering whether the primary system signal can be decoded.

1.3.2 Interference Minimization

Opportunistic utilization of the primary spectrum by the secondary system can be seen as a resource allocation problem. The objective of the secondary system can be formulated to fulfill a certain design target while minimizing the interference at the primary, e.g. energy efficiency of the secondary system [33]. Alternately it can be designed as an optimization problem under the interference temperature constraint at the PRs as the secondary sum rate maximization problem [34, 35].

In a classical wireless network, allocating more power to the users with higher channel gains is generally preferable from a sum rate/capacity perspective. However, in an underlay CRN, the amount of interference created at the PR has to be taken into account as well, when allocating power (or other resources). Therefore, a classical solution to resource allocation problems cannot be readily applied to CRNs. When the SUs access the primary band through orthogonal channels, the optimal power allocation scheme is a waterfilling policy [23]. However, the cutoff values for the channel gains for the said policy are weighted by factors reflecting the interference generated at the PRs [34].

The secondary transmission power impacts the opportunistic utilization of the primary band under the interweave CR model too. Spectrum holes (at a given frequency band) are spatio-temporal events, and therefore the availability of spectral opportunities depend on the transmission power of the ST and the reliability of opportunity detection at the SR. A spectrum hole has to be available over a larger area if an ST is to transmit with a higher transmission power, and hence communicate with a Secondary Receiver (SR) that is further away. On the other hand, the availability of such spectral opportunities is inversely proportional to the coverage area, i.e. spectral opportunities over a smaller coverage area arise more frequently compared to that over a larger area. Therefore, the secondary transmission power has to be carefully designed for optimal transport throughput under the opportunistic access framework for CRN [35].

Approaching the sum-rate optimization problem becomes more difficult in a multiuser CRN with multiple PUs and SUs transmitting simultaneously, where the problem is known to be nonconvex. Under the cognitive interference channel model, several solutions have been proposed to maximize the performance of the secondary system. Ex-

amples include joint beamforming and power control for multi-antenna secondary systems [36]; achieving network equilibrium by penalizing the SUs through imposing time-varying prices corresponding to the interference they create [37]; and applying game theoretic formulations to find the optimum power allocation solution [38].

1.3.3 Superposition Coding and Successive Interference Cancellation

In the overlay CR model discussed earlier, the opportunistic access of the spectrum by the SUs can be facilitated by collaboration between the primary and the secondary systems. In collaborative primary-secondary transmission, the available time period for transmission is divided into two shorter time slots (TS). In the first TS, the primary transmitter transmits its signal, which is simultaneously received and successfully decoded by the PR, the ST and possibly the SR. In the following TS, the ST composes its message by superposition coding the secondary signal on top of the primary signal, and transmit the super-positioned signal using the decode-and-forward relaying strategy. The total available transmission power at the ST should be carefully divided among the primary and the secondary message such that the end-to-end rate at the PR after the two-TS transmission is not penalized by the SU's opportunistic access.

Under certain conditions, the secondary system can nonetheless achieve non-zero rates through such collaborative techniques at the secondary system. The most important of these conditions is that the ST can successfully decode the primary message received in the first TS in order to be able to relay it in the subsequent TS [39–41]. When equal-length time slots are allocated to the primary source and the secondary relay, maximum ratio combination (MRC) of the signals received in the two TSs can be applied to retrieve the primary signal at the PR [39] . If the SR is sufficiently close to the PT, it can receive and decode the primary signal in the first TS with a high probability. Thereafter, the SR can subtract the primary signal from the relayed superimposed signal received in the second TS from the ST, and finally obtain an interference free version of the secondary signal [40]. On the other hand, when the PT is outside the reception range of the SR and hence the SR cannot overhear the primary message, the power allocation at the ST should be such that the SR can decode the secondary signal from the message received in the second TS by employing successive interference cancellation (SIC) technique [41]. However, determining the optimum time and power allocation ratios in some of the above-discussed solutions require (partial) knowledge of the different channel gains at the ST and both the receivers, which may limit the applicability of the such schemes in practical opportunistic spectrum access scenarios.

1.3.4 Dirty Paper Coding

Dirty-paper pre-coding (DPC) or Costa precoding refers to communicating over an Additive White Gaussian Noise (AWGN) channel in the presence of interference that is non-causally known at the transmitter but not at the receiver [42]. In the overlay CR paradigm, the impact of primary interference at the SR can be completely removed by precoding the secondary signal using an appropriate DPC technique, while insuring there is no degradation in the PU communication. In the low-interference regime, where the secondary signal of interest at the SR is stronger than the primary interference, it has been shown in [26] that a scheme involving DPC can achieve the capacity for the AWGN channels. A multi-level DPC scheme for the single user CR channel that is capable of performing very close to the capacity in both low and high rate of interference is proposed in [43].

1.3.5 Interference Alignment

Interference Alignment (IA) is found to achieve full spatial multiplexing gain in a Gaussian interference channel [44]. It was first proposed by Maddah-Ali in [45,46] for the two user Multiple-Input Multiple-Output (MIMO)-X channel. Subsequently this was generalized for the K-user MIMO-IFC by Cadambe and Jafar in [44]. The main idea of IA is to align the transmission of signals from different transmitters such that all the unwanted interference at each receiver overlap with each other. This will allow a transmitter-receiver pair to communicate interference free over the remaining interference free dimensions. In [44], it is shown that by using Interference Alignment (IA), each user in a fully connected K user wireless interference channel can communicate reliably at rates approaching one half of the rates the user can achieve in a single user (interference free) channel.

Due to the separation of interference and information signal subspaces, interference alignment naturally lends itself to systems where the interference is to be avoided and/or minimized, such as the CRN. IA in a CR scenario is studied in [47–49]. In the seminal works on IA in a CR environment [47], a MIMO SU harmlessly coexisting with a MIMO PU is considered. The authors provide a power allocation and an IA scheme for the Secondary Transmitter (ST) such that the interference at the PR does not spill into the PU's desired direction of communication; and the secondary rate is maximized. This scheme is introduced as the Opportunistic Interference Alignment (OIA) scheme. The idea of OIA is generalized into the Opportunistic Spatial Orthogonalization (OSO) in [48]. The authors introduce OSO as a cognitive radio scheme that allows the existence of SUs and hence increases the sum throughput, even if the PUs occupy all the frequency bands all

the time. The proposed scheme exploits spatial dimensions of the channels and the resulting randomness and independence. In the OSO scheme the interference from multiple SU is opportunistically aligned at the direction that is near orthogonal to the PU's signal space at each channel usage. This is in contrast to the commonly employed IA schemes where the secondary transmissions are *pre-shaped* to introduce exploitable structure to the interference at the PRs. On a related note, the concept of constrained IA is introduced in [49]. In this work, an outer bound is developed on the degrees of freedom (DoF) of the secondary users in the presence of a MIMO primary user that maximizes its own rate. In addition, an iterative algorithm that achieves this cognitive IA scheme is presented. All of the above papers, and most other related works investigating IA in a CRN context assume availability of full CSI at the STs, including that of the primary channel. However, recently introduced techniques, such as the blind interference alignment scheme [50], are aimed at overcoming such stringent CSI dependency.

1.4 State-of-The-Art in Cognitive Radio

In this section we present some of the key areas of research in cognitive radio technology and discuss the state-of-the-art in each of these topics.

1.4.1 Information theoretic analysis and fundamental performance limits

The main topics of investigation in Information theoretic analysis of CR technology involves fundamental capacity limits and associated transmission techniques for different CR wireless paradigms. Some of the relevant findings are discussed in the preceding sections of this chapter. Reference [23] provides an excellent survey on information-theoretic capacity results, related bounds, and the degrees of freedom for different CR network paradigms. In a recently published paper [27], the authors have presented new capacity results for several parameter regimes. Furthermore, inner and outer bounds for the general Gaussian cognitive channel, and the capacity within one bps/Hz, are also presented in this work. Moreover, reference [27] provides an excellent and concise summary of the known relevant results to date.

1.4.2 Spectrum Sensing

Sensing the spectrum band for availability of spectrum holes or opportunities for cognitive access is an essential enabling technique for CR technology. In the interweave CR model, sensing is critical as it directly relates to available opportunities. Moreover, spectrum sensing also plays a role in identifying the presence of, and collecting various PU information (e.g., primary message, channel gain, etc.); and hence is also important for other CR models. Reference [51] is one of the very first overview papers on spectrum sensing in CR, wherein the authors provide an overview of the regulatory requirements (such as detection sensitivity, sensing periodicity etc.) and discuss major challenges associated with the practical implementation of spectrum sensing functionality in CR systems. The above reference further addresses different performance tradeoff issues in spectrum sensing.

Most simple spectrum sensing techniques proposed in the literature are based on energy detection. Such spectrum techniques involves estimating the noise power and then comparing the energy of a detected signal against the noise power to determine the presence of a signal. In [52], the authors have used random matrix theory to propose a new sensing method based on the eigenvalues of the covariance matrix of signals received at the secondary users. The proposed spectrum sensing methods overcome the noise uncertainty problem associated with energy-detection based sensing methods, and can be used without requiring any knowledge of signal, channel and noise power.

Hardware limitations restrict the sensing capability of individual CR nodes to narrow bandwidths. Collaborative spectrum sensing among the CR nodes can improve the sensing capability to cover wider bands. Low-overhead wide-band spectrum sensing methods for a CRN with a large number of cooperating nodes operating over a wide bandwidth are proposed in [53]. The proposed method involves using novel matrix completion and joint sparsity recovery algorithms to decode spectrum occupancy from joint spectrum sensing information provided by multiple sensing nodes. The proposed algorithm represent the recent paradigm shift in spectrum sensing techniques towards collaborative and wide band spectrum sensing techniques.

1.4.3 Cognitive Interference Analysis

Despite the intelligence of CR nodes, and careful planning, unwanted interference at the PRs is unavoidable in opportunistic spectrum sharing. It is important to understand and

analyze the cognitive interference received at the PRs in order to minimize its harmful impact on the performance of the primary systems. Cognitive interference analysis usually incorporates developing a model for the statistical representation of the cognitive interference power at the PRs, which then can be used to evaluate various performance measures. One of the earliest works on modeling the distribution of aggregate cognitive interference at a PR is presented in [54], where the secondary interference model is presented in terms of system parameters of a spectrum sensing-based CRN. On a similar note, the Probability Density Function (PDF) of the cognitive network interference power is approximated using the theory of truncated stable distributions in [55], where the authors further demonstrate how different metrics evaluating the primary system performance can be computed using the derived interference model. Reference [56] is one of the very few papers in the literature, which presents findings of real-life spectrum measurement activities and discusses the lessons learned from it. Additionally, a new stochastic model is proposed for the duty cycle distribution which can have multiple applications in DSA research.

In most investigation on cognitive interference analysis, the network is generally modeled as a spatial Poisson point process (PPP), mainly due to its analytical tractability. However, due to opportunistic natures of its access, a CRN is most likely to have a limited number of nodes randomly distributed across a relatively small area, and as such the PPP may not be the most appropriate model for analyzing such a network [57]. Reference [58] addresses the shortcomings of the Poisson model and proposes an alternative that overcomes its drawbacks. On the other hand, references [59, 60] analyze the aggregate cognitive interference by modeling the CRN as a Binomial point process (BPP) instead of the commonly used PPP model.

1.4.4 Spectrum Sharing, Resource Allocation, and Power Control

Resource allocation problems in the spectrum sharing CR model address the optimum utilization of the available resources, including the spectrum access opportunities. In a CRN with multiple primary and secondary users, the optimum design approach should treat all active links as a large interference network, and jointly optimize some measure of the secondary performance under a certain guarantee on the primary performance [61]. However, such joint optimization is difficult to implement, and perhaps not feasible from a practical point of view.

An important survey of dynamic resource allocation schemes for underlay CRN with

emphasis on convex optimization techniques is presented in [61]. In this work, the authors discuss different formulations of resource optimization problem and discusses different probable solutions to the posed problems. Reference [62] is another major work where the ergodic capacity of a single user secondary system coexisting with a single user primary system is analyzed under different coexistence strategies. One of the pioneering works addressing sub-channel and downlink transmission power allocation problem for multi-cell CRNs is presented in [63]. In their investigation, the authors consider a multi-cell CR-enabled orthogonal frequency division multiple access (CR-OFDMA) network that has to control the interference to the PRs alongside coordinating the inter-cell interference in itself. Reference [64] is a significant work on resource allocation in relay-assisted CRNs, wherein relay and power allocation problem for OFDM-based single antennae CR systems are investigated. The authors in [64] have proposed a method to maximize the capacity of a CR user employing relays with a constraint on the total transmission power and an interference temperature constraint at the PRs.

1.4.5 Cross-layer optimization

An important aspect of wireless networks is their dynamic behavior. The conventional protocol stack is inflexible and inefficient since each layer has specific functionalities assigned to it. Moreover, the different protocol layers communicate in a strict manner. By exploiting lower layer information through a cross-layer design concept, performance benefit and efficiency in spectrum and energy usage may be obtained. Such design approach is known as cross-layer optimization. In this section, we briefly discuss few significant contributions in cross-layer analysis of CRNs.

Reference [65] by Urgaonkar and Neely is a significant work on cross-layer modeling and analysis of single-hop cognitive radio networks. In this contribution, the authors use the technique of Lyapunov Optimization to develop a cross-layer (transport and radio link layers) model for scheduling and flow control of data packets at the STs that maximize the throughput utility of the SUs subject to maximum collision constraints for PUs.

A notable work on cross-layer spectrum sensing is [66], wherein a cross-layer based opportunistic multi-channel Medium Access Channel (MAC) protocol, which integrate the spectrum sensing at physical (PHY) layer with the packet scheduling at MAC layer for the wireless ad hoc networks is proposed. The proposed MAC protocol enable the SUs to identify and utilize the leftover frequency spectrum in a way that constrains the level of interference to the PRs.

On a similar note, [67] is another important work addressing the PHY-MAC cross layer performance analysis in an infrastructure based DSA environment. In this study, the authors have developed a queueing analytic framework to study the data link layer Quality of Service (QoS) performance measures for CR users with bursty traffic arrival pattern and correlated channel fading under dynamic channel activity at the PU end.

Cross-layer design has also been considered for multi-antenna CR devices. In [68], the authors present a cross-layer optimized cooperative beamforming technique to forward messages in busy time slots without causing interference to the PUs. The proposed cooperative scheme can achieve cooperative diversity gain and improve the QoS for the SUs without consuming additional idle Time slots (TSs) or temporal spectrum holes.

1.5 Emerging Cognitive Radio Applications

Although Cognitive Radio technology is relatively novel and is still at the early stage of its development, many emerging applications have already been proposed. Several important developments in the past years in spectrum policy rules have accelerated the evolution of emerging CR applications. Most notable of these are the publication of the final rules for unlicensed devices in the TV bands by FCC in September 2010 [69], and the secondary use of the $2360 - 2400$ MHz band for medical body area networks (MBAN) under the IEEE 802.15.4j standard, which is expected to be finalized at the end of 2012 [70]. Standardization efforts to facilitate the secondary usage of TV band and other parts of the spectrum are also being considered by the Electronics Communications Committee (ECC) in Europe [71] and elsewhere. Some of the proposed CR applications are briefly discussed in this section.

1.5.1 Smart Grid Networks

Smart grid refers to the power grid which utilizes a digital processing and communication technology to control appliances at the consumer end; thus saving energy, reducing costs and increasing reliability, efficiency and transparency. Access to a reliable communication network is critically important for the success of smart grids. Typically the smart grid communication network can be divided into three segments: the home area network (HAN) connecting the end user appliances, the advanced metering infrastructure (AMI) or field area network (FAN) that carry information from the HAN to the network

gateway (e.g. the power substations), and the wide area network (WAN) serving as the backbone [72].

CR technology in the television white space (TVWS) is envisioned by the IEEE 802.15 Smart Utility Networks Task Group 4g (IEEE 802.15.4g) as a potential candidate technology for the AMI/FAN as it offers many advantages in terms of bandwidth, reach and cost in certain markets compared to other competing technologies [73].

1.5.2 Public Safety Networks

Public safety workers are increasingly being equipped with wireless devices having communication capabilities to enhance their efficiency and ability to quickly respond to emergency situations. However, the envisioned application is being hampered because the radio spectrum dedicated for public safety usage is becoming highly congested, and due to interoperability issues between different incompatible systems used by different agencies. CR has been identified as a potential technology to support the increasing bandwidth and communication demands of the public safety networks [73]. The opportunistic access supported by CR technology will open up new spectrum bands for public safety use, e.g. the license-exempt TVWS. Furthermore, with the agility accorded by the multi-interface SDR, CR technology can facilitate interoperability of different systems and/or operations over different bands. However, ensuring the high priority access and the stringent connectivity guarantee generally required of public safety networks, is one of the biggest challenges of supporting public safety access through CRNs.

1.5.3 Commercial Cellular Networks

A recent analysis suggests that there will be a likely deficit of 300 MHz in the broadband spectrum by 2014 [74]. The National Broadband Plan published by the FCC in March 2010 recommends meeting this additional spectrum demand by making TV spectrum available for cellular broadband usage [74]. Specifically, CR technology can augment next generation cellular systems such as long term evaluation (LTE) and WiMAX to opportunistically use these newly available spectrums either in the access or backhaul part of the networks [73].

Application of CR technologies in access network can be either in providing *'hotspot'* access at mass gathering locations, such as stadiums and airports; or in extending indoor coverage through deploying femtocell [75] (or femtocell-like pico-cells). On the other

hand, CR can facilitate extending coverage to rural areas by opening the network operators' door to cost-affective backhaul access [73].

1.5.4 Wireless Medical Body Area Networks

The remote monitoring of body status and the surrounding environment is becoming increasingly important for many different medical (and other) applications. Generally small on-body sensor nodes are used for this purpose. Each node has enough information handling and communication capability to process and forward relevant information to a base station for real time diagnosis. The sensor nodes can be wirelessly connected to form an MBAN, which allows the integration of the monitoring sensor nodes and the associated base station(s) [76]. Due to the stringent quality of service (QoS) of the life-critical MBANs, the license-exempt 2.4 GHz industrial, scientific and medical (ISM) band is not suitable for its operation [73]. Conversely, the very-low-power and close-range nature of its operation makes CR technology a suitable candidate in realizing MBANs [70, 76]. In fact, the $2360 - 2400$ MHz has already been allocated for secondary use by MBAN under the IEEE 802.15.4j standard.

1.5.5 Green Wireless Communication via Cognitive Dimension

Green networking and communication approach calls for holistic energy-wise optimization of communication systems to arrest the increasing environmental impact of information and communication technology (ICT), and minimize its harmful effects [77]. CR has been envisaged to ensure energy-wise more efficient communication systems. From the green perspective, CR enables the wise and optimal utilization of the the spectrum, which is a limited natural resource [77]. The "*consume only when necessary*" approach of CRs coupled with the energy efficiency of opportunistic spectrum utilization is an enabling paradigm that will support long term sustainable development of global ICT infrastructure. Nonetheless, a number of trade-offs are entangled with the green-side of CR technology, such as spectrum sensing vs. spectrum utilization tradeoff (including multi-channel power allocation); computational complexity vs. energy consumption tradeoff; hardware complexity vs. financial cost, and others [77].

1.6 Cognitive Radio Testbeds and Standardization Activities

Most research studies and results evaluating CRs rely on a theoretical analysis or computer simulations, which cannot fully characterize the complex heterogenous radio environment of its operation. From the design perspective, it is still not very clear how the end-to-end design of a complete CR system with all the functionalities of the different system architecture layers should be put together. In fact, there are very few works involving test-bed applications or prototype development of CR systems. One of the earliest CR testbeds was developed by the Berkeley Wireless Research Center (BWRC) at the University of California at Berkeley [78].

The BWRC CR testbed hardware architecture is built on the Berkeley Emulation Engine (BEE2), which is a modular scalable FPGA-based computing platform with software design methodology [79]. The software architecture is Simulink-based design flow and BEE2 specific operating system providing an integrated implementation and data acquisition environment during experimentations. The testbed radio interface is a highly reconfigurable 2.4 GHz radio modem connected to the BEE2 platform via fiber link that can be adaptively tuned over 85 MHz of bandwidth. The received signal strength (RSSI) and the automatic gain control (AGC) are measured in real-time, and can be used to perform spectrum sensing. In addition, available Ethernet interface to BEE2 provides connectivity to other networked devices such as 802.11 equipments designated to be the primary users [78]. The emulation scenario of a CR environment with primary and secondary users is reproduced from [78] in Figure 1.3.

Other notable activities in CR testbed development include the OpenAirInterface developed and maintained by Institute Eurécom, France [80]; the IRIS platform developed by Trinity College Dublin, Ireland [81]; and the ASGARD platform of Aalborg University, Denmark [82].

1.6.1 Cognitive Radio in Standardization

The IEEE 802.22 working group on Wireless Regional Area Network (WRAN) was formed in October 2004 with the objective of using CR technology to allow opportunistic access of the TVWS. The target application of IEEE 802.22 WRAN standard is to bring broadband access to low-population-density areas by reusing spectrum allocated to TV

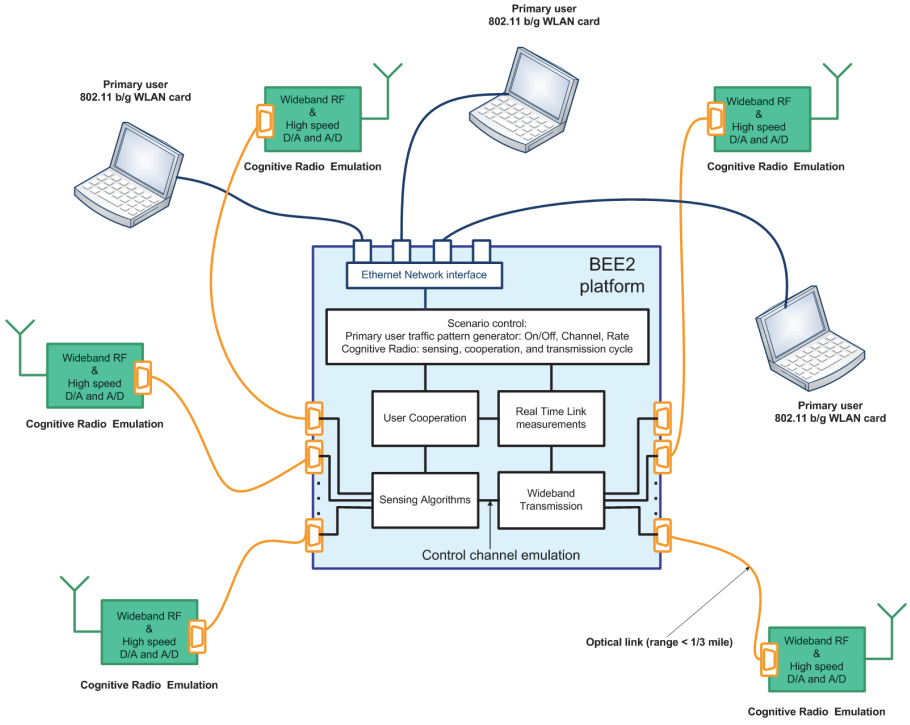

Figure 1.3: Emulation of the cognitive radio BWRC testbed based on BEE2 architecture [78].

broadcast ($54-862$ MHz) on a non-interfering basis. Some key aspects of IEEE 802.22 WRAN standard are summarized from [83, 84] and outlined in this section.

Spectrum Awareness

Geo-location information with assistance from a database, and spectrum sensing are the two methods that are proposed in IEEE 802.22 standard for spectrum awareness. These involve using geo-location information of the CR devices along with data of registered licensed devices from a data base to identify the locally available channels for cognitive access.

System Aspects

The IEEE 802.22 WRAN standard is designed to provide fixed cellular wireless broadband access to rural areas. Each base station can serve a maximum of upto 255 customer premises equipment (CPE) in an area of typically $17-30$ km or more in radius. The minimum peak throughput at the cell edge is 1.5 Mbps in the downlink direction and 384 kbps in the reverse direction.

Physical Layer

The air interface of the IEEE 802.22 standard is based on a single mode 2048-carrier Orthogonal Frequency Division Multiple Access (OFDMA) with support for a channel bandwidth of $6, 7$, or 8 MHz (as per regulation of the country). Initially only Time-Division Duplex (TDD) mode was supported since it is not always possible to have a paired TV channel available. The provisions for incorporating Frequency-Division Duplex (FDD) in the future is also available. The IEEE 802.22 standard does not support multi-antenna terminals due to the large antenna size at the low operating frequencies. Due to the long range of operation, the cyclic prefix length is set to accommodate the associated long propagation delay. As for the adaptive modulation and coding scheme, three constellation sizes (Quaternary Phase Shift Keying (QPSK), 16-Quadrature Amplitude Modulation (QAM), and 64-QAM) and four coding rates ($1/2, 2/3, 3/4$, and $5/6$) are supported, providing a peak data rate of around 23 Mega bits per second (Mbps) at 6 MHz bandwidth.

MAC Layer

The IEEE 802.22 MAC layer have been inspired in part by the IEEE 802.16 MAC standard, and provides mechanisms for flexible and efficient data transmission. However, major enhancement have been made to support cognitive functionality for reliable coexistence with primary users and self-coexistence among other 802.22 systems. The MAC standard is connection oriented with support for unicast, multicast and broadcast access for both management and data. Moreover, the IEEE 802.22 MAC specifies a self-coexistence mechanism based on the Coexistence Beacon Protocol (CBP) to manage mutual interference among collocated WRAN systems due to co-channel operation.

The potential of CR is recognized by the introduction the IEEE 802.22 WRAN standard, which was in fact the recipient of the IEEE Standards Association *'Emerging Technology of the Year Award'* in 2011.

1.7 Scope and Limitations of this Work

The state-of-the-art in various aspects of Cognitive Radio technology have briefly been outlined so far in this chapter. All the above topics lead to many interesting research questions and subjects of study. However, given the limitation of time and resources that constitute a PhD study, the scope of this thesis is confined to investigating a number of issues for a specific CRN model. In this section, we present the scope and limitations of the work, and the rationale behind the delimiting choices made.

Most of the research presented in this thesis consider the underlay cognitive radio model, where the cognitive/secondary network opportunistically accesses the primary spectrum under an interference temperature constraint at the PRs. This PhD study is part of a Nordic project titled "Cross Layer Optimization in Short-Range Wireless Sensor Networks (CROPS) II" with cooperative transmission enabled wireless sensor networks as the primary target application. With this background in mind, the focus of this thesis was limited to the underlay CR model, which is suitable for close range communications. Moreover, simplicity, low-cost and low power consumption is an important requirement for nodes in an wireless sensor network. Such requirements have motivated us to limit most of our studies to scenarios that does not involve active cooperation with the primary system; and also to focus a large part of our investigation on narrowband single antenna users.

In addition, smaller cells such as pico-cells, and femtocells are envisioned to be the key enabling technology supporting the huge data rate requirements of the future communication systems. Furthermore, next generation wireless networks are becoming increasingly heterogeneous due to the number of different systems dynamically co-existing in the same spectrum [85]. Such trends have been an essential motivating factor in limiting our studies to small cells with a limited number of heterogenous users.

The communication distances between different users in a small cell size are usually in the range of tens to hundreds of meters. This implies that the user communication is most often in the interference-limited region rather than the power-limited region. As such, proper understanding and management of the inter-user interference is important in facilitating proper utilization of the radio resources. Proper interference management/coordination is further critical for the opportunistic CR systems. Therefore, *'interference'* has been a central recurring theme in this thesis. At the end of the thesis, we have also presented our recent basic investigation involving hierarchical spectrum usage using advanced physical layer interference management techniques such as beamforming and interference alignment schemes.

An idea remains a theoretical abstraction unless it can be implemented as a real life product. Test beds and implementations of CR systems, which have been briefly discussed in Section 1.6, is an important step in the life cycle of any novel research topic as it enables demonstrating proof of concept; although in practice, it is very difficult to turn ideas into reality in the wireless world. However, test bed development and implementations are beyond the funding term of an individual PhD study period. Moreover, any form of implementation, even in its simplest form, require multilateral skills and inputs from a team of researchers with a long project life cycle. Hence, test bed implementation and proof of concept for the research findings presented in this thesis could not be explored due to the individual nature of the current PhD project, and limited time and resources.

1.8 Typical System Models and Performance Evaluation Parameters

In this section, we present typical communication system models and discuss a few of the commonly used performance evaluation parameters and metrics of a wireless system which have been used in this thesis.

1.8.1 Linear system model

A linear model is a mathematical model of a system based on the use of linear operators, and usually presents a mathematical abstraction of a real-life system which are typically non-linear. Such idealization provides a simple but robust analytical model to analyze the system performance and give valuable insights. Throughout this thesis, the linear system has been adopted to model the wireless communication link between a transmitter and a receiver. Under this model, and considering single antenna devices and a narrowband context, the signal $y(t)$ received at a given receiver at time t is given by

$$y(t) = h(t)x(t) + \sum_j g_j(t)\tilde{x}_j(t) + n(t), \tag{1.1}$$

where $x(t)$ is the transmitted signal from the intended transmitter, $h(t)$ is the channel gain from this transmitter to the receiver, and $n(t)$ is the received noise signal at the receiver which is typically modeled as zero mean AWGN with variance N_0. The linear system model can also capture any interference(s) received from other co-channel interferers, as shown in (1.1), where $\tilde{x}_j(t)$ represents the transmitted signal from an interfering transmitter with channel gain from that transmitter to the intended receiver denoted by $g_j(t)$. Furthermore, the above narrowband model could also represent one sub channel in a wideband Frequency-Division Multiplexed (FDM) system.

The channel gains $h(t)$ and $g_j(t)$ are generally modeled as random variable with a known distribution, the exact choice of which depends on the considered scenario. The Rayleigh, Rician and the Nakagami-m fading models are the most typically used distributions.

1.8.2 Commonly used Key Performance Indicator Metrics

The performance of any given system can be measured using a number of different metrics, with each metrics conveying one or some aspect of the system performance. It is common to consider a number of different metrics in evaluating a system performance in order to reflect the overall performance of the system. Throughout this thesis, a number of system performance metrics have been used to evaluate the performance of the presented analyses and proposed schemes/algorithms.

One of the most commonly used Key Performance Indicators (KPIs) of a system is the received Signal-to-Interference-plus-Noise Ratio (SINR), which is a measure of the ratio of the received signal power to the sum interference plus noise power. Considering the

system model of (1.1), the SINR γ at the intended received is given by [86]

$$\gamma = \frac{|h(t)x(t)|^2}{\sum_j |g_j(t)\tilde{x}_j(t)|^2 + N_0}. \tag{1.2}$$

The SINR of a communication link succinctly represents the physical layer performance, and can be easily translated to other performance indicators such as the capacity and the BER. For example, under the Gaussian distribution assumption on the received interference and noise and considering that a capacity-achieving coding is used, the capacity $C(\gamma)$ of a communication link with received SINR γ is famously given by the Shannon's rate as $C(\gamma) = \log_2(1+\gamma)$ [87].

Alongside the physical layer KPIs such as the SINR and the capacity, considering higher-level KPIs such as the end-to-end delay, or the system goodput (which reflects the loss in capacity due to overheads) can further help to evaluate the overall system performance. Besides, other important system level performance indicators include for example the coverage area of a network, and its Area Spectral Efficiency (ASE). The network coverage is simply the geographical area within which a user can be served by a network at least with a minimum acceptable service quality. The ASE, on the other hand, is defined as the sum of the maximum average data rates/Hz/unit area supported by a cell's base station [88]. It is a measure of the efficiency or the quality of the coverage area of the network. Both of these KPIs reflect a network level performance and are influenced by higher level design issues such as the frequency reuse distance, cell sizes, antenna sectorization etc. [88].

1.9 Key Contributions of this Thesis

A detailed list of the original contributions of this thesis are presented in this Section. But first we present, what we believe are, the *three* most important contributions of this thesis as a synopsis.

1.9.1 Synopsis of Key Contributions

- A generalized model for the interference at a legacy receiver from a coexisting heterogeneous next generation narrowband is derived in this thesis, where the transmitters can have different transmit powers, admission rates and path loss exponents.

Applications of the derived model in performance evaluation of the legacy system, as well as system design of the next generation system are then demonstrated. In addition, the derived model is used to propose a simple distributed power allocation algorithm for the secondary system.

- A novel hybrid cooperation scheme for an interference temperature constrained CRN is presented in Chapter 2 of this thesis. The proposed scheme is found to utilize the diversity gain accorded by the cooperative communication with insignificant penalty in terms of the multiplexing gain of direct communication.
- At an attempt at exploring how to achieve the maximum utility benefit for an underlay CRN given the interference temperature constraint at the PRs, we propose a measure of the achievable rate utility of the SUs with respect to the interference at the PRs; and present a distributed resource allocation algorithm that maximizes the sum of this proposed measure across the SUs.

1.9.2 Original Contributions of the Papers Included in This Thesis

The main contributions of the following papers, which constitute this thesis, are summarily described below.

Paper A – Interference Modeling in Heterogeneous Next Generation Wireless Networks - and its Applications

N. H. Mahmood, F. Yilmaz, M.-S. Alouini, and G. E. Øien, "Heterogeneous Next Generation Wireless Network Interference Model - and its Applications", Submitted to Wiley International Journal on Wireless Communications and Mobile Computing, August 2012.

Partial results of this work have been published in the following three conference papers:

- *N. H. Mahmood, F. Yilmaz, M.-S. Alouini and G E. Øien,"Cognitive Interference Modeling with Applications in Power and Admission Control", in Proceedings of the IEEE Symposium on New Frontiers in Dynamic Spectrum Access Networks (DySPAN 2012)* [89].
- *N. H. Mahmood, F. Yilmaz, M.-S. Alouini and G E. Øien, "On the Ergodic Capacity of Legacy Systems in the Presence of Next Generation Interference", in Proceedings of The Eighth International Symposium on Wireless Communication Systems*

(ISWCS'11), Aachen, Germany, November 2011. pp. 462-466 [90].

- *N. H. Mahmood, F. Yilmaz, and M.-S. Alouini, "A Generalized and Parameterized Interference Model for Cognitive Radio Network", in Proceedings of the 12th IEEE International Workshop on Signal Processing Advances in Wireless Communications (SPAWC 2011), San Francisco, USA, June 2011. pp. 76-80* [91].

Next generation wireless systems facilitating better utilization of the scarce radio spectrum have emerged as a response to inefficient rigid spectrum assignment policies. These are comprised of intelligent radio nodes that opportunistically operate in the radio spectrum of existing primary systems; yet unwanted interference at the primary receivers is unavoidable. In order to design efficient next generation systems and to minimize their harmful consequences, it is necessary to realize their impact on the performance of primary systems. In this work, a generalized framework for the performance analysis of such primary systems in the presence of interference from next generation systems is presented.

The most important contributions of this work are as follows. First, a generalized unified framework to evaluate the impact of the interference power from a narrowband NGwN at the receiver of a coexisting narrowband primary system is presented, where the underlying nodal distribution of the Next Generation wireless Network (NGwN) is modeled as a Binomial Point Process (BPP) instead of the commonly considered Poisson Point Process (PPP). Furthermore, power control and admission control at the Opportunistic Transmitters (OTs) are considered. Second, we consider the Path Loss Exponent (PLE) to be a Random Variable (RV), instead of it being fixed over the coverage area. Empirical studies have reported that even a small cell can have different types of terrain property, such as buildings, trees and open area, resulting in the PLE to vary over the area of a single cell [92–94]. Such an analysis is important as future wireless networks are becoming increasingly more heterogeneous in which different users belonging to different networks can experience different slow fading effects. Finally, we introduce and adopt a bounded path loss model which overcomes the shortcomings of the commonly used model which limits transmitter receiver separation distance to be greater than unity.

Paper B – On Hybrid Cooperation in Underlay Cognitive Radio Networks

N. H. Mahmood, F. Yilmaz, G. E. Øien and M.-S. Alouini, "On Hybrid Cooperation in Underlay Cognitive Radio Networks", Submitted to the IEEE Transactions on Wireless

Communications, September 2012.

Partial results of this work have been published in the following conference paper:

- *N. H. Mahmood, F. Yilmaz, G. E. Øien and M.-S. Alouini, "On Hybrid Cooperation in Underlay Cognitive Radio Networks", in Proceedings of the 46th Asilomar Conference on Signals, Systems and Computers (Asilomar 2012)* [95].

In certain wireless systems where transmitters are subject to a strict received power constraint, such as in an underlay CRN, cooperative communication helps to improve the coverage area and the outage performance of a network, and is a promising strategy to enhance the network performance. However, this comes at the expense of increased resource utilization. To balance the performance gain against the possible over-utilization of resources, we propose and analyze an adaptive-cooperation technique for underlay CRNs termed as hybrid-cooperation, whereby the SUs cooperate adaptively to enhance the capacity and the error performance of the network. The bit error rate, the capacity and the outage performance of the network under the proposed hybrid cooperation technique are analyzed in this paper, and compared against the traditional cooperative scheme. Findings of analytical performance analyses are further validated numerically through selected computer-based Monte-Carlo simulations. *The proposed scheme is found to achieve significantly higher capacity at comparable BER compared to the conventional amplify-and-forward cooperation scheme.*

Paper C – A Relative Rate Utility based Distributed Power Allocation Algorithm for Cognitive Radio Networks

N. H. Mahmood, G. E. Øien, L. Lundheim and U. Salim, "A Relative Rate Utility based Distributed Power Allocation Algorithm for Cognitive Radio Networks", in Proceedings of the 2012 International WDN Workshop on Cooperative and Heterogeneous Cellular Networks (WDN-CN2012) held in conjunction with IEEE PIMRC 2012 [96].

In an underlay Cognitive Radio Network, multiple secondary users coexist geographically and spectrally with multiple PUs under a constraint on the maximum received interference power at the PRs. Given such a setting, one may ask "how to achieve maximum utility benefit at the SUs given the imposed interference temperature constraint"? We attempt at answering the above question by proposing a distributed power allocation algorithm that takes into consideration the inter-secondary interference, as well as that between the STs and the PRs. The impact of the inter-secondary interference on the rate performance

is quantified through an *'interference price'*, which is a measure of the marginal rate at the SRs per unit secondary interference contributed by other interfering SRs. The main contribution of this work is a proposal to measure and then maximize the relative achievable rate utility of the SUs with respect to the interference it generates at the PRs. This is achieved using the introduced measure of *'relative rate utility'*. Unlike most previous works, this measure is unique for each ST, reflecting the facts that: i) different STs will cause different levels of interference at the PRs, even for the same amount of transmit power; and ii) the achievable rate for a given transmit power level is different for different SUs. In addition, with the proposed algorithm, the secondary system can operate independently from the primary system and still satisfy the interference temperature constraint at all PRs.

Paper D – Interference Coordination Techniques for Cognitive Radio Networks Under Zero Interference Constraint at Primary Receivers

N. H. Mahmood and G. E. Øien, "Generalized Hierarchical Spectrum Usage under Spatio-orthogonal Co-existence Policy", submitted for possible publicaiton to the IEEE Wireless Communication and Networking Conference (IEEE-WCNC) 2013.

The wireless channel is inherently broadcast in nature, where multiple links interfere with each other. Dealing with interference in the wireless link mostly involve one or more of the following: i) interference avoidance, ii) interference rejection, and iii) interference exploitation. In this work, we investigate different interference management techniques for hierarchical spectrum usage, where different systems communicate using the same wireless channel under different operating conditions. More specifically, we propose a scheduling scheme, and study different transmit precoder design principles for an opportunistic wireless systems accessing the spectrum of a legacy system under strictly "no interference" policy. The proposed schemes, which utilize the spatial degrees of freedom accorded by multiple antennas, are found to result in significant sum rate performance of the opportunistic system without affecting the operation of the legacy system. Computer based Monte-Carlo simulations are used to validate the performance of the proposed algorithms.

1.10 Possible future works

In this concluding section, we present some ideas for possible extension of the work disseminated in this thesis.

1.10.1 Empirical Heterogeneous Networks Interference Model

In *paper A*, we have developed an unified statistical model for the sum interference power at a target PR from a set of interfering STs, each with different probabilities of becoming active and different transmission powers. Such network interference modeling has applications to dynamic spectrum access and HetNets, among others. The derived Moment Generating Function (MGF) of the interference distribution involves an weighted sum of the special Beta function. Under certain circumstances and for some applications, computation of the MGF may be computationally intensive. Therefore, it would be interesting to approximate the derived MGF, possibly using known distributions. Moreover, numerically comparing the derived distribution MGF with the MGF of other known distributions, such as the Gaussian Mixture and the Symmetric Alpha Stable distribution would allow comparing the proposed model with other models for similar interference scenarios. Furthermore, empirically measuring the interference power for practical scenarios of opportunistic spectrum access, and then using the obtained data to derive an interference model may present a more realistic model and help to capture impacts of heterogeneous network access that cannot be modeled theoretically.

1.10.2 Relay selection with correlated channels

The work presented in *paper B* proposes a novel hybrid cooperative scheme for cognitive radios that improves the capacity of a relay assisted communication link without significantly affecting its error performance. However, the proposed scheme involves the best relay selection strategy, where the relay offering the best performance (e.g. maximum SINR) is selected at each communication slot involving a relay. This entails a significant signaling overhead since all associated CSI is required at the base station (or any other centralized node) to determine the best relay.

As a possible extension of the proposed scheme, other relay selection strategies can be investigated that can further improve the system throughput. One idea can be to explore relay selection based on the average system performance (e.g. best average SINR). Initial

investigation have shown that such a technique greatly impacts the diversity gain of the relays due to the uncorrelated channel assumption. However, wireless channels in practice are correlated over the coherence time and bandwidth. Hence, it will be interesting to investigate the performance of such '*best average*' relay selection techniques under correlated channel model assumptions.

1.10.3 Optimum Resource Allocation Schemes with Cooperation between the Secondary and the Primary Systems

A relative rate utility based power allocation algorithm for interference temperature constrained CRN is proposed in *paper C*. The PRs are not assumed to cooperate with the STs in the considered scenario. However, the boundary between the so called primary and secondary system is becoming blurred and the paradigm is shifting towards all cognitive network, or networks where both the primary and the secondary users belong to the same operator. Hence, it may be conceivable in the future to assume some sort of cooperation among the users. Under such a scenario, it would be interesting to compare what gains can be achieved from such cooperation versus the price (overheads) of establishing the said cooperation. On a different note, we have considered that the entire channel bandwidth is always available to all the users. However, under strong interference conditions, rate-wise it may be more beneficial to suppress interference by orthogonal transmissions or by using advanced receiver techniques. Therefore, the current work can be extended to investigate the optimum channel allocation schemes and advanced receiver design principles in addition to the power assignment problem.

The STs are assumed to be able to estimate the ST-PR channel sufficiently well, and to be synchronized among each other. It will be interesting to investigate algorithms that are robust to the uncertainty in the primary channel information (in terms of error and delay in the CSI), as well as any drift in synchronization among the STs.

1.10.4 Interference Alignment Schemes with Minimum Information Exchange

In the work presented in *paper D*, full cooperation between the primary and secondary network is assumed. Such an assumption results in scenarios that can serve as a benchmark with high backhaul capacity and instantaneous CSI across different nodes. As an extension of the presented work, we would like to investigate what is the requirement on

the backhaul capacity, and how sensitive is the proposed scheme to CSI errors/delays. More specifically, we would like to quantify the requirements of instantaneous channel knowledge, and measure the impact of errors (in terms of inaccuracies as well as delays) on the performance of the proposed IA schemes. Furthermore, we would also like to investigate practical 'statistical interference alignment' schemes that utilized the channel statistics instead of the instantaneous values and hence are not sensitive to CSI inaccuracies or delays.

1.11 Other Papers

In addition to papers A-D, the author also carried out the following research which resulted in a conference publication, but is not formally part of this dissertation as it is not central to the thesis topic.

On the Impact of Primary User Localization on Rate Performance of CR systems

N. H. Mahmood, M. Brandt-Pearce, G. E. Øien, On the Impact of Primary User Localization on Rate Performance of CR Systems, in Proceedings of 5th IEEE Annual International Conference on Wireless Internet (WICON 2010), Singapore, March 1-3, 2010, pp. 1-8.

This paper investigates how localization knowledge of primary users impacts the sum-rate performance of a secondary system in an underlay cognitive radio setting. Two different probabilistic models for the primary users' location information are assumed, one uniform distribution and the other with Gaussian distribution. The interplay between the achievable rate of the secondary system and the primary users' location information under the AWGN and a fading channel model are presented and analyzed. Investigations are carried out for different propagation environments, localization models and primary-secondary user settings. Results show that the relationship between the secondary system sum-rate and the primary users' location information depends on the number of primary and secondary users, as well as the propagation environment. Empirical expressions for the sum-rate are proposed for different localization probability distributions.

Bibliography

[1] C. V. N. I. (VNI), "Cisco® visual networking index (VNI) global mobile data traffic forecast update, 2011 - 2016," Cisco Systems, Inc., White paper, Feb. 2012.

[2] J. Rebello. (2011, Apr.) More than 1 billion devices to have embedded wireless networking capability. [Online]. IHS iSuppli. http://tinyurl.com/6mpuwjg.

[3] P. Steenkiste, D. Sicker, G. Minden, and D. Raychaudhuri, "Future directions in cognitive radio network research," NSF Workshop Report, Arlington, VA, USA, Tech. Rep., Mar. 2009.

[4] J. Mitola, "The software radio architecture," *Communications Magazine, IEEE*, vol. 33, no. 5, pp. 26 –38, May 1995.

[5] F. S. P. T. Force, "Report of the spectrum efficiency working group," Federal Communications Commission, Tech. Rep., 2002.

[6] I. F. Akyildiz, W.-Y. Lee, M. C. Vuran, and S. Mohanty, "NeXt generation/dynamic spectrum access/cognitive radio wireless networks: A survey," *Computer Networks*, vol. 50, no. 13, September 2006.

[7] "The xG architectural framework v1.0," DARPA Next Generation Working Group, 2003.

[8] J. Mitola III and G. Q. Maguire Jr., "Cognitive radio: making software radios more personal," *IEEE Personal Communications*, vol. 6, no. 4, pp. 13 –18, Aug. 1999.

[9] J. Mitola III, "Cognitive radio: An integrated agent architecture for software defined radio," Ph.D. dissertation, Royal Institute of Technology (KTH), Sweden, May 2000.

[10] S. Haykin, "Cognitive radio: Brain-empowered wireless communications," *IEEE Journal on Selected Areas in Communications*, vol. 23, no. 2, pp. 201–220, Feb. 2005.

[11] C. Ramming, "Cognitive networks," in *The 23rd DARPA Systems and Technology Symposium (DARPATech)*, Anaheim, CA, USA, Mar. 2004.

[12] M. Sifalakis, M. Mavrikis, and G. Maistros, "Adding Reasoning and Cognition to the Internet," in *3rd Hellenic Conference on Artificial Intelligence (EETN) - proceedings companion volume*, Athens,Greece, May 2004, pp. 365–375.

[13] Q. Mahmoud, Ed., *Cognitive Networks: Towards Self-Aware Networks*. West Sussex, England: John Wiley & Sons, 2007.

[14] FCC-03-289, "Establishment of an interference temperature metric to quantify and manage interference and to expand available unlicensed operation in certain fixed, mobile and satellite frequency bands," Federal Communications Commission, Tech. Rep., Nov. 2003.

[15] P. J. Kolodzy, "Interference temperature: a metric for dynamic spectrum utilization," *International Journal of Network Management*, vol. 16, no. 2, pp. 103–113, Mar. 2006.

[16] Q. Zhao and B. Sadler, "A survey of dynamic spectrum access," *IEEE Signal Processing Magazine*, vol. 24, no. 3, pp. 79 –89, May 2007.

[17] J. P. de Vries and K. A. Sieh, "Reception-oriented radio rights: Increasing the value of wireless by explicitly defining and delegating radio operating rights," *Telecommunications Policy*, vol. 36, no. 7, pp. 522–530, Aug. 2012.

[18] T. Maseng and T. Ulversøy, "Dynamic frequency broker and cognitive radio," in *The IET Seminar on Cognitive Radio and Software Defined Radios: Technologies and Techniques*, 2008.

[19] S. Srinivasa and S. Jafar, "The throughput potential of cognitive radio: A theoretical perspective," in *40th Asilomar Conference on Signals, Systems and Computers (ACSSC '06)*, Nov. 2006, pp. 221–225.

[20] S. Pollin, "Coexistence and dynamic sharing in cognitive radio networks," in *Cognitive Wireless Communication Networks*, E. Hossain and V. Bhargava, Eds. New York, USA: Springer, 2007.

[21] Y. Li and A. Nosratinia, "Hybrid opportunistic scheduling in cognitive radio networks," *IEEE Transactions on Wireless Communications*, vol. 11, no. 1, pp. 328 –337, Jan. 2012.

[22] M. Gastpar, "On capacity under receive and spatial spectrum-sharing constraints," *IEEE Transactions on Information Theory*, vol. 53, no. 2, pp. 471–487, Feb. 2007.

[23] A. Goldsmith, S. A. Jafar, I. Maric, and S. Srinivasa, "Breaking Spectrum Gridlock With Cognitive Radios: An Information Theoretic Perspective," *Proceedings of the IEEE*, vol. 97, no. 5, pp. 894–914, May 2009.

[24] R. Zhang and Y. Liang, "Exploiting Multi-Antennas for opportunistic spectrum sharing in cognitive radio networks," *IEEE Journal of Selected Topics in Signal Processing*, vol. 2, no. 1, pp. 88 –102, Feb. 2008.

[25] I. Maric, R. D. Yates, and G. Kramer, "Capacity of interference channels with partial transmitter cooperation," *IEEE Transactions on Information Theory*, vol. 53, no. 10, pp. 3536–3548, Oct. 2007.

[26] W. Wu, S. Vishwanath, and A. Arapostathis, "Capacity of a class of cognitive radio channels: Interference channels with degraded message sets," *IEEE Transactions on Information Theory*, vol. 53, no. 11, pp. 4391 –4399, Nov. 2007.

[27] S. Rini, D. Tuninetti, and N. Devroye, "Inner and outer bounds for the gaussian cognitive interference channel and new capacity results," *IEEE Transactions on Information Theory*, vol. 58, no. 2, pp. 820 –848, Feb. 2012.

[28] C. Stevenson, G. Chouinard, Z. Lei, W. Hu, S. Shellhammer, and W. Caldwell, "IEEE 802.22: The first cognitive radio wireless regional area network standard," *IEEE Communications Magazine*, vol. 47, no. 1, Jan. 2009.

[29] S. Mishra, R. Tandra, and A. Sahai, "Coexistence with primary users of different scales," in *Proceedings of the 2nd IEEE International Symposium on New Frontiers in Dynamic Spectrum Access Networks (DySPAN)*, Apr. 2007, pp. 158 –167.

[30] N. Sai Shankar, "Efficiency and coexistence strategies for cognitive radio," in *Cognitive Radio, Software Defined Radio, and Adaptive Wireless Systems*, H. Arslan, Ed. Dordrecht, The Netherlands: Springer, 2007, pp. 189–234.

[31] O. Bakr, M. Johnson, B. Wild, and K. Ramchandran, "A Multi-Antenna framework for spectrum reuse based on Primary-Secondary cooperation," in *Proceedings of the 3rd IEEE International Symposium on New Frontiers in Dynamic Spectrum Access Networks (DySPAN)*, Oct. 2008, pp. 1 – 5.

[32] P. Popovski, H. Yomo, K. Nishimori, R. Di Taranto, and R. Prasad, "Opportunistic interference cancellation in cognitive radio systems," in *Proceedings of the 2nd*

IEEE International Symposium on New Frontiers in Dynamic Spectrum Access Networks (DySPAN), Apr. 2007, pp. 472 – 475.

[33] Z. Hasan, G. Bansal, E. Hossain, and V. Bhargava, "Energy-efficient power allocation in OFDM-based cognitive radio systems: A risk-return model," *IEEE Transactions on Wireless Communications*, vol. 8, no. 12, pp. 6078 –6088, Dec. 2009.

[34] G. Bansal, M. Hossain, and V. Bhargava, "Optimal and suboptimal power allocation schemes for OFDM-based cognitive radio systems," *IEEE Transactions on Wireless Communications*, vol. 7, no. 11, pp. 4710 –4718, Nov. 2008.

[35] W. Ren, Q. Zhao, and A. Swami, "Power control in cognitive radio networks: How to cross a Multi-Lane highway," *IEEE Journal on Selected Areas in Communications*, vol. 27, no. 7, pp. 1283 –1296, Sep. 2009.

[36] F. Wang and W. Wang, "Sum rate optimization in interference channel of cognitive radio network," in *Proceedings of the IEEE International Conference on Communications (ICC)*, May 2010, pp. 1 –5.

[37] M. Hong and A. Garcia, "Equilibrium pricing of interference in cognitive radio networks," *IEEE Transactions on Signal Processing*, vol. 59, no. 12, pp. 6058 –6072, Dec. 2011.

[38] G. Scutari, D. Palomar, F. Facchinei, and J. Pang, "Monotone games for cognitive radio systems," in *Distributed Decision Making and Control*, ser. Lecture Notes in Control and Information Sciences, R. Johansson and A. Rantzer, Eds. Springer Berlin / Heidelberg, 2012, vol. 417, pp. 83 – 112.

[39] Y. Han, A. Pandharipande, and S. Ting, "Cooperative decode-and-forward relaying for secondary spectrum access," *IEEE Transactions on Wireless Communications,*, vol. 8, no. 10, pp. 4945 – 4950, Oct. 2009.

[40] E. Shin and D. Kim, "Time and power allocation for collaborative Primary-Secondary transmission using superposition coding," *IEEE Communications Letters*, vol. 15, no. 2, pp. 196 – 198, Feb. 2011.

[41] T. Kim and D. Kim, "Cooperative primary-secondary transmission using superposition coding and successive interference cancellation," in *Proceedings of the International Conference on Computing, Networking and Communications (ICNC), 2012*, Feb. 2012, pp. 277 – 281.

[42] M. Costa, "Writing on dirty paper (Corresp.)," *IEEE Transactions on Information Theory*, vol. 29, no. 3, pp. 439 – 441, May 1983.

[43] M. Uppal, G. Yue, Y. Xin, X. Wang, and Z. Xiong, "A Multi-Level design for Dirty-Paper coding with applications to the cognitive radio channel," in *Proceedings of IEEE Global Telecommunications Conference (GLOBECOM), 2011*, Dec. 2011, pp. 1 – 5.

[44] V. Cadambe and S. Jafar, "Interference alignment and degrees of freedom of the K-user interference channel," *IEEE Transactions on Information Theory*, vol. 54, no. 8, pp. 3425 – 3441, Aug. 2008.

[45] M. A. Maddah-Ali, S. A. Motahari, and A. K. Khandani, "Communication over MIMO X channels: Signaling and performance analysis," University of Waterloo, Tech. Rep. UW-ECE-2006-27, 2006.

[46] M. Maddah-Ali, A. Motahari, and A. Khandani, "Communication over MIMO X channels: Interference alignment, decomposition, and performance analysis," *IEEE Transactions on Information Theory*, vol. 54, no. 8, pp. 3457 –3470, Aug. 2008.

[47] S. Perlaza, N. Fawaz, S. Lasaulce, and M. Debbah, "From spectrum pooling to space pooling: Opportunistic interference alignment in MIMO cognitive networks," *IEEE Transactions on Signal Processing*, vol. 58, no. 7, pp. 3728 –3741, July 2010.

[48] C. Shen and M. Fitz, "Opportunistic spatial orthogonalization and its application in fading cognitive radio networks," *IEEE Journal of Selected Topics in Signal Processing*, vol. 5, no. 1, pp. 182 –189, Feb. 2011.

[49] M. Amir, A. El-Keyi, and M. Nafie, "Constrained interference alignment and the spatial degrees of freedom of MIMO cognitive networks." *IEEE Transactions on Information Theory*, vol. 57, no. 5, pp. 2994 – 3004, 2011.

[50] S. A. Jafar, "Blind Interference Alignment" *IEEE Journal of Selected Topics in Signal Processing*, vol. 6, no. 3, pp. 216–227, Jun. 2012.

[51] A. Ghasemi and E. Sousa, "Spectrum sensing in cognitive radio networks: requirements, challenges and design trade-offs," *IEEE Communications Magazine*, vol. 46, no. 4, pp. 32 – 39, Apr. 2008.

[52] Y. Zeng and Y.-c. Liang, "Eigenvalue-based spectrum sensing algorithms for cognitive radio," *IEEE Transactions on Communications,*, vol. 57, no. 6, pp. 1784 – 1793, Jun. 2009.

[53] J. Meng, W. Yin, H. Li, E. Hossain, and Z. Han, "Collaborative spectrum sensing from sparse observations in cognitive radio networks," *IEEE Journal on Selected Areas in Communications,*, vol. 29, no. 2, pp. 327 – 337, Feb. 2011.

[54] A. Ghasemi, "Statistical characterization of interference in cognitive radio networks," in *Proceedings of the IEEE 19th International Symposium on Personal, Indoor and Mobile Radio Communications (PIMRC)*, sept. 2008, pp. 1 – 6.

[55] A. Rabbachin, T. Q. S. Quek, H. Shin, and M. Z. Win, "Cognitive network interference," *IEEE Journal on Selected Areas in Communications*, vol. 29, no. 2, pp. 480 – 493, Feb. 2011.

[56] M. Wellens and P. Mähönen, "Lessons learned from an extensive spectrum occupancy measurement campaign and a stochastic duty cycle model," *Mobile Networks and Applications*, vol. 15, no. 3, pp. 461 – 474, Jun. 2010.

[57] J. G. Andrews, R. K. Ganti, M. Haenggi, N. Jindal, and S. Weber, "A primer on spatial modeling and analysis in wireless networks," *IEEE Communications Magazine*, vol. 58, no. 11, pp. 2 – 9, Nov. 2010.

[58] B. Canberk, I. Akyildiz, and S. Oktug, "Primary user activity modeling using first-difference filter clustering and correlation in cognitive radio networks," *IEEE/ACM Transactions on Networking*, vol. 19, no. 1, pp. 170 – 183, Feb. 2011.

[59] S. Srinivasa and M. Haenggi, "Modeling interference in finite uniformly random networks," in *Proceedings of International Workshop on Information Theory for Sensor Networks (WITS 2007)*, Santa Fe, New Mexico, USA, June 2007.

[60] H. de Lima Carlos, M. Bennis, K. Ghaboosi, and M. Latva-aho, "On interference analysis of self-organized femtocells in indoor deployment," in *IEEE GLOBECOM 2010 Workshop on Femtocell Networks*, Miami, Florida, USA, Dec. 2010, pp. 659 – 663.

[61] R. Zhang, Y.-c. Liang, and S. Cui, "Dynamic resource allocation in cognitive radio networks," *IEEE Signal Processing Magazine*, vol. 27, no. 3, pp. 102 – 114, May 2010.

[62] M. Khoshkholgh, K. Navaie, and H. Yanikomeroglu, "Access strategies for spectrum sharing in fading environment: Overlay, underlay, and mixed," *IEEE Transactions on Mobile Computing*, vol. 9, no. 12, pp. 1780 – 1793, Dec. 2010.

[63] K. W. Choi, E. Hossain, and D. I. Kim, "Downlink subchannel and power allocation in Multi-Cell OFDMA cognitive radio networks," *IEEE Transactions on Wireless Communications*, vol. 10, no. 7, pp. 2259 – 2271, Jul. 2011.

[64] D. Bharadia, G. Bansal, P. Kaligineedi, and V. Bhargava, "Relay and power allocation schemes for OFDM-Based cognitive radio systems," *IEEE Transactions on Wireless Communications*, vol. 10, no. 9, pp. 2812 –2817, Sep. 2011.

[65] R. Urgaonkar and M. Neely, "Opportunistic scheduling with reliability guarantees in cognitive radio networks," *IEEE Transactions on Mobile Computing*, vol. 8, no. 6, pp. 766 –777, june 2009.

[66] H. Su and X. Zhang, "Cross-Layer based opportunistic MAC protocols for QoS provisionings over cognitive radio wireless networks," *IEEE Journal on Selected Areas in Communications*, vol. 26, no. 1, pp. 118 –129, Jan. 2008.

[67] M. Rashid, M. Hossain, E. Hossain, and V. Bhargava, "Opportunistic spectrum scheduling for multiuser cognitive radio: a queueing analysis," *IEEE Transactions on Wireless Communications*, vol. 8, no. 10, pp. 5259 –5269, Oct. 2009.

[68] J. Liu, W. Chen, Z. Cao, and Y. Zhang, "Cooperative beamforming for cognitive radio networks: A Cross-Layer design," *IEEE Transactions on Communications*, vol. 60, no. 5, pp. 1420 –1431, May 2012.

[69] "Unlicensed operations in the TV broadcast bands, second memorandum opinion and order," FCC 10-174, Sep. 23 2010.

[70] IEEE 802.15 WG on Wireless Personal Area Network (WPAN) Sub Group on Medical Body Area Networks (MBAN). Accessed on June 23, 2012. [Online]. Available: http://www.ieee802.org/15/pub/TG4j.html

[71] SE 43: Cognitive radio systems in white spaces. Accessed on July 02, 2012. [Online]. Available: http://www.cept.org/ecc/groups/ecc/wg-se/se-43

[72] W. Wang, Y. Xu, and M. Khanna, "A survey on the communication architectures in smart grid." *Computer Networks*, vol. 55, no. 15, pp. 3604–3629, Jul. 2011.

[73] J. Wang, M. Ghosh, and K. Challapali, "Emerging cognitive radio applications: A survey," *IEEE Communications Magazine*, vol. 49, no. 3, pp. 74 –81, Mar. 2011.

[74] FCC, "Mobile broadband: The benefits of additional spectrum," OBI tech. report no. 6, Tech. Rep., Oct. 2010.

[75] G. Gür, S. Bayhan, and F. Alagöz, "Cognitive femtocell networks: an overlay architecture for localized dynamic spectrum access [Dynamic spectrum management]," *IEEE Wireless Communications,*, vol. 17, no. 4, pp. 62 –70, Aug. 2010.

[76] S. Ullah, H. Higgins, B. Braem, B. Latre, C. Blondia, I. Moerman, S. Saleem, Z. Rahman, and K. Kwak, "A comprehensive survey of wireless body area networks," *Journal of Medical Systems*, vol. 36, no. 3, pp. 1065–1094, 2012.

[77] G. Gür and F. Alagöz, "Green wireless communications via cognitive dimension: an overview," *IEEE Network*, vol. 25, no. 2, pp. 50 –56, Apr. 2011.

[78] D. B. Čabrić, "Cognitive radios: System design perspective," Ph.D. dissertation, University of California, Berkeley, California, USA, Dec. 2007.

[79] C. Chang, J. Wawrzynek, and R. Brodersen, "BEE2: a high-end reconfigurable computing system," *IEEE Design Test of Computers*, vol. 22, no. 2, pp. 114 – 125, Apr. 2005.

[80] F. Kaltenberger, R. Ghaffar, R. Knopp, H. Anouar, and C. Bonnet, "Design and implementation of a single-frequency mesh network using openairinterface," *EURASIP Journal on Wireless Communications and Networking*, vol. 2010, pp. 19:1–19:12, Apr. 2010. [Online]. Available: http://dx.doi.org/10.1155/2010/719523

[81] P. Sutton, J. Lotze, H. Lahlou, S. Fahmy, K. Nolan, B. Ozgul, T. Rondeau, J. Noguera, and L. Doyle, "Iris: an architecture for cognitive radio networking testbeds," *IEEE Communications Magazine*, vol. 48, no. 9, pp. 114 –122, Sep. 2010.

[82] O. Tonelli, G. Berardinelli, A. Cattoni, T. S£rensen, and P. Mogensen, "Software architecture design for a dynamic spectrum allocation-enabled cognitive radio testbed," in *Proceedings of the European Signal Processing Conference (EUSIPCO)*. Barcelona, Spain: European Association for Signal Processing (EURASIP), Sep. 2011.

[83] C. Stevenson, G. Chouinard, Z. Lei, W. Hu, S. Shellhammer, and W. Caldwell, "Ieee 802.22: The first cognitive radio wireless regional area network standard," *IEEE Communications Magazine*, vol. 47, no. 1, pp. 130 –138, Jan. 2009.

[84] IEEE 802.22 Working Group on Wireless Regional Area Networks. Accessed on July 03, 2012. [Online]. Available: http://www.ieee802.org/22/

[85] A. Ghosh, N. Mangalvedhe, R. Ratasuk, B. Mondal, M. Cudak, E. Visotsky, T. Thomas, J. Andrews, P. Xia, H. Jo, H. Dhillon, and T. Novlan, "Heteroge-

neous cellular networks: From theory to practice," *IEEE Communications Magazine*, vol. 50, no. 6, pp. 54 –64, Jun. 2012.

[86] M. K. Simon and M.-S. Alouini, *Digital Communication over Fading Channels*, 2nd ed. New Jersey, USA: John Wiley & Sons, Dec. 2005.

[87] T. M. Cover and J. A. Thomas, *Elements of Information Theory*, 2nd ed. John Wiley & Sons, Jul. 2006.

[88] M.-S. Alouini and A. J. Goldsmith, "Area spectral efficiency of cellular mobile radio systems," *IEEE Transaction on Vehicular Technology*, vol. 48, no. 4, pp. 1047–1066, Jul. 1999.

[89] N. H. Mahmood, F. Yilmaz, M.-S. Alouini, and G. E. Øien, "Cognitive interference modeling with applications in power and admission control," in *Proceedings of the IEEE International Symposium on Dynamic Spectrum Access Networks (DySPAN 2012)*, Colorado, USA, Oct. 2012.

[90] N. H. Mahmood, F. Yilmaz, M.-S. Alouini, and G. E. Øien, "On the ergodic capacity of legacy systems in the presence of next generation interference," in *8th IEEE International Symposium on Wireless Communication Systems, ISWCS 2011*, Aachen, Germany, November 2011.

[91] N. H. Mahmood, F. Yilmaz, and M.-S. Alouini, "A generalized and parameterized interference model for cognitive radio networks," in *12th IEEE International Workshop on Signal Processing Advances in Wireless Communications (SPAWC '11)*, San Francisco, USA, June 2011.

[92] V. Erceg, L. J. Greenstein, S. Y. Tjandra, S. R. Parkoff, A. Gupta, B. Kulic, A. A. Julius, and R. Bianchi, "An empirically based path loss model for wireless channels in suburban environments," *IEEE Journal on Selected Areas in Communication*, vol. 17, no. 7, pp. 1205–1211, Jul. 1999.

[93] M. C. Walden and F. J. Rowsell, "Urban propagation measurements and statistical path loss model at 3.5 GHz," in *Proceedings of IEEE Antennas and Propagation Society International Symposium*, Hawaii, USA, Jul. 2005, pp. 363–366.

[94] G. Mao, B. Anderson, and B. Fidan, "Path loss exponent estimation for wireless sensor network localization," *Computer Networks*, vol. 51, no. 10, pp. 2467 – 2483, Jul. 2007.

[95] N. H. Mahmood, F. Yilmaz, G. E. Øien, and M.-S. Alouini, "On hybrid cooperation in underlay cognitive radio networks," in *Proceedings of the 46th Asilomar Conference on Signals, Systems and Computers*, California, USA, Nov. 2012.

[96] N. H. Mahmood, G. E. Øien, U. Salim, and L. Lundheim, "A relative rate utility based distributed power allocation algorithm for cognitive radio networks," in *Proceedings of the PIMRC International WDN Workshop on Cooperative and Heterogeneous Cellular Networks*, Sydney, Australia, Sep. 2012.

[97] N. H. Mahmood, G. E. Øien, and M. Brandt-Pearce, "On the impact of Primary User Localization Information on Rate performance of Secondary Systems," in *Proceedings of the Wireless Internet Conference (WICON '10)*, Singapore, Mar. 2010, pp. 1 – 8.

Paper A

Interference Modeling for Heterogeneous Next Generation Wireless Networks - and its Applications

Nurul Huda Mahmood, Ferkan Yilmaz, Mohamed-Slim Alouini and Geir Egil Øien

Submitted to Wiley International Journal on Wireless Communications and Mobile Computing, August 2012.

Partial results of this work have been published in Proceedings of The 12th IEEE International Workshop on Signal Processing Advances in Wireless Communications (SPAWC 2011), San Francisco, USA, June 22-24 2011. pp. 76-80; The Eighth International Symposium on Wireless Communication Systems (ISWCS11), Aachen, Germany, November 5-9 2011. pp. 462-466; and the IEEE Symposium on New Frontiers in Dynamic Spectrum Access Networks (DySPAN 2012), Washington, USA, October 16-19 2012.

Chapter 2

Interference Modeling for Heterogeneous Next Generation Wireless Networks - and its Applications

Nurul Huda Mahmood, Ferkan Yilmaz, Mohamed-Slim Alouini and Geir E. Øien

Abstract - Next generation wireless systems facilitating better utilization of the scarce radio spectrum have emerged as a response to inefficient rigid spectrum assignment policies. These are comprised of intelligent radio nodes that opportunistically operate in the radio spectrum of existing primary systems; yet unwanted interference at the primary receivers is unavoidable. In order to design efficient next generation systems and to minimize their harmful consequences, it is necessary to realize their impact on the performance of primary systems. In this work, a generalized framework for the interference analysis of such a next generation system is presented where the different opportunistic transmitters may transmit with different powers and transmission probabilities. The analysis is built around a model developed for the statistical representation of the interference at the primary receivers, which is then used to evaluate various performance measures of the primary system. Applications of the derived interference model is designing the next generation network system parameters are also demonstrated. Such an approach provides an unified and generalized framework using which a wide range of performance measures can be analyzed. Findings of analytical performance analyses are confirmed through selected computer-based Monte-Carlo simulations.

Keywords – Next generation networks, cognitive radio network, interference model, power allo-

cation scheme.

2.1 Introduction

Recent advances in communication technologies have facilitated the introduction of next generation wireless systems such as Cognitive Radio Networks (CRN) [1, 2], cognitive Wireless Sensor Networks (WSN) [3] or femtocell networks [4]. In a certain CRN setup, namely the *underlay* cognitive radio (CR) model, the secondary users (SU) coexist with the primary users (PU) in the same time-frequency slot by guaranteeing to respect an imposed interference temperature constraint [1]. Similarly in a femtocell network, the femtocell base station (F-BS) operates in the same frequency band of a macrocell network within its operating area [4].

Harmful interference from these next generation opportunistic systems at the legacy or primary receivers is unavoidable in scenarios where different systems simultaneously communicate over a shared radio medium. It is therefore necessary to analyze and properly understand the interworking of these next generation opportunistic interference with the primary systems, in order to design efficient next generation systems, and to minimize their impact on the performance of the primary system.

In this work, we consider a narrowband next generation opportunistic system coexisting with a narrowband primary system in the same geo-spectral location where the transmissions of the opportunistic transmitters (OT) interfere at the primary receiver (PR). The different OTs are considered to be active with different probabilities and are able to transmit with different transmission powers. An unified statistical model for the sum interference power from such a NGwN at a PR located at the cell-centre is derived, and various examples of its applications are demonstrated. The problem studied is important as next generation wireless networks (NGwN) are becoming increasingly heterogeneous due to such co-existence paradigms [5]. Specific examples of the considered setting can be a cognitive radio networks (CRN) opportunistically coexisting with a licensed system, or a femtocell network operating in the presence of a macrocell network.

Due to various factors such as mobility and randomness in possible user locations, the locations of the opportunistic users in a NGwN can be modeled as realizations of random spatial point processes. Such an assumption allows us to analyze the problem in hand using techniques from stochastic geometry and point processes [6, 7]. In most studies of such kind, the network is generally modeled as a spatial Poisson point process (PPP),

mainly due to its analytical tractability [7].

The opportunistic operation of the NGwNs under consideration in this investigation imply that such networks usually operate with a limited number of nodes. For example, constraints in the form of a maximum interference temperature at a PR practically limit the number of SUs that will be able to share the spectrum with a licensed system in a CRN [1]. Similarly F-BS deployed at home or in small businesses serve a limited number subscribers at most [4]. Such a network, with a limited number of nodes randomly distributed across a relatively small area, is better modeled as a Binomial point process (BPP) instead of a PPP [7]. More precisely, a BPP is defined as the random pattern formed by N independent and identically distributed (i.i.d.) random points uniformly distributed inside a bounded region $\mathcal{S}$ [6]. With this argument, the distribution of the OTs in this contribution is modeled as a BPP instead of a PPP.

Prior research has focused on characterizing the interference for and/or analyzing the performance of primary systems in the presence of particular next generation network. Some examples of previous related research include [8–12]. In [9], the distribution of the aggregate interference from cognitive users is statistically modeled using the cumulants of the aggregate interference, and the results are used to approximate the probability of harmfully interfering with a licensed receiver in terms of the sensing capability and density of the CRs, as well as the underlying fading distribution. On a similar note, the outage probability for licensed systems in the presence of CR interferers, where the licensed receiver is protected by a circular prohibited transmission area (termed as guard zone) is analyzed in [10]. In [12], the cognitive network interference power with power control at the SUs is statistically modeled, where the authors approximate the probability density function (PDF) of the interference power by a truncated stable distribution and demonstrate how different metrics evaluating the primary system performance can be computed using the derived interference model.

In all the above works, the statistical representation of the interference is derived by modeling the CRN as a *"Poisson field of interferers"*. Reference [8, 11], on the other hand, consider a BPP model for the network. The analysis in [8] is limited to finding the moment generating function (MGF) of the interference in a WSN as an integral over the fading distribution of the channel, and then numerically finding the cumulants of the interference distribution from the expression for the MGF. In [11], the authors provide an analytical framework for assessing the uplink interference power at the center of an indoor deployment scenario in a femtocell network.

In this work, we analyze the impact of the interference power from a general and nar-

rowband NGwN on the performance of a coexisting narrowband primary system, and investigate its role in designing various secondary system parameters. To evaluate the impact, we first develop a unified statistical model for the aggregate narrowband interference power experienced at the PR. We then demonstrate how the developed interference model can be used to evaluate the performance of the coexisting primary system in terms of different metrics such as outage probabilities and ergodic capacity. Furthermore, we also describe how this model can be used by the NGwN to determine various system parameters such as the transmission power and the number of active transmitters under an imposed interference temperature constraint.

The most important contributions of this work are as follows. First, we present a generalized unified framework to evaluate the impact of the interference power from a narrowband NGwN at the receiver of a coexisting narrowband primary system, where the underlying nodal distribution of the NGwN is modeled as a BPP instead of the commonly considered PPP. Furthermore, power control and admission control at the OTs are also considered. Second, we consider the path loss exponent (PLE) to be a random variable (RV), instead of it being fixed over the coverage area. Empirical studies have reported that even a small cell can have different types of terrain property, such as buildings, trees and open area, resulting in the PLE to vary over the area of a single cell [13–15]. This analysis is important as future wireless networks are becoming increasingly more heterogeneous in which different users belonging to different networks can experience different slow fading effects [5]. Finally, we introduce and adopt a bounded path loss model which overcomes the shortcomings of the commonly used model which limits transmitter receiver separation distance to be greater than unity.

The remainder of this paper is organized as follows. The system model is elaborated in Section 5.2. Statistical representation of the generalized interference model is presented in Section 2.3, and 2.5. Various applications of the derived interference model are demonstrated in Sections 2.4 and 2.6, which are then numerically validated in Section 4.5. Finally, Section 5.5 concludes the paper.

2.2 System Model

We consider a NGwN with N active interfering transmitters uniformly distributed across an annular ring shaped cell $\mathcal{S}$ of outer radius B and inner radius A, in the two-dimensional plane $\mathbb{R}^2$. The interfered PR is located at the origin of the cell, and is communicating with an transmitter that is stationary at a location known to all the terminals. It can either be

a primary base station in the downlink direction of the primary system, or a primary user equipment communicating with the base station in the uplink direction. Information about the location of the communicating transmitter is generally readily available. Otherwise such information is easy to obtain by a one-time location update through cooperation among the terminals [18]. The considered setting is general enough to describe a cellular as well as an ad-hoc scenario for the NGwN.

Generalized Bounded Path Loss Model

In the next generation networks described in Section 5.1, the opportunistic transmitter location is independent of that of the PRs, and can be arbitrarily close to it. Thus, the generally used unbounded path loss model ($\beta(r) = r^{-\alpha}$), where r is the transmit-receiver separation distance in meters and α is the PLE, results in an amplification of the transmitted signal for $r < 1$ and has a singularity at $r = 0$. This leads to *"significant deviations from a realistic performance"* [19]. To overcome this limitation, Inaltekin *et. al.* proposed the distance dependent bounded path loss model defined in [19] as $\beta(r) = (1+r)^{-\alpha}$. In the context of the NGwNs described earlier, we consider a generalized scenario for the path loss experienced by interference signal, where the OT and the PR can be arbitrarily close to each other. To represent this, we denote the minimum possible physical transmitter-receiver separation to be $1-\varepsilon$, where ε is any real positive number, such that $\varepsilon \leq 1$ (thus, the inner radius of $\mathcal{S}$ is $A = 1-\varepsilon$). With this minimum transmitter-receiver separation distance, we introduce the *generalized bounded path loss model* defined for $r > (1-\varepsilon)$ as

$$\beta(r) \triangleq (\varepsilon + r)^{-\alpha}. \tag{2.1}$$

It is easily observed that (2.1) satisfies the following required properties of a bounded path loss model outlined in [19]:
Boundedness: $\beta(r)$ approaches 1 as r approaches $1-\varepsilon$; *decay rate:* $\beta(r)$ approaches $r^{-\alpha}$ as r approaches $+\infty$; and *smoothness:* $\beta(r)$ is a monotonously decreasing function of r and is differentiable everywhere.

Interference Power Representation

Under a narrowband assumption, the interference power at the PR from a given OT is given by $I = p\,g\,\beta(r)$, where p is the transmission power and g is the composite fast and slow statistical variation of the channel. The composite fading power gain is modeled by

a Gamma/Log-normal distribution [20, 21], and the path loss model is as given in (2.1) with r being a realization of the RV $\mathcal{R}$ representing the Euclidean distances between the OT and the PR. Considering uniform distribution of a user for $A \leq r \leq B$, the PDF of $\mathcal{R}$ is given by [6]

$$f_{\mathcal{R}}(r) = \frac{2r}{B^2 - A^2}. \tag{2.2}$$

The PLE α is also considered a RV. Based on the data presented in [14] and [15], we model the PDF of α as a Gamma distribution shifted by 2 (i.e. $\alpha = \xi + 2$, where ξ is Gamma distributed). However, our analysis is equally valid for other possible discrete or continuous, empirically or mathematically-derived probability distribution models for the PLE.

2.3 Statistical Representation of the Interference Power from a Single OT

Let us first consider interference from a single OT randomly located in $\mathcal{S}$ with transmit power p_1, and let the interference power from this OT at the PR be $I_1 = p_1 g \hat{r}$, where $\hat{r} \triangleq (\varepsilon + r)^{-\alpha}$. Defining the MGF to be a function of the complex variable s with a negative argument, the MGF of I_1 is given by $\mathcal{M}_{I_1}(s; A, B, p_1) = \int\int\int e^{-s p_1 g \hat{r}} f_G(g) dg\, f_{\hat{r}}(\hat{r}) d\hat{r}\, f_\alpha(\alpha) d\alpha$, where $f_G(g)$, $f_{\hat{r}}(\hat{r})$ and $f_\alpha(\alpha)$ are respectively the distributions of the composite fading power gain, the changed variable $\hat{r}$ and the PLE α.

The PDF of the Gamma/Log-normal composite fading distribution is given by [20, eq. 2.57]

$$f_G(g) = \int_0^\infty \frac{m^m g^{m-1}}{w^m \Gamma(m)} \exp\left(-\frac{m g}{w}\right) \frac{\psi}{\sqrt{2\pi}\sigma w} \exp\left[-\frac{(10\log_{10} w - \mu)^2}{2\sigma^2}\right] dw, \tag{2.3}$$

where $\psi = 10/\ln 10$, μ (dB) and σ (dB) are the mean and the standard deviation (SD) of the underlying Log-normal shadow fading distribution, and m is the fading-parameter of the underlying Gamma distribution. Using (2.2), the definition of the MGF given above and conditional expectations, the MGF of the interference power from the considered

single OT can be readily expressed as

$$\begin{aligned}\mathcal{M}_{I_1}(s) &= \mathbb{E}\left[\mathcal{M}_{I_1}(s|\alpha)\right] \\ &= \mathbb{E}\left[\frac{2/\alpha}{B^2-A^2}\int_{\frac{1}{(\varepsilon+B)^{\alpha}}}^{\frac{1}{(\varepsilon+A)^{\alpha}}}\frac{\hat{r}^{-1}\mathcal{M}_g(sp_1\hat{r})}{\left(\hat{r}^{\frac{-2}{\alpha}}-\varepsilon\hat{r}^{\frac{-1}{\alpha}}\right)^{-1}}d\hat{r}\right], \end{aligned} \tag{2.4}$$

where $\mathcal{M}_g(s)$ is the MGF of the composite Gamma/Log-normal fading given by [20, eq. 2.58] as

$$\mathcal{M}_g(s) \simeq \frac{1}{\sqrt{\pi}}\sum_{n=1}^{N_p} H_{x_n}\left(1+\frac{10^{\left(\sqrt{2}\sigma x_n+\mu\right)/10}s}{m}\right)^{-m}, \tag{2.5}$$

with x_n and H_{x_n} respectively being the n^{th} root and the n^{th} weight factor of the N_p-order Hermite polynomial and are given by Abramowitz and Stegun [22, Table (25.10)]. The above approximation is highly accurate when the order of the Hermite polynomial, $N_p \geq 20$. Let us further define the constants, $\{k_n\}_{n=1}^{N_p}$ as $k_n \triangleq 10^{\left(\sqrt{2}\sigma x_n+\mu\right)/10}$. We can therefore rewrite the MGF conditioned on the PLE α, $\mathcal{M}_{I_1}(s|\alpha)$, given in (2.4) as

$$\mathcal{M}_{I_1}(s|\alpha) = \frac{2}{\alpha\sqrt{\pi}}\sum_{n=1}^{N_p}\frac{H_{x_n}\left(\Phi_{I_n}^{(1)}(s|\alpha)-\Phi_{I_n}^{(2)}(s|\alpha)\right)}{B^2-A^2}, \tag{2.6}$$

where $\Phi_{I_n}^{(1)}(s|\alpha)$, and $\Phi_{I_n}^{(2)}(s|\alpha)$ are respectively given by

$$\Phi_{I_n}^{(1)}(s|\alpha) = \int_{(\varepsilon+B)^{-\alpha}}^{(\varepsilon+A)^{-\alpha}}\left(1+\frac{s\,p_1\,k_n\,\hat{r}}{m}\right)^{-m}\hat{r}^{-\frac{2}{\alpha}-1}\,d\hat{r},$$

$$\Phi_{I_n}^{(2)}(s|\alpha) = \int_{(\varepsilon+B)^{-\alpha}}^{(\varepsilon+A)^{-\alpha}}\varepsilon\left(1+\frac{s\,p_1\,k_n\,\hat{r}}{m}\right)^{-m}\hat{r}^{-\frac{1}{\alpha}-1}\,d\hat{r}.$$

After some algebraic manipulations, the first integration $\left(\Phi_{I_n}^{(1)}(s|\alpha)\right)$ can be reduced in closed form to

$$\begin{aligned}\Phi_{I_n}^{(1)}(s|\alpha) &= e^{-j\pi\left(\frac{2}{\alpha}+m\right)}\left(\frac{k_n s p_1}{m}\right)^{\frac{2}{\alpha}}\times \\ &\quad \mathrm{B}\left(-\frac{m(\varepsilon+A)^{\alpha}}{k_n s p_1},-\frac{m(\varepsilon+B)^{\alpha}}{k_n s p_1};\frac{2}{\alpha}+m,1-m\right), \end{aligned} \tag{2.7}$$

where $j=\sqrt{-1}$ is the imaginary unit and $\mathrm{B}(z1,z2;a,b)$ is the generalized incomplete

Beta function defined as the difference of two incomplete Beta functions, i.e. $\mathrm{B}(z1,z2;a,b) = \mathrm{B}(z1;a,b) - \mathrm{B}(z2;a,b)$ [23]. The incomplete Beta function $\mathrm{B}(z;a,b)$ is defined in [22, eq. 6.6.1] as $\mathrm{B}(z;a,b) \triangleq \int_0^z t^{a-1}(1-t)^{b-1}dt$. The Beta function is a special mathematical function whose functional implementation is readily available in most mathematical software packages such as Matlab, Mathematica and Maple. Its derivatives with respect to (w.r.t.) the different variables are also well defined.

Following similar steps, we can reduce the second integration $\left(\Phi_{I_n}^{(2)}(s|\alpha)\right)$ in closed form to

$$\begin{aligned}\Phi_{I_n}^{(2)}(s|\alpha) &= \varepsilon e^{-j\pi\left(\frac{1}{\alpha}+m\right)}\left(\frac{k_n s p_1}{m}\right)^{\frac{1}{\alpha}} \times \\ &\quad \mathrm{B}\left(-\frac{m(\varepsilon+A)^{\alpha}}{k_n s p_1}, -\frac{m(\varepsilon+B)^{\alpha}}{k_n s p_1}; \frac{1}{\alpha}+m, 1-m\right). \end{aligned} \tag{2.8}$$

The final expression for the conditional MGF of a single user interference power at the PR is then obtained by plugging the closed-form expressions given in (2.7) and (2.8) into (2.6) above, and is thereafter given by

$$\begin{aligned}\mathcal{M}_{I_1}(s|\alpha) = \frac{2}{B^2-A^2}\sum_{n=1}^{N_p}\frac{H_{x_n}}{\alpha\sqrt{\pi}}\Bigg\{ &\frac{\mathrm{B}\left(-\frac{m(\varepsilon+A)^{\alpha}}{k_n s p_1}, -\frac{m(\varepsilon+B)^{\alpha}}{k_n s p_1}; \frac{2}{\alpha}+m, 1-m\right)}{\exp\left\{j\pi\left(\frac{2}{\alpha}+m\right)\right\}\left(\frac{k_n s p_1}{m}\right)^{-2/\alpha}} - \\ &\frac{\mathrm{B}\left(-\frac{m(\varepsilon+A)^{\alpha}}{k_n s p_1}, -\frac{m(\varepsilon+B)^{\alpha}}{k_n s p_1}; \frac{1}{\alpha}+m, 1-m\right)}{\varepsilon^{-1}\exp\left\{j\pi\left(\frac{1}{\alpha}+m\right)\right\}\left(\frac{k_n s p_1}{m}\right)^{-1/\alpha}}\Bigg\}. \end{aligned} \tag{2.9}$$

Final MGF of Single User Interference Power

Having obtained the interference power MGF conditioned on the PLE α, we now evaluate the expectation over α in (2.4) in order to obtain the unconditioned MGF of the single user interference power.

The final expectation over α in (2.4) requires a cumbersome integration of (2.9) over a shifted Gamma distribution. To obtain results in a simple and compact form, we can instead approximate this integration by evaluating it numerically. In this contribution, the numerical integration is carried out by first truncating the PDF of the PLE in order to contain its infinite support to a finite range. Only the parts of the PDF that has negligible probability distribution are truncated. The expectation over the PLE is then evaluated by approximating the integration as a weighted sum, where the weight coefficients w_q

and the abcissas α_q are obtained using the extended Trapeziodal rule outlined in [22, eq. 25.4.2]. The number of terms n_q is chosen sufficiently large so as to make the error term negligible. Moreover, due to this numerical integration approach, the results of this work remain valid for any other underlying analytical or empirically derived distribution of the PLE.

With this numerical integration approach, the expectation over α in (2.4) can now be expressed as a weighted sum of (2.9). More precisely the closed form expression for the MGF of the single user interference power at the PR is derived in closed form as

$$\begin{aligned}\mathcal{M}_{I_1}(s;A,B,p_1) &= \frac{2}{B^2-A^2}\sum_{q=1}^{n_q}\frac{w_q}{\alpha_q\sqrt{\pi}}\sum_{n=1}^{N_p}H_{x_n}\times \\ &\left\{\frac{\mathrm{B}\left(-\frac{m(\varepsilon+A)^{\alpha_q}}{k_n s p_1},-\frac{m(\varepsilon+B)^{\alpha_q}}{k_n s p_1};\frac{2}{\alpha_q}+m,1-m\right)}{\exp\left[j\pi\left(\frac{2}{\alpha_q}+m\right)\right]\left(\frac{k_n s p_1}{m}\right)^{\frac{-2}{\alpha_q}}}-\right. \\ &\left.\frac{\mathrm{B}\left(-\frac{m(\varepsilon+A)^{\alpha_q}}{k_n s p_1},-\frac{m(\varepsilon+B)^{\alpha_q}}{k_n s p_1};\frac{1}{\alpha_q}+m,1-m\right)}{\varepsilon^{-1}\exp\left[j\pi\left(\frac{1}{\alpha_q}+m\right)\right]\left(\frac{k_n s p_1}{m}\right)^{\frac{-1}{\alpha_q}}}\right\}. \end{aligned} \tag{2.10}$$

2.4 Applications of the Interference Model in the NGwN System Parameter Design

The interference power MGF derived in the previous section provides a robust tool that can be used in a number of ways in evaluating the primary system performance as well as designing various NGwN system parameters. In order to get an insight into its practical appeal and as an illustrative example, in this section we demonstrate how the derived interference model can be used to calculate the mean interference power at the PR from a single OT averaged over all the possible user locations in the region $\mathcal{S}$. By the relation between the MGF of a RV and its mean, the mean interference power $\bar{I}_1(p_1,A,B)$ is given by

$$\bar{I}_1(p_1,A,B) = -\frac{\partial}{\partial s}\mathcal{M}_{I_1}(s;A,B,p_1)\Big|_{s=0}. \tag{2.11}$$

For the want of space, we have omitted the lengthy but relatively straight-forward derivation of $\bar{I}_1(p_1,A,B)$, which involves expressing the incomplete Beta function in terms of the Gauss-Hypergeometric function using [22, eq. 6.6.8], some algebraic manipulations

and then differentiating the Gauss-Hypergeometric function w.r.t. s using [22, eq. 15.2.1]. The final expression for the single user mean interference power at the PR is derived as

$$\bar{I}_1(p_1,A,B) = \frac{2p_1\sum_{n=1}^{L} H_{x_n}k_n}{\sqrt{\pi}(B^2-A^2)} \times \left\{ \frac{\varepsilon\left((\varepsilon+B)^{1-\alpha}-(\varepsilon+A)^{1-\alpha}\right)}{\alpha-1} - \frac{(\varepsilon+B)^{2-\alpha}-(\varepsilon+A)^{2-\alpha}}{\alpha-2} \right\}. \quad (2.12)$$

Applications of the above derived expression for the mean interference power in various NGwN system parameter design are detailed in Section 2.6.

2.5 MGF of the Sum Interference Power

In this section, we build on the single user interference power MGF obtained earlier to derive the MGF of the sum interference power from the N OTs uniformly distributed in $\mathcal{S}$ around the PR, where each OT may possibly transmit with different transmission probabilities and different transmission powers. This is motivated by the fact that power decays rapidly with distance and hence a receiver is most affected by the interference power from the users that are close to it [12]. Thus, giving higher chance to the OTs that are further away from the PR to transmit, may result in more efficient utilization of the limited radio resource in a CRN. Imposing a *guard zone* around the PR is an example of this principle in practice, wherein only the OTs that further than a given distance to the PR are allowed to transmit [10].

Let the entire cell under investigation be divided into J disjoint sub-regions of annular rings $\mathcal{S}_j$ such that $\mathcal{S}_1 \cup \cdots \cup \mathcal{S}_J = \mathcal{S}$ as shown in Fig. 2.1. Furthermore, let the outer and the inner radius of each sub-region be given by R_{j-1} and R_j respectively, and with $R_0 = B$ and $R_J = A$. With such a division of the entire cell, the OTs in the different sub-regions can be prioritized differently, possibly depending on the radius of the sub-region in which the OTs are located. Let the probability of transmission from the sub-region $\mathcal{S}_j$ be denoted by ρ_j. The MGF, $\mathcal{M}_{I_{\mathcal{S}}^J}(s)$, of the sum interference power from the N interferers uniformly distributed across the entire cell, where each OT may transmit with different transmission probabilities, is derived in this section.

MGF of the Interference Power from the Sub-region $\mathcal{S}_j$

To derive the MGF of the sum interference power from the entire region, let us first focus on a specific sub-region $\mathcal{S}_j$. Let the number of OTs in this region be k_j, where each OT can be active with probability ρ_j ($0 \leq \rho_j \leq 1$) and transmission power p_j independently of the other interferers. Let the sum interference power from the k_j interferers in this case be denoted by $I_{\mathcal{S}_j}^{k_j}$. Given this setting, let Λ denote the RV representing the number of active OTs and its realization be given by λ, where $\lambda \in \{0, 1, \ldots, k_j\}$. Due to the properties of the adopted BPP model, the probability distribution of Λ is by definition binomial, and is given by $f_\Lambda(\lambda) = \binom{k_j}{\lambda} \rho^\lambda (1-\rho)^{k_j - \lambda}$ [6].

By the independence assumption among the interference from the different OTs, the MGF of the sum interference power from k active (out of the k_j available) interferers is straightforwardly given by $\mathcal{M}_{I_{S_j|k}}(s) = \left(\mathcal{M}_{I_1}(s; R_j, R_{j-1}, p_j)\right)^k$. The MGF $\mathcal{M}_{I_{S_j}}^{k_j}(s)$ of the total interference power $I_{\mathcal{S}_j}^{k_j}$ may be evaluated using conditional probability as $\mathcal{M}_{I_{S_j}}(s|k_j) = \mathbb{E}_k\left[\mathcal{M}_{I_{S_j|k}}(s)\right]$. Using the law of total probability, this MGF is given by $\mathcal{M}_{I_{S_j}}(s|k_j) = \sum_{k=0}^{k_j} f_\Lambda(k) \mathcal{M}_{I_{S_j|k}}(s)$. After some algebraic manipulations, the final expression for $\mathcal{M}_{I_{S_j}}(s|k_j)$ is given as

$$\mathcal{M}_{I_{S_j}}(s|k_j) = \left(1 + \rho_j \left[\mathcal{M}_{I_1}(s; R_j, R_{j-1}, p_j) - 1\right]\right)^{k_j}, \tag{2.13}$$

where $\mathcal{M}_{I_1}(s; R_j, R_{j-1}, p_j)$ is given by (2.10).

PDF of the Interferer Distribution

Next, let us look at the distribution of the different interfering OTs across the entire cell. Under the uniform distribution assumption, the probability that any given OT lies in the sub-region $\mathcal{S}_j$ is given by $\tau_j = \frac{\nu(\mathcal{S}_j)}{\nu(\mathcal{S})}$, where $\nu(\mathcal{A})$ is the area of $\mathcal{A}$ [6]. Let K_j denote the RV representing the number of interferers in $\mathcal{S}_j \; \forall j \in \{1, 2, \ldots, J\}$. It can be observed that, by construction, the joint distribution of each RV K_j taking the value k_j, such that $\sum_j k_j = N$, is given by the multinomial probability distribution [6]

$$f_{K_1,\ldots,K_J}(k_1, \ldots, k_J) = \frac{N!}{k_1! k_2! \ldots k_J!} \tau_1^{k_1} \tau_2^{k_2} \ldots \tau_J^{k_J}. \tag{2.14}$$

MGF of the Sum Interference Power

Let $\mathcal{M}_{I_S^J}(s)$ be the MGF of the sum interference power from the N interferers uniformly distributed across the entire cell as described above. Using the law of total probability, $\mathcal{M}_{I_S^J}(s)$ is given by $\mathcal{M}_{I_S^J}(s) = \mathbb{E}[\mathcal{M}_{I_{S_1}}(s|k_1)\mathcal{M}_{I_{S_2}}(s|k_2)\ldots\mathcal{M}_{I_{S_J}}(s|k_J)]$, where the $J-1$ fold expectation is over the RVs $K_1, K_2, \ldots, K_{J-1}$[1], whose joint distribution is given by (2.14). Using (2.13) and (2.14), the above expectation can be expressed as $\mathcal{M}_{I_S^J}(s) = \sum_{k_1=0}^{N}\sum_{k_2=0}^{N-k_1}\cdots\sum_{k_{J-1}=0}^{N-\sum_{j=1}^{J-2}k_j}\frac{N!}{k_1!k_2!\ldots k_J!}\times\left(\tau_1\mathcal{M}_{I_{S_1}}(s|1)\right)^{k_1}\left(\tau_2\mathcal{M}_{I_{S_2}}(s|1)\right)^{k_2}\cdots\left(\tau_J\mathcal{M}_{I_{S_J}}(s|1)\right)^{k_{J-1}}$, where $\mathcal{M}_{I_{S_J}}(s|1)$ is as given by (2.13).

Finally, after some algebraic manipulations, this sum can be succinctly expressed as

$$\mathcal{M}_{I_S^J}(s) = \left(\tau_1\mathcal{M}_{I_{S_1}}(s|1) + \tau_2\mathcal{M}_{I_{S_2}}(s|1) + \cdots + \tau_J\mathcal{M}_{I_{S_J}}(s|1)\right)^N. \tag{2.15}$$

2.6 Applications of the Derived Interference Model

Application of the derived interference power MGF in evaluating various secondary system parameters is demonstrated in Section 2.4. In this section, we continue that discussion further by presenting examples of how the derived sum interference power MGF can be used to design a simple, yet robust and completely distributed power allocation algorithm for the OTs. Applications of the sum interference power MGF in the performance evaluation of the primary system in terms of various performance metrics such as outage probabilities and ergodic capacity, are also shown.

2.6.1 Power Allocation Algorithm for the OTs

Many of the existing power allocation algorithms for different next generation systems assume perfect knowledge of the OT-PR channel [24]. In reality, this may not always be available without active cooperation of the primary system, especially for passive PRs such as TV receivers. However, statistical information about the OT-PR channels can easily be obtained or estimated using well known techniques [25].

Due to the generally imposed interference-temperature constraint at the PR, controlling the interference power from the OTs at a PR is an important task, for which power control

[1] K_J is completely determined by the $J-1$ other RVs: $K_J = N - \sum_{j=1}^{J-1} K_j$.

at the OTs plays an important role [26]. In this part, we demonstrate how the derived sum interference power MGF can be used to allocate the transmission powers of the OTs under an average interference temperature constraint Q. Following (2.11), the mean interference power $\bar{I}_S$ from the N OTs uniformly distributed across the different regions of the entire cell, with different transmission probabilities for each sub-region, can be obtained from the MGF of the sum interference power given in (2.15). After some algebraic manipulations, the average sum interference power is obtained as

$$\bar{I}_S = N \sum_{j=1}^{J} \tau_j \rho_j \bar{I}_1(p_j, R_j, R_{j-1}), \tag{2.16}$$

where $\bar{I}_1(p_j, R_j, R_{j-1})$ is defined in (2.12).

With this expression for the mean interference power, the transmission powers of the OTs can be chosen such that the mean interference power does not exceed the average interference temperature threshold Q. A very simple yet distributed strategy can be to allow all OTs to transmit with equal power. However, this would mean that a OT which is close to the PR (and hence results in relatively higher interference) transmits with the same power as a OT that is much further away from the PR. To overcome this limitation, we propose two simple power assignment techniques where the transmit powers of the OTs are inversely proportional to the interference they create at the PR.

Power Assignment Technique - I

In the first proposal, let the total interference power constraint be divided such that the interference contribution from each sub-region Q_j is the same, i.e. $Q_j = \frac{Q}{J}, \forall j$.

Power Assignment Technique - II

Alternatively, the total interference power constraint can be distributed among the different regions in proportion to the relative size of each region, so as to better reflect the interference contribution from each region. In such a case, the interference contribution from each sub-region Q_j can be chosen as $Q_j = \tau_j Q$, where τ_j is defined earlier.

Having determined the tolerable interference contributions from each region, the transmit powers of the OTs in each sub-region that would guarantee to meet the region-wise mean

interference constraint Q_j is straightforwardly derived using (2.12) and (2.16) as

$$p_j \leq \frac{\frac{Q_j\sqrt{\pi}\left(R_{j-1}^2-R_j^2\right)}{2N\tau_j\rho_j\varepsilon\sum_{n=1}^{L}H_{x_n}k_n}}{\frac{\tilde{R_{j-1}}^{1-\alpha}-\tilde{R_j}^{1-\alpha}}{\alpha-1}-\frac{\tilde{R_{j-1}}^{2-\alpha}-\tilde{R_j}^{2-\alpha}}{\varepsilon(\alpha-2)}}. \tag{2.17}$$

This is a very simple and yet distributed method of assigning transmission powers at the OTs which neither requires any cooperation among the OTs or with the PR; nor any instantaneous CSI. However, the proposed power allocation strategy does not guarantees any particular performance of the secondary system, and therefore it is more suitable for implementation in simple and low-cost secondary systems with minimal QoS constraints and a distributed network architecture. A particular examples of such a secondary systems can be the information gathering nodes of a cognitive wireless sensor network.

Other Applications

The above-derived MGF can also be used to determine other secondary system parameters. For a given transmit power and under an average interference temperature constraint, the number of active OTs to be allowed in a CRN at any given time (N), or the activity rates of the users in the different sub-regions (ρ_j), can be determined from the expression for $\bar{I}_S$ given in (2.16).

2.6.2 Main Performance Evaluation of the Primary system

The sum interference power MGF derived in Section 2.5 can also be used as a tool to analyze the performance of primary systems in the presence of the interference from the NGwN. This performance can be evaluated using a number of different measures, such as the outage probability, the bit error probability, capacity (ergodic or instantaneous) or the signal-to-interference-plus-noise-ratio (SINR) [20]. In this paper, we illustrate the application of the tools developed in this work in evaluating the outage probability and the ergodic capacity of the primary system in the presence of next generation interference.

Ergodic Capacity of Primary System

The ergodic capacity of a communication system, C_l is a measure of the maximum number of bits that can be successfully received on average by the receiver. Let ϕ denote the power

of the received signal of interest at the PR. Assuming that the primary transmitter (PT) transmits with power $\tilde{p}$ and the fading power gain experienced by the primary signal is given by $\tilde{g}$, ϕ is given by $\phi = \tilde{p}\,\tilde{g}\,(\tilde{\varepsilon}+\tilde{r})^{-\tilde{\alpha}}$, where $\tilde{r}$ and $\tilde{\alpha}$ are the known Euclidean PT-PR distance and the PLE respectively. Under the realistic assumption that $\tilde{r} \gg 1$, the minimum PT-PR separation distance $\tilde{\varepsilon}$ in the above expression approaches zero, and thus $(\tilde{\varepsilon}+\tilde{r})^{-\tilde{\alpha}} \to \tilde{r}^{-\tilde{\alpha}}$. We have earlier observed that the variation in the PLE value is due to the variations in the terrain property at different locations within the cell. Since we assume that the PT and the PR locations are fixed and known, we can readily assume that the PLE for the primary channel is a constant.

The instantaneous capacity of a receiver depends on its instantaneous SINR. In this particular case, the SINR at the PR is given by $\lambda_l = \frac{\phi}{I_S+\mathcal{Z}}$, where $\mathcal{Z}$ is the additive white Gaussian noise (AWGN) power at the receiver. Assuming that Shannon capacity can be achieved at every resource slot, a lower bound on the PR instantaneous capacity conditioned on λ_l is given by the famous Shannon's capacity formula for AWGN channels, $\log_2(1+\lambda_l)$ [27]. The ergodic capacity C_l can be obtained by taking the expectation of this instantaneous capacity over the distribution of the SINR, i.e. $C_l = \mathbb{E}_{\lambda_l}[\log_2(1+\lambda_l)]$. The direct method for calculating this expectation requires a complicated two fold integration over the PDFs of I_S and ϕ, and cannot be solved easily. Instead, we follow the procedures adopted by Hamdi in [28] to evaluate the capacity of transmit diversity over correlated Rayleigh fading. By virtue of the independence assumption of ϕ and I_S, we obtain a simple closed form expression for the ergodic capacity involving the MGF obtained earlier in this paper. This expression, which is given below, involve a single integration that can be easily computed using any available mathematical softwares such as *Mathematica*®, or any other suitable numerical integration technique. The expression for the PR ergodic capacity is given by

$$C_p = \frac{1}{\ln(2)} \int_0^\infty \frac{\mathcal{M}_{I_S}(\frac{s}{\mathcal{Z}})\left(1-\mathcal{M}_\phi(\frac{s}{\mathcal{Z}})\right)}{s} \exp(-s)\, ds, \tag{2.18}$$

where $\mathcal{M}_\phi(s)$ is the MGF of ϕ. The MGF of the commonly used fading models are given in [20].

Interference Outage Probability

Considering the interference temperature constraint, the *interference outage probability*, P^I_{out}, at the PR can be defined as the event that the sum interference power exceeds the threshold Q. Thus, $P^I_{out} = \Pr[I_S > Q] = 1 - F_{I_S}(Q)$, where $F_{I_S}(r)$ is the cumulative distri-

bution function (CDF) of I_S. Using the relationship between the CDF and the MGF, the outage probability can be found from the inverse Laplace transform (ILT) of the derived sum interference power MGF, and is given as [20, eq. 1.6]

$$P_{out}^{I} = 1 - \frac{1}{2\pi j} \oint \frac{\mathcal{M}_{I_S}(s)}{s} \exp(sQ)\, ds. \tag{2.19}$$

SINR Outage Probability

In most practical cases, the probability of outage at a radio receiver depends on the SINR rather than just the interference power itself. To capture this influence, we introduce the *SINR outage probability* P_{out}^{SINR}, which is probability that the SINR at the PR falls below a given threshold, θ_{th}. Following the PR signal model described in Section 2.6.2, the SINR outage probability is given as $P_{out}^{\text{SINR}} = \Pr\left[\frac{\phi}{I_S+\mathcal{Z}} < \theta_{\text{th}}\right] = \Pr[\phi - (I_S+\mathcal{Z})\theta_{\text{th}} < 0]$. By introducing the variable $\zeta = \phi - (I_S+\mathcal{Z})\theta_{\text{th}}$, P_{out}^{SINR} can be written in terms of the CDF of ζ $F_\zeta(\zeta)$, as $P_{out}^{\text{SINR}} = F_\zeta(0)$.

By virtue of the inversion theorem presented in [29], the CDF of an univariate RV X can be obtained from its characteristic function (CF) $\mathcal{C}_X(t)$ as $F_X(x) = \frac{1}{2} - \frac{1}{\pi}\int_0^\infty \frac{\Im\{\exp(-itx)\mathcal{C}_X(t)\}}{t}\, dt$, where $\Im\{\cdot\}$ denotes the imaginary part. Using the fact that the CF of a scaled sum of two independent RVs are the product of their appropriately scaled individual CFs and the relationship between the CF and the MGF of a RV, the CF of ζ is given by $\mathcal{C}_\zeta(t) = \mathcal{C}_\phi(t)\hat{\mathcal{M}}_{I_S}(j\theta_{th}t)$, where $\hat{\mathcal{M}}_{I_S}(s)$ is the MGF of $I_S + \mathcal{Z}$. Using this relation, the SINR outage probability can therefore be obtained in terms of a single integration as

$$P_{out}^{\text{SINR}} = \frac{1}{2} - \frac{1}{\pi}\int_0^\infty \frac{\Im\left\{\mathcal{C}_\phi(t)\hat{\mathcal{M}}_{I_S}(j\theta_{\text{th}}t)\right\}}{t} dt. \tag{2.20}$$

Outage Probability Calculations

For most practical scenarios, it is not easy to evaluate the integrals (3.21) and (2.20) analytically. In this contribution, we have used the Euler summation technique [30] and the inversion theorem [29] by following the procedures outlined in [31, 32] to efficiently evaluate the outage probability expressions given in (3.21) and (2.20) numerically.

2.7 Numerical Results

In this section, we present some selected computer-based numerical Monte-Carlo simulation results to validate and to demonstrate the accuracy of the above obtained analytical results. Unless otherwise mentioned, the following parameters of the composite Gamma/log-normal fading distribution are assumed for the simulations: m-parameter $m = 2$, SD and mean of log-normal shadowing, $\sigma = 6$ dB and $\mu = 0$ dB and the transmission power of the OTs $p_j = 1$. The parameter values of the unshifted Gamma distribution for the PLE, ξ, are obtained by model fitting data presented in [14], and are $m_\xi = 6.5$ and $\bar{\gamma}_\xi = \frac{m_\xi}{3}$. In order to get an accurate result from the numerical integrations, the order of the Hermite polynomial is set at $N_p = 30$; and the integrations are performed using Mathematica®. The Monte-Carlo simulation results are obtained by averaging each test case over at least $50,000$ runs using Matlab®.

2.7.1 Secondary Sum Rate Performance with Power Allocation Algorithm

The secondary sum rate curves for the proposed power allocation schemes are plotted against the number of OTs (N) in Fig. 2.2, and are compared against the sum rate curve for equal transmit power. The interference threshold Q is set at 30 dB higher than the noise power. The SU area is divided into four regions with the different radii $R = [100, 50, 20, 10, 5]$. The secondary channel model is the same as that considered for the secondary to primary system.

For the secondary system, a cellular system with orthogonal transmissions is assumed, i.e. there are no inter-secondary interference. Results are presented for the scenarios where the secondary base station (SBS) is at the cell origin (i.e., co-located with the PR) and at the cell edge.

The variation of the secondary sum rate (with respect to) w.r.t. to the interference threshold is presented in Fig. 2.3, where the secondary sum rate curves from ten OTs are plotted against the interference threshold Q (normalized by the noise power N_0).

At very stringent interference thresholds, there is hardly any room for the SUs to operate, and a low sum rate is observed for all the presented cases. However, the sum rate performance is relatively better when the SBS is at the cell edge compared to when it is at the cell centre. This is because in the former case, the SUs that are close to the SBS (at the

cell edge) have higher transmit powers and thus can achieve relatively higher rate despite the strict interference constraint.

On the other hand, when the interference constraint at the PR is relaxed, all the OTs transmit with relatively higher powers. In this case, a higher sum rate is observed when the SBS is at the cell centre compared to when it is at the cell edge. This is due to the fact that for the latter case, there are some OTs at the other end of the cell edge with high path loss, in contrast with the former case where the OTs are uniformly distributed around the SBS.

From the presented results, the advantages of having different transmit powers for OTs in different regions can be readily appreciated. Compared the performance of the proposed power assignment strategies against that with equal power, sum-rate gains of as high as seven-fold when the SBS is at the cell edge, and about five-fold when the SBS is at the cell centre, are observed. Moreover, it is found that the having a region-wise interference contribution that is proportional to the area of each region (i.e. $Q_j = \tau_j Q$) always yields better performance compared to the other considered cases.

2.7.2 Ergodic Capacity of Primary System

The ergodic capacity of the PR for different numbers of interferers distributed across a cell with radius, $R = 50$ m is shown in Figure 2.4. A Rayleigh fading channel is assumed for the primary channel with $\tilde{r} = 20$ m and $\tilde{\alpha} = 4$. Results with shadowing for the OT-PR channel are compared with that for fading only (i.e. no shadowing). As expected, observe that shadowing has a negative impact on the primary system ergodic capacity, and the influence becomes more evident with increasing number of OTs.

Figure 2.5 presents the ergodic capacity of the primary system in the presence of interference from 5 OTs distributed across the entire cell with different cell sizes. Results for the proposed path loss model and compared with that using the commonly used model, $\beta(r) = r^{-\alpha}$ (marked by $\varepsilon = 0$). As intuitively expected, the ergodic capacity of the primary user is much higher when the OTs are spread out across a larger area, due to the fact that interference power decays rapidly with distance. Furthermore, the difference in performance resulting from the proposed path loss model is evident, especially when the cell size is small.

2.7.3 Interference Outage Probabilities

Interference outage probabilities at the PR for different number of OTs and different values of the SD of shadow fading are presented in Figure 2.6. The interference threshold values are normalized by the mean interference power from a single interferer. Most notably, the interference outage probabilities are found to increase for strong shadowing conditions ($\sigma = 6$ dB) compared to no or light shadowing. This is because stronger shadowing introduces greater variations in the interference power at the receiver, thus increasing the probability of the interference power exceeding the threshold Q_{th}. Furthermore, it is also observed that the interference outage probabilities increases with an increase in the number of OTs. This can be attributed to the fact that independent interference powers are additive.

Figure 2.7 presents interference outage probability results for different cell size. For each cell size, the interference threshold is normalized by the mean interference power for the respective case with $\varepsilon = 1$ (so that the two curves for each cell size can be compared against the same threshold). The number of OTs $N = 5$ and $\sigma = 2$ dB. We observe that there is in fact *"significant deviations"* between the performance of the two different path loss models, which is more evident for smaller cell sizes, and at higher interference thresholds. Comparing the results presented in Figure 2.7 with that in Figure 2.5, it is interesting to observe that the differences in the ergodic capacity of the primary system for the different path loss models are not as significant compared to the differences in the outage probabilities. This also highlights the importance of considering different performance measures when evaluating a system.

We further observe that a PR experiences less interference when the interferers are spread around, which conforms to the earlier finding in with ergodic capacity. Furthermore, note that the outage probability falls abruptly at higher Q_{th} for smaller cell sizes. When the cell size is small, the variance of the interference power is also small as the interferers are closer to each other. Thus the probabilities of the interference power being much larger than the mean becomes very low, as can be seen from the results presented in Figure 2.7. From these findings, we can deduce that *the usual assumption that the sum interference can be treated as a Gaussian RV (by virtue of the Central Limit Theorem) is only valid for densely distributed interferers.* A similar finding is also independently reported in [12].

Impact of the Guard Zone

In this last part, we study the impact of imposing a guard zone around the PR. The impact of the guard zone of radius R on the interference outage probability is presented in Figure 2.8. Results are presented for a scenario with 10 OTs uniformly distributed across cells of different outer radius B with inner radius $A = 1$ m. We observe that even a small guard zone of 5 m can significantly reduce the outage probability at the PR. These results also highlight the importance of accurate PR localization by the NGwN when a guard zone is enforced around the PRs.

2.7.4 SINR Outage Probabilities

The *SINR outage probabilities* with different number of OTs uniformly distributed across a cell of radius $R = 50$ m, are presented in Figure 2.9. A Rayleigh faded primary channel is considered with $\tilde{r} = 5$ and the PLE $\tilde{\alpha} = 4$. Figure 2.10 shows the *SINR outage probabilities* for different cell radii with $N = 5$ and $\sigma = 2$ dB. Here, $\tilde{r}$ for each curve is chosen such that the mean SINR is 10 dB for each case. The presented results corroborate with those presented in Figures 2.6 and 2.10, and further validate the observations made in Section 2.7.3.

2.7.5 Mean Interference Power

The simulated and analytical mean interference power curves from each region for different numbers of OTs uniformly distributed across a cells with region-wise radii $R = [100, 50, 20, 5]$ (i.e. $J = 3$) are presented and compared in Fig. 2.11. The analytical and numerical mean interference powers are found to match closely, demonstrating the accuracy of the derived interference model.

Mean Interference Power with Guard Zone

In some CRN setups, the PR is protected by a guard zone around itself, within which active transmission from the OTs are forbidden [33]. The mean interference power from the OTs in a CRN with such a guard zone imposed around the PR is presented in Fig. 2.12. There are two sub-regions in this analysis, with $\rho_1 = 1$ and $\rho_2 = 0$. Results are presented for different cell sizes (i.e. different R and B) and for different numbers of OTs

N, where only the OTs in the outer ring are active. The simulation results are compared with the analytical mean interference power, and are found to match closely.

2.8 Concluding Remarks

In this work we have derived a model for the interference power from the OTs of a NGwN at a PR located at the centre of a cell, where the OTs can have different transmission probabilities and/or different transmission powers. We have also demonstrated how the derived interference model can be used to design different system parameters for the NGwN and develop a very simple yet robust and distributed power allocation algorithm. Applications of the interference model in evaluating various primary system performance are also shown. All presented results are validated by computer based Monte-Carlo simulation to substantiate the accuracy of the derived model and its applications.

A clear understanding of the intricacies of interference caused by next generation networks on a primary system, and its implications on the performance as well as network parameters of both the systems, will help researchers and practitioners design improved and efficient next generation systems which enhances the optimum utilization of the scarce radio spectrum.

Acknowledgment

This work was conducted while N. H. Mahmood was visiting King Abdullah University of Science and Technology (KAUST), and was in part by KAUST.

Bibliography

[1] S. Haykin, "Cognitive radio: Brain-empowered wireless communications," *IEEE Journal on Selected Areas in Communication*, vol. 23, no. 2, Feb. 2005.

[2] I. F. Akyildiz, W.-Y. Lee, M. C. Vuran, and S. Mohanty, "Next generation/dynamic spectrum access/cognitive radio wireless networks: A survey," *Computer Networks*, vol. 50, no. 13, pp. 2127–2159, Sep. 2006.

[3] A. S. Zahmati, S. Hussain, X. Fernando, and A. Grami, "Cognitive Wireless Sensor Networks: Emerging topics and recent challenges," in *IEEE Toronto International Conference on Science and Technology for Humanity (TIC-STH '09)*, Toronto, Canada, Sep. 2009, pp. 593 –596.

[4] V. Chandrasekhar, J. G. Andrews, and A. Gatherer, "Femtocell networks: A survey," *IEEE Communications Magazine*, vol. 46, no. 9, pp. 59 –67, Sep. 2008.

[5] A. Ghosh, N. Mangalvedhe, R. Ratasuk, B. Mondal, M. Cudak, E. Visotsky, T.A. Thomas, J.G. Andrews, P. Xia, H.S. Jo, H.S. Dhillon, and T.D. Novlan, "Heterogeneous cellular networks: From theory to practice," *IEEE Communications Magazine*, vol. 50, no. 6, pp. 54 –64, June 2012.

[6] J. Illian, A. Penttinen, H. Stoyan, and D. Stoyan, *Statistical Analysis and Modelling of Spatial Point Patterns*, John Wiley & Sons, West Sussex, England, 1st edition, Jan. 2008.

[7] J. G. Andrews, R. K. Ganti, M. Haenggi, N. Jindal, and S. Weber, "A primer on spatial modeling and analysis in wireless networks," *IEEE Communications Magazine*, vol. 58, no. 11, pp. 2–9, Nov. 2010.

[8] S. Srinivasa and M. Haenggi, "Modeling interference in finite uniformly random networks," in *Proceedings of International Workshop on Information Theory for Sensor Networks (WITS 2007)*, Santa Fe, New Mexico, USA, June 2007.

[9] A. Ghasemi, "Statistical characterization of interference in cognitive radio networks," in *IEEE 19th International Symposium on Personal, Indoor and Mobile Radio Communications (PIMRC'08)*, Cannes, France, Sep. 2008, pp. 1–6.

[10] R. Dahama, K.W. Sowerby, and G.B. Rowe, "Outage probability estimation for licensed systems in the presence of cognitive radio interference," in *IEEE 69th Vehicular Technology Conference (VTC-Spring '09)*, Barcelona, Spain, Apr. 2009, pp. 1 –5.

[11] H.M. de Lima Carlos, M. Bennis, K. Ghaboosi, and M. Latva-aho, "On interference analysis of self-organized femtocells in indoor deployment," in *IEEE GLOBECOM 2010 Workshop on Femtocell Networks*, Miami, Florida, USA, Dec. 2010, pp. 659 –663.

[12] A. Rabbachin, T. Q. S. Quek, H. Shin, and M. Z. Win, "Cognitive network interference," *IEEE Journal on Selected Areas in Communications*, vol. 29, no. 2, pp. 480–493, Feb. 2011.

[13] V. Erceg, L. J. Greenstein, S. Y. Tjandra, S. R. Parkoff, A. Gupta, B. Kulic, A. A. Julius, and R. Bianchi, "An empirically based path loss model for wireless channels in suburban environments," *IEEE Journal on Selected Areas in Communication*, vol. 17, no. 7, pp. 1205–1211, Jul. 1999.

[14] M. C. Walden and F. J. Rowsell, "Urban propagation measurements and statistical path loss model at 3.5 GHz," in *Proceedings of IEEE Antennas and Propagation Society International Symposium*, Hawaii, USA, Jul. 2005, pp. 363–366.

[15] G. Mao, B.D.O. Anderson, and B. Fidan, "Path loss exponent estimation for wireless sensor network localization," *Computer Networks*, vol. 51, no. 10, pp. 2467 – 2483, Jul. 2007.

[16] N. H. Mahmood, F. Yilmaz, and M.-S. Alouini, "A generalized and parameterized interference model for cognitive radio networks," in *12th IEEE International Workshop on Signal Processing Advances in Wireless Communications (SPAWC '11)*, San Francisco, USA, June 2011.

[17] N. H. Mahmood, F. Yilmaz, M.-S. Alouini, and G. E. Øien, "On the ergodic capacity of legacy systems in the presence of next generation interference," in *8th IEEE International Symposium on Wireless Communication Systems, ISWCS 2011*, Aachen, Germany, November 2011.

[18] J. T. Flåm, G. M. Kraidy, and D. J. Ryan, "Using a sensor network to localize a source under spatially correlated shadowing," in *71th IEEE Vehicular Technology Conference (VTC Spring '10)*, Taipei, Taiwan, May 2010, pp. 1–5.

[19] H. Inaltekin, M. Chiang, H. V. Poor, and S. B. Wicker, "On unbounded path-loss models: Effects of singularity on wireless network performance," *IEEE Journal on Selected Areas in Comm.*, vol. 27, no. 9, pp. 1078–1092, Sep. 2009.

[20] M. K. Simon and M.-S. Alouini, *Digital Communication over Fading Channels*, John Wiley & Sons, New Jersey, USA, 2nd edition, Dec. 2005.

[21] M.-S. Alouini and A. J. Goldsmith, "Area spectral efficiency of cellular mobile radio systems," *IEEE Transaction on Vehicular Technology*, vol. 48, no. 4, pp. 1047–1066, Jul. 1999.

[22] M. Abramowitz and I. Stegun, Eds., *Handbook of Mathematical Functions with Formulas, Graphs, and Mathematical Tables*, Dover Publications, New York, USA, 2nd edition, 1972.

[23] E. W. Weisstein, "Incomplete beta function," Mathworld, `http://mathworld.wolfram.com`.

[24] L. Musavian and S. Aïssa, "Capacity and power allocation for spectrum-sharing communications in fading channels," *IEEE Transactions on Wireless Communications*, vol. 8, no. 1, pp. 148 –156, Jan. 2009.

[25] K. Werner and M. Jansson, "Estimating MIMO channel covariances from training data under the Kronecker model," *Signal Processing*, vol. 89, pp. 1–13, January 2009.

[26] Wei Ren, Qing Zhao, and Ananthram Swami, "Power control in cognitive radio networks: How to cross a Multi-Lane highway," *IEEE Journal on Selected Areas in Communications*, vol. 27, no. 7, pp. 1283 –1296, Sept. 2009.

[27] T. M. Cover and J. A. Thomas, *Elements of Information Theory*, John Wiley & Sons, 2nd edition, Jul. 2006.

[28] K. A. Hamdi, "A useful lemma for capacity analysis of fading interference channels," *IEEE Transaction on Communications*, vol. 58, no. 2, pp. 411–416, Feb. 2010.

[29] J. Gil-Pelaez, "Note on the inversion theorem," *Biometrika*, vol. 38, no. 3/4, pp. 481–482, Dec. 1951.

[30] J. Abate and W. Whitt, "Numerical inversion of Laplace transforms of probability distributions," *ORSA Journal on Computing*, vol. 7, no. 1, pp. 36–43, 1995.

[31] Y.-C. Ko, M.-S. Alouini, and M. K. Simon, "Outage probability of diversity systems over generalized fading channels," *IEEE Transaction on Communications*, vol. 48, no. 11, pp. 1783–1787, Nov. 2000.

[32] Q. T. Zhang, "Outage probability in cellular mobile radio due to Nakagami signal and interferers with arbitrary parameters," *IEEE Transaction on Vehicular Technology*, vol. 45, no. 2, pp. 364–372, May 1996.

[33] A. Hasan and J. G. Andrews, "The guard zone in wireless ad hoc networks," *IEEE Transactions on Wireless Communications*, vol. 6, no. 3, pp. 897–906, Mar. 2007.

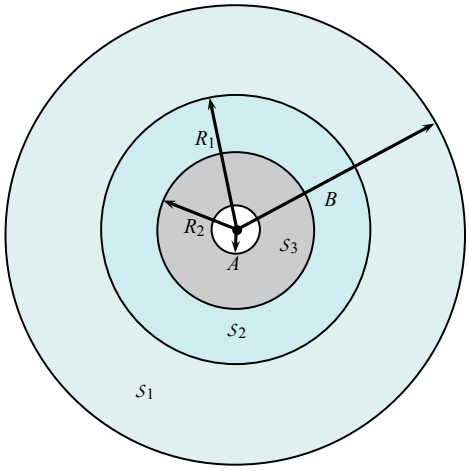

Figure 2.1: System Setup with the entire cell divided into three regions ($J = 3$). The uniformly distributed OTs (filled squares) are interfering at the PR located at the cell centre.

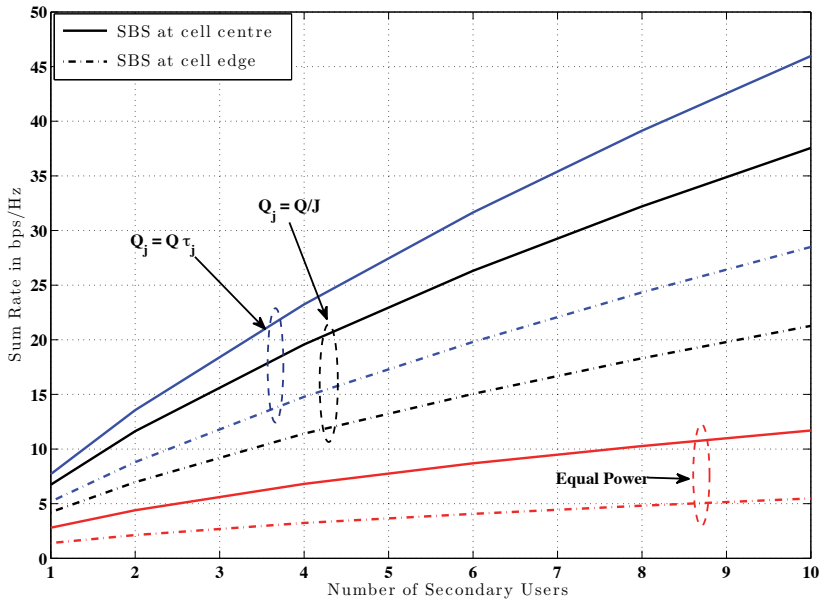

Figure 2.2: Secondary sum rate vs. N for different power assignment techniques. $J = 4$ ($R = [100, 50, 20, 10, 5]$) and $Q = N_0 + 30$ dB.

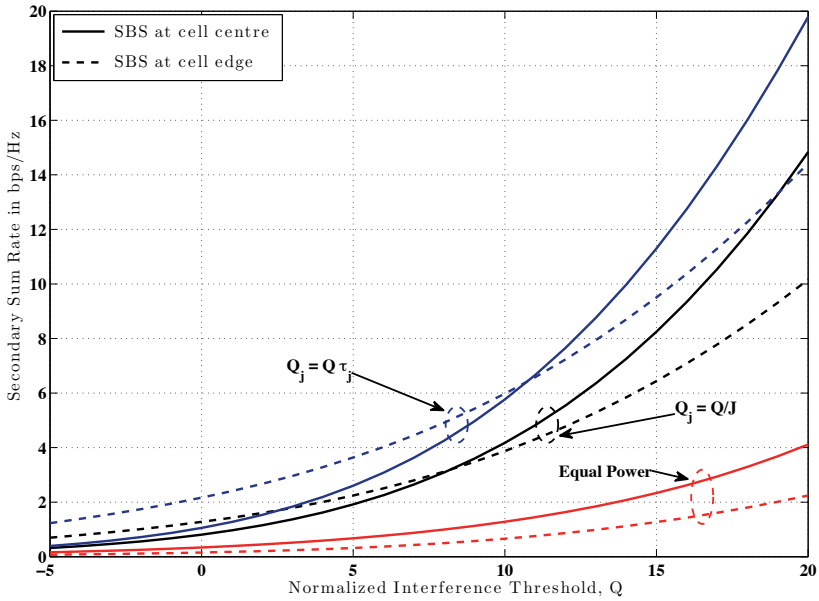

Figure 2.3: Secondary sum rate with 10 SUs vs Q (normalized by N_0). $J = 4$ with $R = [100, 50, 20, 10, 5]$.

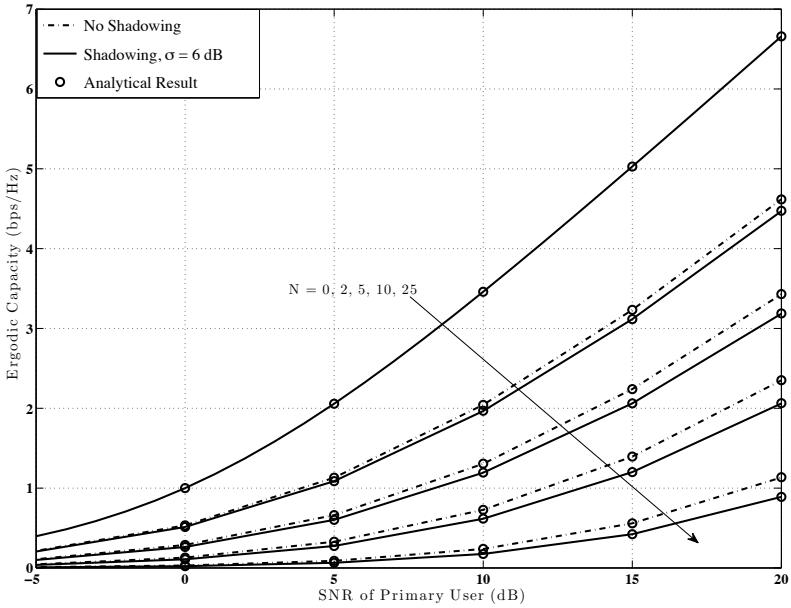

Figure 2.4: Ergodic capacity of the PR for different number of OTs N, and for different fading condition. Radius of cell $B = 50$ m, $\varepsilon = 1$, $\tilde{r} = 20$ m, $\tilde{\alpha} = 4$.

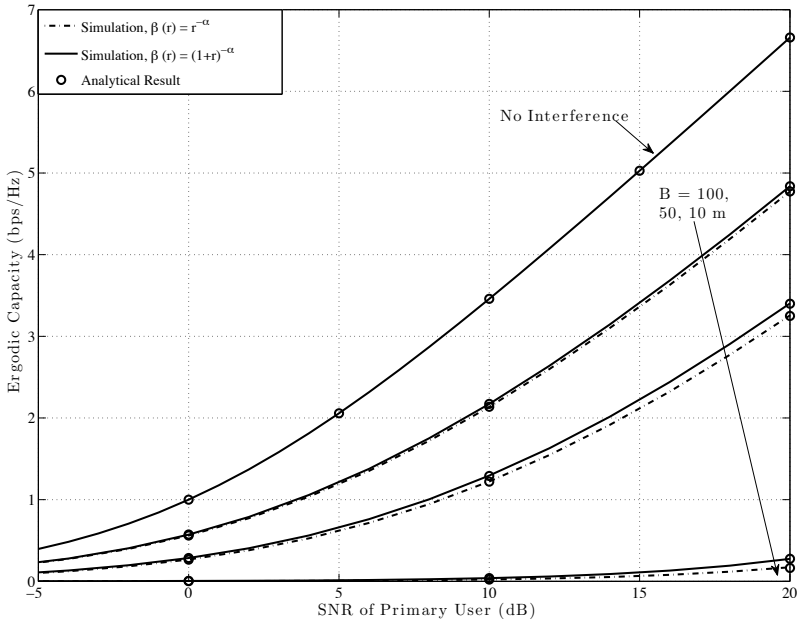

Figure 2.5: Ergodic capacity of the PR in the presence of interference from entire cell for different cell radius B, and different path loss models. Number of OTs $N = 5$, and SD of shadowing, $\sigma = 2$ dB.

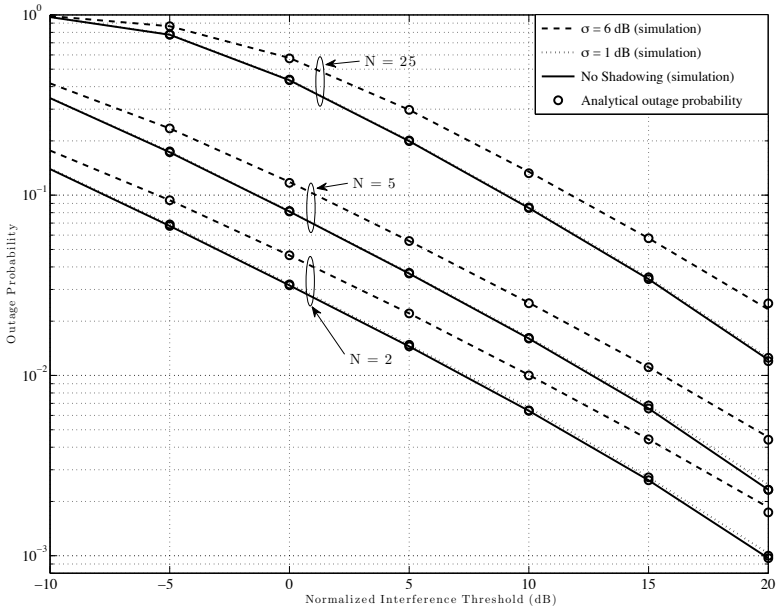

Figure 2.6: Interference outage probabilities at the PR due to interference from entire cell for different number of OTs N, and for different fading conditions. Radius of cell $B = 50$ m, and $\varepsilon = 1$. Interference threshold is normalized by mean interference power from a single OT.

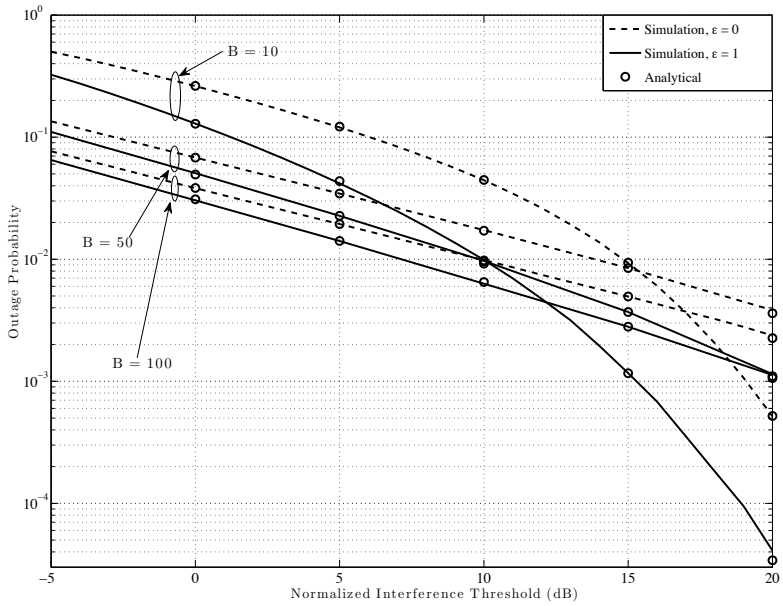

Figure 2.7: Interference outage probabilities at the PR due to interference from entire cell for different cell radius B, and different path loss models. Number of OTs $N = 5$, and the SD of shadowing $\sigma = 2$ dB. Interference threshold is normalized by the mean interference power for each cell radii with $\varepsilon = 1$.

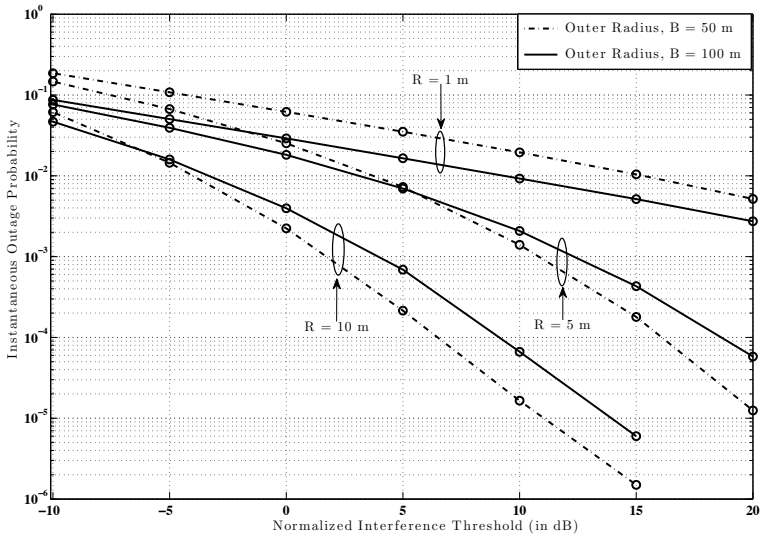

Figure 2.8: Instantaneous outage probability for the case when the cell is divided into two disjoint annular regions at radius R with $N = 10$, where only the OTs in the outer ring are active. All the users are uniformly distributed in a cell of outer radius B and inner radius $A = 1$. The interference threshold is normalized by the mean interference power from a single OT for each cell size (B) with R=1.

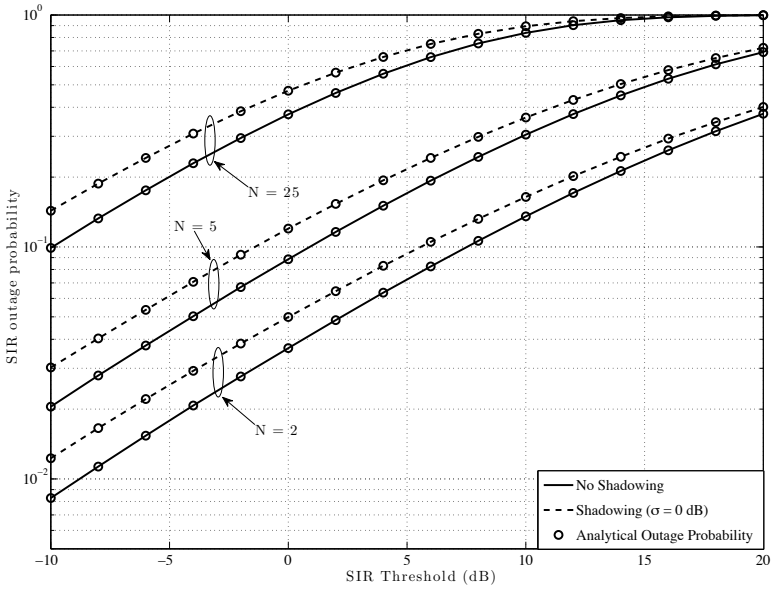

Figure 2.9: SINR outage probabilities at the PR with different number of OTs N, and for different fading conditions. Radius of cell $B = 50$ m, and $\varepsilon = 1$. A Rayleigh fading channel is considered for the primary system with $\tilde{r} = 20$ m and $\tilde{\alpha} = 4$.

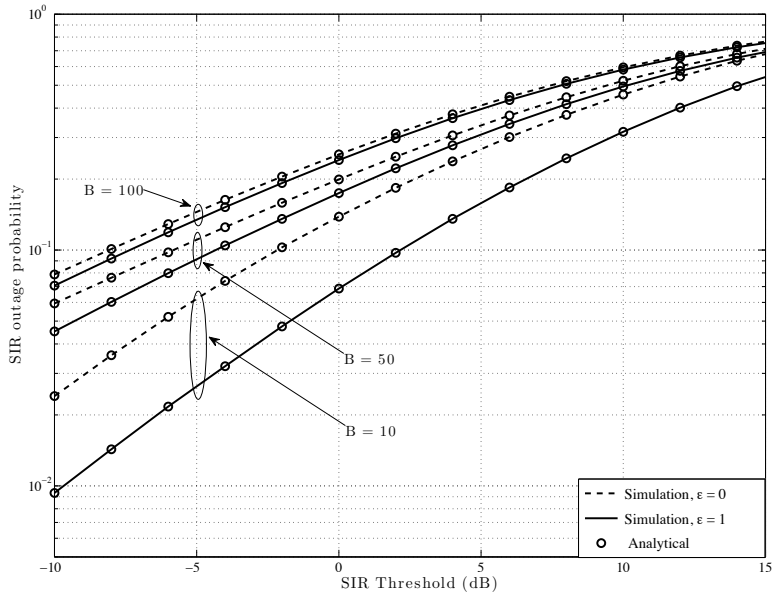

Figure 2.10: SINR outage probabilities at the PR for different cell radius B with $\varepsilon = 1$, shadowing SD $\sigma = 2$ dB and number of OTs $N = 5$. A Rayleigh fading channel is considered for the primary system with PLE $\tilde{\alpha} = 4$. The separation distance $\tilde{r}$ is chosen such that the mean SINR is 20 dB for curves for each cell radius.

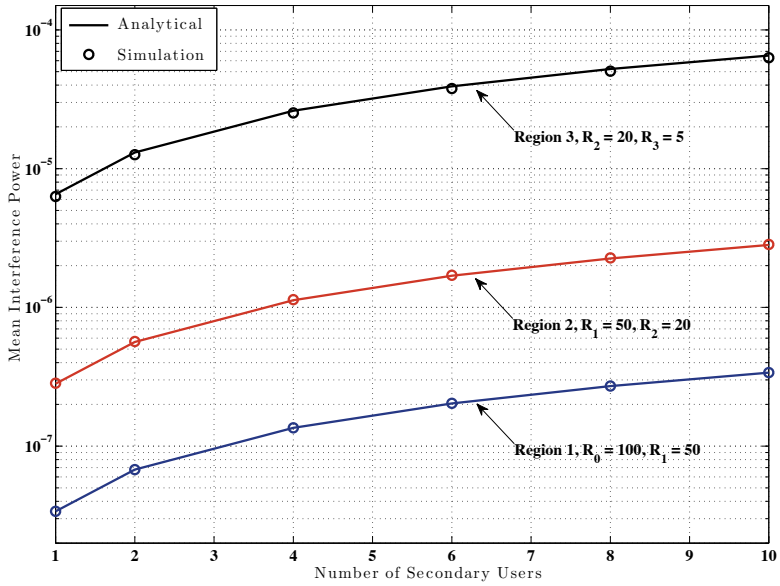

Figure 2.11: Region-wise mean interference power vs. N with $p_j = 1 \forall j$.

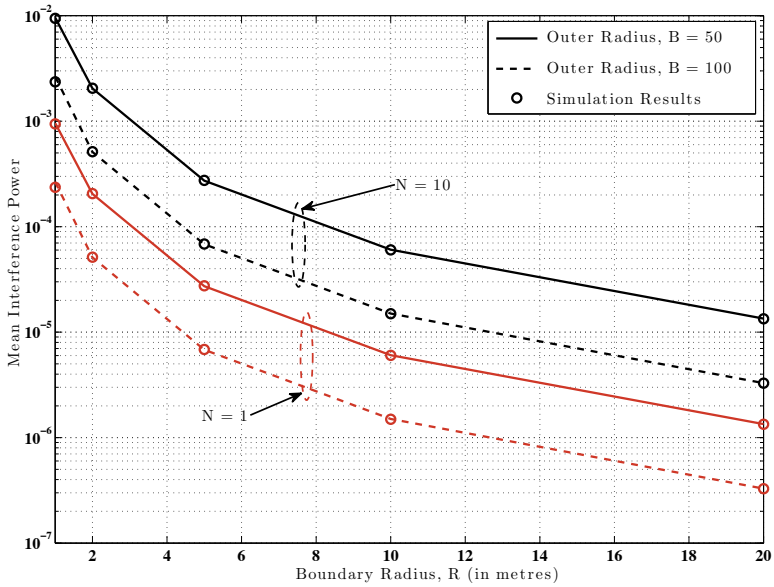

Figure 2.12: Mean interference power when the cell is divided into two disjoint annular regions at radius R. The N total OTs are uniformly distributed in a cell of outer radius B and inner radius $A = 1$. For the active OTs $p_j = 1$.

Paper B

On Hybrid Cooperation in Underlay Cognitive Radio Networks

Nurul Huda Mahmood, Ferkan Yilmaz, Geir Egil Øien and Mohamed-Slim Alouini

Submitted to IEEE Transaction on Wireless Communication, September 2012.

Partial results of this work have been published in the Conference Records of the 46th Asilomar Conference on Signals, Systems and Computers (Asilomar 2012), Pacific Groove, CA, USA, November 2012.

Chapter 3

On Hybrid Cooperation in Underlay Cognitive Radio Networks

Nurul Huda Mahmood, Ferkan Yilmaz, Geir E. Øien and Mohamed-Slim Alouini

Abstract - In certain wireless systems where transmitters are subject to a strict received power constraint, such as in an underlay cognitive radio network, cooperative communication helps to improve the coverage area and the outage performance of a network, and is a promising strategy to enhance the network performance. However, this comes at the expense of increased resource utilization. To balance the performance gain against the possible over-utilization of resources, we propose and analyze an adaptive-cooperation technique for underlay cognitive radio networks termed as hybrid-cooperation, whereby the secondary users cooperate adaptively to enhance the capacity and the error performance of the network. The bit error rate, the capacity and the outage performance of the network under the proposed hybrid cooperation technique are analyzed in this paper, and compared against the traditional cooperative scheme. Findings of analytical performance analyses are further validated numerically through selected computer-based Monte-Carlo simulations. The proposed scheme is found to achieve significantly higher capacity at a much lower BER compared to the conventional amplify-and-forward cooperation scheme.

Keywords – Underlay cognitive radio network, hybrid cooperation, cooperative communication, amplify and forward relaying.

3.1 Introduction

The rapid progress towards the much coveted *Anytime, Anywhere, Anything* wireless communication paradigm has turned the available radio spectrum into a scarce resource, resulting in a flurry of research into its systematic but opportunistic utilization. CRNs have emerged as a potential solution to overcome this scarcity, where licensed/primary and

opportunistic/secondary users may use the same spectrum under different coexistence policies [1]. One such proposed policy is the underlay CRN model, where the PUs are protected from unwanted SU interference through strict constraints on the maximum received interference power at their receivers [2].

The restriction on the received power at the PRs has an impact on the performance and the coverage area of a CRN [3], but this can be possibly improved by means of advanced signal processing techniques. Cooperative communication is such a paradigm that allows different users in a wireless network to collaborate and share each other's resources through distributed signal processing. Thus a particular user may transmit data of its own, or assist another user by forwarding its message through acting as a relay, hence generating diversity and enhancing the coverage. The most simple and commonly used cooperative method is the Amplify-and-Forward (AF) scheme, in which the relay just amplifies the received noisy version of the transmitted message signal and forwards it to the destination or to another node [4].

Inspired by the potential of CRN and cooperative communication, cooperative cognitive radio networks (C-CRN) have recently been investigated as a means of improving the performance of the CRN using the following approaches: cooperation with PUs [5] and cooperation among the SUs in the overlay [6] as well as the underlay [7, 8] CRN model. We limit the scope of this study to an underlay CRN scenario.

In [7], a performance-improving, decode-and-forward (DF) cooperation diversity scheme, with best-relay selection for multiple-relay CRNs under a constraint on the primary outage probability is proposed, and an exact closed-form expression for the secondary outage probability is derived. The authors in [8] have proposed a secondary relay selection scheme with binary secondary transmit power that maximizes the end-to-end secondary SNR under an interference threshold constraint at the PR. Subsequently, the authors have derived the secondary BER and outage probability under the proposed scheme.

The use of multiple channel resources in cooperative communication leads to interesting trade-offs between the system's resource utilization and the diversity gain. Cooperative communication is found to be spectrally inefficient especially when the source-destination channel is good [8]. To balance the performance gain against the possible over-utilization of resources, in this paper, we propose a novel adaptive cooperation technique for underlay CRN, which we have termed as "*Hybrid Cooperation*"; and analyze its performance in a C-CRN with STs that can transmit with variable transmission powers. In the proposed technique, cooperation through the relays is conditioned on the QoS of the secondary link measured in terms of the received SNR. Cooperative communication is utilized only when

the secondary link SNR falls below a given SNR threshold λ. In this work we have derived the MGF of the end-to-end SNR under the proposed hybrid cooperation scheme with AF relaying, and analyzed different performance measures of the secondary system in terms of its BER and outage probability using the derived MGF. We further outline the procedures to determine the SNR threshold λ that can achieve a favorable balance between the multiplexing and the diversity gain. The performance of the proposed scheme is moreover compared against that of an equivalent conventional C-CRN in order to demonstrate the performance gains from the proposed novel hybrid cooperation technique.

The remainder of the paper is organized as follows: in Section 5.2, we introduce the detailed system model and the proposed hybrid cooperative communication protocol. Statistical representation of the end-to-end SNR at the SBS is derived in 3.3. In Section 3.4 and Section 3.5, different performance measures of the secondary system are evaluated using the derived statistical representation of the SNR. Finally the paper is concluded in Section 5.5.

3.2 System Model

We consider an underlay CRN operating in the presence of a PR as shown in Figure 3.1. The CRN consists of a source SU (S_s) communicating with the destination SBS (S_d) with L other SUs that may potentially act as relays. The source and the potential relay SU's communication is assumed to take place across two different resource slots. In the following sequel, the set of the potential receivers include the SBS and each of the L relays, whereas the relays and the source ST constitute the set of the potential transmitters.

The interference from the Primary Transmitter (PT) at the SRs are assumed negligible. This is possible if the PT is assumed to be outside the reception range of the SRs, or by treating the primary interference as noise under the assumption that the primary system uses a random Gaussian codebook [8]. Such assumption simplifies the analysis of the secondary system, and helps to reach some intelligible results and an understanding of the performance bounds of the proposed techniques under different scenarios. However, in practice the inter-system interference may in some scenarios have a slightly different distribution compared to the Gaussian model [9]. Precise interference models can be incorporated to get more refined results if and when necessary, and is left as a possible future extension of this work.

In contrast to the SRs, interference from the STs at the PR cannot be similarly neglected

due to the opportunistic nature of the secondary communication. The unwanted secondary interference at the PR is controlled by imposing a limit on the maximum interference power received from the STs. This requires the STs to adjust the transmission power to ensure that the secondary interference power at the PR does not exceed a given interference temperature threshold Q_{th}. Let p_l and φ_l denote the transmission power of a ST S_l, and the random fading power gain of its channel to the PR. The above-mentioned interference temperature constraint can therefore be expressed as $p_l\varphi_l \leq Q_{th}$. In addition, the physical properties of the STs and regulatory requirements also impose an additional constraint on the transmission power p_l such that $p_l \leq P_l$, where P_l is its maximum allowed transmission power of SU S_l. Putting these two constraints together, and assuming that each ST transmits at the maximum possible transmit power, the transmission power of SU S_l is given by $p_l = \min(\frac{Q_{th}}{\varphi_l}, P_l)$.

Let the signal received at a potential SR S_k from a potential ST S_l be given by $y_k = \sqrt{p_l\phi_{lk}x_l} + n_k$, where ϕ_{lk} is the random fading power gain of the ST-SR channel, x_l is the unit power Gaussian message symbol and n_k is the independent zero mean circularly symmetric AWGN term at the SR, with its power given by N_0. Under this model, the received SNR γ_{lk} at the SR is given by $\gamma_{lk} = p_l\phi_{lk}/N_0$.

All random channel gains in this work are assumed to follow a block fading channel model such that the channel state of each user is constant over each resource slot, but changes independently across resource slots and across users. The channel gains are modeled using the Rayleigh fading model. Thus, the corresponding power gain is an exponential distributed random variable [10]. Information about the ST-PR channels are assumed to be known with sufficient accuracy, and synchronized at the respective ST. This can be obtained by cooperation with the PR using some pilot signals, or by using some sort of centralized band manager with global CSI [11]. Such global CSI assumption gives an upper bound on the achievable performance of the proposed cooperation technique.

Amplify and Forward Relaying

In the considered AF relaying scheme, communication between the source and the SBS through a relay takes place over two orthogonal TSs. The source's transmission in the first TS is received by the SBS and the potential relays. In the subsequent TS, the relay amplifies the received signal subject to the interference temperature and the maximum power constraint, and forwards it to the SBS. At the SBS, the message signals received over the two independent TSs are then combined using the Maximum Ratio Combining (MRC) technique.

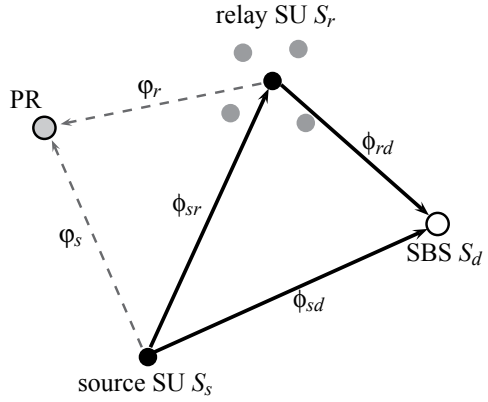

Figure 3.1: The System Model represented by a source SU communicating with the SBS. The SU may communicate directly with the SBS or with the help of relays as shown in this figure. All secondary transmissions are assumed to interfere at the PR.

It can be easily shown that the SNR γ_l of the message signal received at the SBS through the relay S_l is given by

$$\gamma_l = \frac{\gamma_{sl}\gamma_{ld}}{\gamma_{sl}+\gamma_{ld}+N_0}. \tag{3.1}$$

The above exact expression for the SNR can be approximated by its upper bound $\gamma_l \leq \min(\gamma_{sl},\gamma_{ld})$ [12], which is more tractable than (3.1) itself. Furthermore, the above approximation is found to be tight in the mid-to-high SNR regime.

3.2.1 Proposed Hybrid Cooperation Technique

In the hybrid cooperative communication proposed in this paper, the source's first preferance is to communicate through the direct link without involving the relays in order to avoid using additional resource slots. However, the help of a relay is incorporated when the SNR of the signal received through the direct link at the destination SBS (γ_{sd}^{d}) falls below a given SNR threshold λ. In that case, the source to destination communication occurs over two TSs. The SNR of the MRC combined signal at the destination SBS after the two TS is then given by $\gamma_{sd}^{\mathrm{r}} = \gamma_{sd}^{(1)} + \gamma_{sd}^{(2)}$, where the superscript indicates the associated TS. The proposed hybrid cooperation technique is summarized as a flowchart in Fig. 3.2.

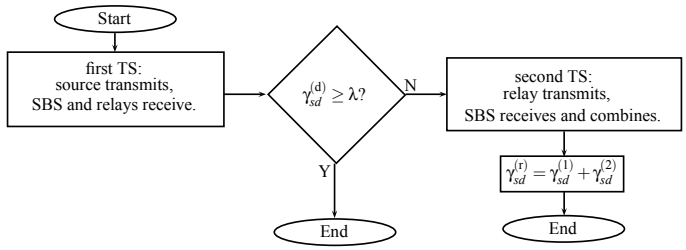

Figure 3.2: Flowchart of a successful transmission with the proposed Hybrid Cooperation technique

The SNR Threshold λ

The choice of the SNR threshold λ is a critical parameter in the proposed hybrid cooperation technique. A small value of λ will push more traffic through the direct link, resulting in a reduced diversity gain since the diversity offered by the relay will be utilized less often. On the other hand, a larger λ value will result in an increased use of the relay channel at the expense of throughput or multiplexing gain. Therefore, the SNR threshold λ has to be "smartly" chosen to strike a balance between the diversity offered by the relay link and the increased utilization of resource slots through the direct link. The best choice of λ will be discussed in the passage of this paper.

3.3 Statistical Representation of the SNR

The statistical representation of the SNR of the signal received from the source SU at the SBS is derived in terms of its MGF in this section. In order to derive the MGF of the final SNR, we first derive the PDF of the ST power profile. Using this power profile, we then independently derive the distributions of the SNR of the direct signal from the source SU at the SBS, and that through the relay. Finally the desired MGF is obtained from the derived individual distributions.

3.3.1 Distribution of the SU Power Profile

The transmission power of a ST S_l under the interference temperature and maximum power constraint constraints is given by

$$p_l = \begin{cases} P_l & \varphi_l \leq \frac{Q_{th}}{P_l} \\ \frac{Q_{th}}{\varphi_l} & \text{otherwise.} \end{cases} \tag{3.2}$$

Using the distribution of the exponential random variable φ_l as given in [10, Eq. 2.7], the PDF of this power profile $f_{P_l}(p)$ is readily obtained as

$$f_{p_l}(p) = \begin{cases} \frac{Q_{th}}{\Omega_{\varphi,l}} p^{-2} \exp\left(-\frac{Q_{th}}{p\Omega_{\varphi,l}}\right) & 0 \leq p < P_l \\ 1 - \exp\left(-\frac{Q_{th}}{P_l\Omega_{\varphi,l}}\right) & p = P_l \\ 0 & \text{otherwise.} \end{cases} \tag{3.3}$$

where $\Omega_{\varphi,l} = \mathbb{E}[\varphi_l]$, with $\mathbb{E}[\cdot]$ denoting the statistical expectation operation. Without loss of generality, henceforth we consider the same maximum transmission power for all STs, i.e. $P_l = P \forall l$. Furthermore, let us define the variables $q_l := \frac{P\Omega_{\varphi,l}}{Q_{th}}$ and $\rho_{lk} := \frac{P\Omega_{\phi,lk}}{N_0}$.

3.3.2 Statistics of the Direct Link SNR

As the initial step of our analysis, we first derive the PDF, the Cumulative Distribution Function (CDF) and the MGF of the SNR, γ_{lk}, of the message signal received at the SR S_k through a direct link from the ST S_l. Note that, S_l can be the source or any of the relays and S_k can be the SBS or any of the relays.

PDF and CDF of the Direct Link SNR

In order to obtain the PDF $f_{\gamma,lk}(r)$ of γ_{lk}, first we consider its PDF conditioned on the transmission power p_l. Under the exponential distribution assumption on ϕ_{lk}, the conditional PDF $f_{\gamma,lk}(r|p)$ is simply given as $f_{\gamma,lk}(r|p) = \frac{N_0}{p\Omega_{\phi,lk}} \exp\left(-\frac{rN_0}{p\Omega_{\phi,lk}}\right)$ [10], where $\Omega_{\phi,lk} = \mathbb{E}[\phi_{lk}]$.

The PDF $f_{\gamma,lk}(r)$ of γ_{lk} is then obtained by averaging $f_{\gamma,lk}(r|p)$ over the distribution of p_l, i.e. $f_{\gamma,lk}(r) = \mathbb{E}[f_{\gamma,lk}(r|p)]$. Using (3.3) and after some algebraic manipulations, the PDF

of γ_{lk} is readily derived as

$$f_{\gamma,lk}(r) = \frac{e^{-r\rho_{lk}}}{\rho_{lk}}\left(1 - e^{-1/q_l}\right) + \frac{e^{-r/\rho_{lk}-1/q_l}}{\rho_{lk}+rq_l}\left(1 + \frac{\rho_{lk}q_l}{\rho_{lk}+rq_l}\right). \tag{3.4}$$

The CDF of γ_{lk}, defined as $F_{\gamma,lk}(r) \triangleq \int_0^r f_{\gamma,lk}(u)\,du$, is then straightforwardly evaluated as

$$F_{\gamma,lk}(r) = 1 - e^{-r/\rho_{lk}} + \frac{\rho_{lk}q_l e^{-r/\rho_{lk}-1/q_l}}{\rho_{lk}+rq_l}. \tag{3.5}$$

PDF of the Direct Source-Destination Communication

Let γ_{sd} represent the SNR of the signal received at the SBS from the source ST through the direct link. In our proposed hybrid-cooperative communication, γ_{sd} is differentiated into two different sets of realizations corresponding to whether the communication through the relay is invoked or not. Let $\gamma_{sd}^{(\mathrm{d})}$ $\left(\gamma_{sd}^{(1)}\right)$ represent the case when the cooperation of a relay is not required (is required), i.e. $\gamma_{sd}^{(\mathrm{d})} := \gamma_{sd} \geq \lambda$ $\left(\gamma_{sd}^{(1)} := \gamma_{sd} < \lambda\right)$.

We may analyze the proposed hybrid-cooperation technique by considering $\gamma_{sd}^{(\mathrm{d})}$ and $\gamma_{sd}^{(1)}$ as two different RVs. Since the RV $\gamma_{sd}^{(\mathrm{d})}$ is only defined for $\lambda \leq \gamma_{sd}^{(\mathrm{d})} < \infty$, its PDF is given by

$$f_{\gamma,sd}^{(\mathrm{d})}(r) = \begin{cases} \frac{1}{1-F_{\gamma,sd}(\lambda)} f_{\gamma,sd}(r) & r \geq \lambda \\ 0 & \text{otherwise,} \end{cases} \tag{3.6}$$

where $f_{\gamma,sd}(r)$ and $F_{\gamma,sd}(r)$ are given by (3.4) and (3.5) respectively. Subsequently, the MGF of $\gamma_{sd}^{(\mathrm{d})}$ is given by $\mathcal{M}_{\gamma,lk}^{(\mathrm{d})}(s) = \int_\lambda^\infty \exp(-sr) f_{\gamma,sd}^{(\mathrm{d})}(r)\,dr$, and can be expressed as

$$\mathcal{M}_{\gamma,sd}^{(\mathrm{d})}(s;\lambda) = \frac{1}{1-F_{\gamma,sd}(\lambda)} \left\{ \frac{e^{-\lambda/\rho_{sd}(1+s\rho_{sd})}}{1+s\rho_{sd}} \left[\frac{s\rho_{sd} - \lambda q_s/\rho_{sd}}{1+\lambda q_s/\rho_{sd}} e^{-1/q_s} + 1 \right] + \frac{s\rho_{sd}}{q_s} e^{s\rho_{sd}/q_s} \mathrm{Ei}\Big(-(1+s\rho_{sd})\,(1/q_s + \lambda/\rho_{sd}) \Big) \right\}, \tag{3.7}$$

where $\mathrm{Ei}(x) \triangleq -\int_{-x}^\infty \frac{\exp(-t)}{t}\,dt$ is the Exponential Integral [13, Eq. 5.1.2].

Similarly, the PDF of the RV $\gamma_{sd}^{(1)}$, which is defined for $0 \leq r < \lambda$, is given by $f_{\gamma,sd}^{(1)}(r) =$

$\frac{f_{\gamma,sd}(r)}{F_{\gamma,sd}(\lambda)}$ (within the defined range); and its corresponding MGF is given by

$$\mathcal{M}^{(1)}_{\gamma,sd}(s;\lambda) = \frac{1}{F_{\gamma,sd}(\lambda)} \left\{ \frac{1 - e^{-\lambda/\rho_{sd}(1+s\rho_{sd})} + se^{-1/q_s}}{1+s\rho_{sd}} - \frac{\left(\frac{s\rho_{sd}}{q_s} - \frac{\lambda q_s}{\rho_{sd}}\right) e^{-\lambda/\rho_{sd}(1+s\rho_{sd})-1/q_s}}{(1+s\rho_{sd})(1+\lambda q_s/\rho_{sd})} + \right.$$
$$\left. \frac{s\rho_{sd}}{q_s} e^{s\rho_{sd}/q_s} \left[\mathrm{Ei}\Big(-\frac{s\rho_{sd}}{q_s} - \frac{1}{q_s} \Big) - \mathrm{Ei}\Big(-(1+s\rho_{sd})\,(1/q_s + \lambda/\rho_{sd}) \Big) \right] \right\}. \quad (3.8)$$

3.3.3 Statistical Representation of the SNR Through the Relay Link

The upper bound on the SNR of the signal from the source ST received at the SBS through a relay S_l is given by $\gamma_l \leq \min(\gamma_{sl}, \gamma_{ld})$ [12], where the PDF and the CDF of γ_{sl} (and similarly γ_{ld}) are given in (3.4) and (3.5) respectively. By approximating γ_l with the above upper bound, and applying results from order statistics, the CDF of γ_l can be approximated in terms of the individual CDFs of γ_{sl} and γ_{ld} as $F_{\gamma,l}(r) \approx F_{\gamma,sl}(r) + F_{\gamma,ld}(r) - F_{\gamma,sl}(r)F_{\gamma,ld}(r)$ [14].

If we assume that the relay is located such that its channel to the source ST and the SBS are identically distributed, and if the distribution of its channel to the PR is similarly that of the source ST-PR channel, then we have the equality $F_{\gamma,sl}(r) = F_{\gamma,ld}(r)$. Hence the approximate CDF of γ_l can be further simplified as $F_{\gamma,l}(r) \approx F_{\gamma,sl}(r)\left(2 - F_{\gamma,sl}(r)\right)$, where γ_{sl} represents both the source-relay and the relay-SBS direct link SNR. Such an assumption further upper bounds γ_l since the minimum of two independent RVs is maximized when they are distributed identically.

The approximate PDF of γ_l is thereafter readily given by $f_{\gamma,l}(r) \approx 2f_{\gamma,sl}(r)\left(1 - F_{\gamma,sl}(r)\right)$. The MGF derived using this approximation gives a lower bound on the exact MGF of the γ_l. Hence, the resulting lower bound on the MGF of γ_l is given by $\mathcal{M}_{\gamma,l}(s) \geq 2\mathcal{M}_{\gamma,sl}(s) - \mathcal{M}_{f_{\gamma,sl}F_{\gamma,sl}}(s)$.

In the above expression, $\mathcal{M}_{\gamma,sl}(s) \triangleq \int_0^\infty \exp(-sr) f_{\gamma,sl}(r)\,dr$. On a similar note, $\mathcal{M}_{f_{\gamma,sl}F_{\gamma,sl}}(s) \triangleq 2\int_0^\infty \exp(-sr) f_{\gamma,sl}(r)F_{\gamma,sl}(r)\,dr$. The expression for $\mathcal{M}_{\gamma,sl}(s)$ can be obtained by taking the limit of (3.7) as $\lambda \to 0$, and is readily obtained as

$$\mathcal{M}_{\gamma,sl}(s) = \frac{1+s\rho_{sl}e^{-1/q_s}}{1+s\rho_{sl}} - \frac{s\rho_{sl}}{q_s} e^{s\rho_{sl}/q_s} \mathrm{Ei}\left(-\frac{s\rho_{sl}}{q_s} - \frac{1}{q_s} \right). \quad (3.9)$$

By deriving $\mathcal{M}_{f_{\gamma,sl}F_{\gamma,sl}}(s)$ and after some algebraic manipulation the expression for the

lower bound on $\mathcal{M}_{\gamma,l}(s)$ is finally obtained as

$$\mathcal{M}_{\gamma,l}(s) \geq \frac{2\left(1+s\rho_{sl}e^{-1/q_s}\right)}{2+s\rho_{sl}} - \left(\frac{\rho_{sl}}{q_s}+\frac{\rho_{sl}}{2+s\rho_{sl}}\right)se^{-2/q_s} - \frac{\frac{2s\rho_{sl}}{q_s}e^{s\rho_{sl}/q_s}\mathrm{Ei}\left(-\frac{s\rho_{sl}}{q_s}-\frac{2}{q_s}\right)}{\left(1+\frac{s\rho_{sl}}{2q_s}+\frac{1}{q_s}-e^{1/q_s}\right)^{-1}}. \tag{3.10}$$

3.3.4 Statistics of the Final SNR at SBS

When a single relay is used, the SNR of the signal received at the SBS through the relay in the second TS is given by γ_l, i.e. $\gamma_{sd}^{(2)} = \gamma_l$. Hence, the end-to-end SNR of the MRC combined signal at the SBS after a two TS transmission stage involving a single relay is given by $\gamma_{sd}^{(\mathrm{r})} = \gamma_{sd}^{(1)} + \gamma_l$. Under the independence assumption on the direct signal and that through the relay, the MGF $\mathcal{M}_{\gamma,sd}^{(\mathrm{r})}(s)$ of $\gamma_{sd}^{(\mathrm{r})}$ is the product of the MGFs of the individual SNRs, i.e. $\mathcal{M}_{\gamma,sd}^{(\mathrm{r})}(s) \geq \mathcal{M}_{\gamma,sd}^{(1)}(s)\mathcal{M}_{\gamma,l}(s)$, where $\mathcal{M}_{\gamma,sd}^{(1)}(s)$ and $\mathcal{M}_{\gamma,l}(s)$ are given by (3.8) and (3.10) respectively. Finally, considering the proposed hybrid cooperation technique, the lower bound on the MGF of the final SNR γ at the SBS is eventually given by

$$\mathcal{M}_{\gamma}(s) \geq \left(1-F_{\gamma,sd}(\lambda)\right)\mathcal{M}_{\gamma,sd}^{(\mathrm{d})}(s;\lambda) + F_{\gamma,sd}(\lambda)\mathcal{M}_{\gamma,sd}^{(1)}(s;\lambda)\mathcal{M}_{\gamma,l}(s). \tag{3.11}$$

3.4 Performance Analysis of the Proposed Hybrid Cooperation Technique

Different metrics for the performance evaluation of the proposed hybrid cooperation technique are analyzed, and the design of the best SNR threshold λ is investigated in this section.

3.4.1 Error Rate Calculation

Following the unified approach presented in [10], the error rate for a wide variety of M-ary modulation schemes can be evaluated using the MGF of the received SNR. For example, the average Symbol Error Rate (SER) resulting from the considered MRC reception across L independent diversity streams with M-ary Phase Shift Keying (MPSK) modulation over generalized fading channels can be deduced from the MGF of the received SNR

as [10, 9.15]

$$\zeta_s(\rho,q)=\frac{1}{\pi}\int_0^{(M-1)\pi/M}\prod_{l=1}^{L}\mathcal{M}_l\left(\frac{\sin^2(\pi/M)}{\sin^2 x}\right)dx, \tag{3.12}$$

where $\mathcal{M}_l$ is the MGF of the received SNR through the l^{th} branch through the corresponding generalized fading channel.

As an illustrative example we present the BER of Binary Phase Shift Keying (BPSK) modulation for the considered system in this contribution. The BER of the proposed hybrid cooperation technique with BPSK modulation can be evaluated using the MGF derived in (3.11) as

$$\zeta_b(\rho,q)=\frac{1}{\pi}\int_0^{\frac{\pi}{2}}\mathcal{M}_\gamma\left(\frac{1}{\sin^2 x}\right)dx, \tag{3.13}$$

which gives a lower bound on the BER of the proposed hybrid cooperation scheme. With the above simplified expression, the BER can be readily evaluated by a single integral using any available mathematical softwares or simple numerical techniques. BER curves of the proposed hybrid cooperation technique for different threshold SNRs λ are plotted against the maximum transmit power (normalized by the noise power) $\frac{P}{N_0}$ in Figure 3.3. The presented simulation results for the approximate BER is obtained by approximating γ_l with its lower bound as discussed earlier, and yields a lower bound on the BER. Simulation results for the approximate BER are compared against analytical results evaluated using (3.13) and are found to match closely. Only simulation results are presented for the exact BER since it is difficult to evaluate analytically.

All simulation results presented throughout this paper were carried out in Matlab® using the Monte-carlo simulation technique. Results for each presented scenarios have been obtained by averaging over many runs (at least $100,000$).

3.4.2 Ergodic Capacity

In this section, we demonstrate how the ergodic capacity of the secondary system under the proposed hybrid cooperation scheme can be evaluated using the earlier derived MGF. Assuming the Shannon capacity can be achieved at every resource slot, the instantaneous secondary capacity conditioned on the received SNR is given by the famous Shannon's capacity formula for AWGN channels, $C(\gamma)=\log_2(1+\gamma)$ [15]. The ergodic capacity can thereafter be obtained by taking the expectation of this instantaneous capacity over the distribution of γ. Considering the proposed hybrid cooperation technique, a $(1-F_{\gamma,sd}(\lambda))$ fraction of the communication occurs over a single TS during which the SNR of the

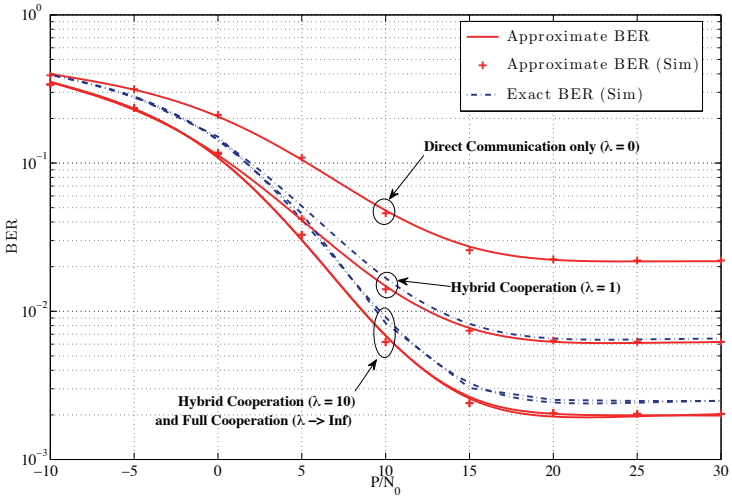

Figure 3.3: The BER under the proposed hybrid cooperation with a single relay. $\Omega_{\phi,sd} = \Omega_{\varphi,s} = \Omega_{\varphi,l} = -3$ dB, $\Omega_{\phi,sl} = \Omega_{\phi,ld} = 0$ dB, and $Q_{th} = N_0 + 10$ dB.

received signal at the SBS is given by $\gamma_{sd}^{(\mathrm{d})}$. In the remaining $F_{\gamma,sd}(\lambda)$ fraction, the SNR $\gamma_{sd}^{(\mathrm{r})}$ is received over a communication phase involving two TSs. Combining these two time divisions, the end-to-end ergodic capacity of the secondary communication for the proposed scheme is given by

$$C(\rho_{sd},\rho_{sl},q_s;\lambda) = \Big(1-F_{\gamma,sd}(\lambda)\Big)\mathbb{E}\left[\log_2(1+\gamma_{sd}^{(\mathrm{d})})\right] + \frac{F_{\gamma,sd}(\lambda)}{2}\mathbb{E}\left[\log_2(1+\gamma_{sd}^{(1)}+\gamma_l)\right]. \tag{3.14}$$

The direct method for calculating the above expectation requires complicated integrations over the distributions of $\gamma_{sd}^{(\mathrm{d})}$, $\gamma_{sd}^{(1)}$ and γ_l, and cannot be evaluated easily. Instead, we simplify the above expression by applying an useful lemma proposed by Hamdi in [16] to evaluate the capacity involving multiple integrals. By virtue of the independence assumption on the different SNRs, we obtain a simple closed form expression for the upper bound on the ergodic capacity of the secondary system involving the MGFs obtained earlier in this paper, as given by

$$C(\rho_{sd},\rho_{sl},q_s;\lambda) \le \frac{\big(1-F_{\gamma,sd}(\lambda)\big)}{\ln 2}\int_0^\infty \frac{1-\mathcal{M}_{\gamma,sd}^{(\mathrm{d})}(z;\lambda)}{z}\exp(-z)\,dz + \frac{F_{\gamma,sd}(\lambda)}{2\ln 2}\int_0^\infty \frac{1-\mathcal{M}_{\gamma,sd}^{(1)}(z;\lambda)\mathcal{M}_{\gamma,sd}^{(2)}(z)}{z}\exp(-z)\,dz, \tag{3.15}$$

where $\ln(x)$ is the natural logarithm. The integrand in (3.15) is a continuous and bounded non-negative quantity in the range of integration, and as such can be easily computed using any suitable numerical integration techniques or available mathematical softwares. The ergodic capacity curves with a single relay and for difference choices of the threshold SNR λ for the setup presented in Figure 3.3 is shown in Figure 3.4.

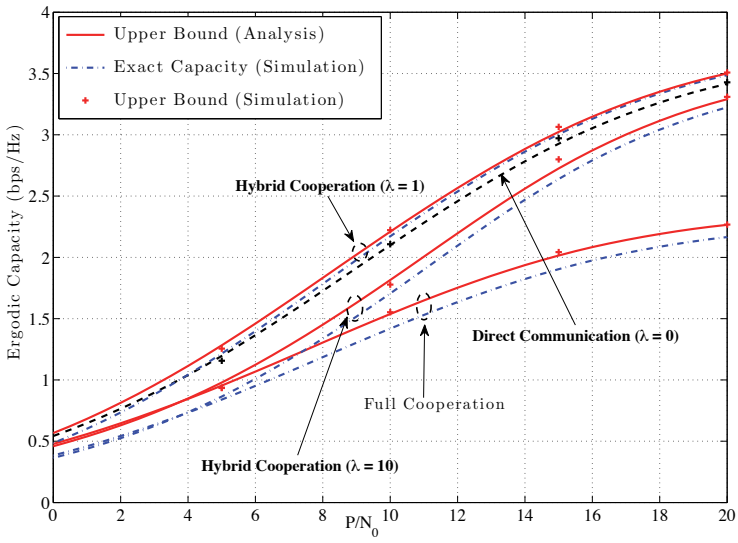

Figure 3.4: Ergodic Capacity with proposed hybrid cooperation for one relay. $\Omega_{\phi,sd} = \Omega_{\varphi,s} = \Omega_{\varphi,l} = -3$ dB, $\Omega_{\phi,sl} = \Omega_{\phi,ld} = 0$ dB, and $Q_{th} = N_0 + 10$ dB.

We can appreciate the potential gains of the proposed hybrid cooperation scheme by comparing Figure 3.3 and Figure 3.4. First of all, we observe the well known fact that relays provide diversity gain at the expense of rate penalty. This is evident from the curves corresponding to $\lambda = 0$ and $\lambda \to \infty$, where one of them displays higher capacity with higher BER ($\lambda = 0$), whereas the other exhibits better BER performance at the expense of the capacity ($\lambda \to \infty$). In contrast, however, interesting findings are observed for the curves representing the hybrid cooperation scheme. By comparing the curves representing the direct communication case with that of hybrid cooperation scheme with $\lambda = 1$, *we observe that the proposed scheme results in a higher throughput at a much lower BER*. On the other hand, when the SNR threshold λ is increased to 10, the BER of the hybrid cooperation scheme is almost equal to that with full cooperation, whereas the resulting throughput is comparable to the no cooperation scenario. Thus, with the proposed scheme, the BER performance gain accorded by the relays can be achieved at a significantly higher capacity gain. In addition, the curves presented in the above figure highlight the importance of

choosing an appropriate value of the the SNR threshold λ, the choice of which is discussed in the passage of this paper. In addition, the upper bound on the ergodic capacity given by (3.15) is found to be tighter for the proposed scheme compared to the full cooperation technique as is evident from Figure 3.4.

3.4.3 Determining the SNR Threshold

In the source ST to the SBS communication, the choice between the link through the relay and the direct link is determined by the SNR threshold λ. A higher value of λ will force more traffic through the relay, resulting in diversity gain in exchange of increased resource utilization. Conversely, a lower value of λ will result in increased multiplexing gain at the expense of the received SNR, which in turn may lead to higher BER. Therefore, the SNR threshold λ has to be carefully chosen to strike an appropriate balance between the diversity-multiplexing tradeoff. In this section, we outline how the SNR threshold λ can be chosen such that there is no significant BER penalty for the increased resource utlization due to the proposed hybrid cooperation.

The BER contribution of the direct communication (i.e. when a relay is not utilized) depends strongly on the SNR threshold λ. Since the SNR of the direct link is always greater than the SNR threshold λ, its value can be appropriately chosen to guarantee any given target BER. Therefore, to ensure that there is no significant impact on the BER due to the proposed hybrid cooperation technique, the SNR threshold λ should be chosen such that the BER contribution of the direct link is insignificant compared to that through a relay link with the conventional cooperative scheme.

For any given channel condition, and a given modulation/coding scheme, let ζ_{FC} be the BER that can be achieved with full cooperation (i.e. when $\lambda \to \infty$). Using (3.13), ζ_{FC}, which is independent of λ, can be evaluated as

$$\zeta_{\text{FC}}(\rho_{sd}, \rho_{sl}, q_s) = \frac{1}{\pi} \int_0^{\frac{\pi}{2}} \mathcal{M}_{\gamma,sd}\left(\frac{1}{\sin^2 x}\right) \mathcal{M}_{\gamma,l}\left(\frac{1}{\sin^2 x}\right) dx, \tag{3.16}$$

where $\mathcal{M}_{\gamma,sd}(s)$ and $\mathcal{M}_{\gamma,l}(s)$ are the MGFs given by (3.10) and (3.9) respectively.

Similarly, the BER of the direct communication link with the proposed hybrid cooperation for the same channel condition can be evaluated as $\zeta_{\text{DC}}(\rho_{sd}, q_s; \lambda) = \frac{1-F_{\gamma,sd}(\lambda)}{\pi} \int_0^{\frac{\pi}{2}} \mathcal{M}^{(\text{d})}_{\gamma,sd}\left(\frac{1}{\sin^2 x}\right) dx$. To ensure negligible impact on the BER due to the proposed hybrid cooperation technique, let us choose λ such that $\zeta_{\text{DC}}(\rho_{sd}, q_s; \lambda) \ll \zeta_{\text{FC}}(\rho_{sd}, \rho_{sl}, q_s)$.

It is easily observed that determining λ to satisfy the above condition is not straightforward since it requires solving a complicated integral of the MGF. To simplify the analysis, we approximate the integration involved in evaluating $\zeta_{\mathrm{DC}}(\rho_{sd}, q_s; \lambda)$ by a two-point trapezoidal sum [13, Eq. 25.4.1] as (see Appendix 3.7 for proof and associated conditions)

$$\zeta_{\mathrm{DC}}(\rho_{sd}, q_s; \lambda) \approx \frac{e^{\frac{\rho_{sd}}{q_s}-u}}{4}\left\{\frac{\rho_{sd}}{uq_s}\left(\frac{1}{u+1}+\frac{1}{\rho_{sd}}\right)+\frac{1}{1+\rho_{sd}}\left(e^{1/q_s}-1\right)\right\}, \tag{3.17}$$

where $u \triangleq (1+\rho_{sd})(1/q_s+\lambda/\rho_{sd})$. As a rule of thumb, let λ be such that $\zeta_{\mathrm{DC}}(\rho_{sd}, q_s; \lambda) \leq \frac{\zeta_{\mathrm{FC}}}{100}$. Hence, the problem of finding λ can be constituted as determining the smallest u that satisfies

$$\frac{\rho_{sd}}{uq_s}e^{\frac{\rho_{sd}}{q_s}-u}\left(\frac{1}{u+1}+\frac{1}{\rho_{sd}}\right)+\frac{\left(e^{1/q_s}-1\right)e^{\frac{\rho_{sd}}{q_s}-u}}{1+\rho_{sd}}-\frac{\zeta_{\mathrm{FC}}(\rho_{sd}, \rho_{sl}, q_s)}{25} \leq 0, \quad , \tag{3.18}$$

where $u \geq \left(\frac{\rho_{sd}}{q_s}+\frac{1}{q_s}\right) > 0$. The above equation can be readily solved for u by using suitable numerical methods. Due to lack of space, the details of the solution is relegated to Appendix 3.7.

Finally, the best choice of the SNR threshold λ for which there is no significant BER penalty with the proposed hybrid cooperation scheme is obtained from u as

$$\hat{\lambda} = \lceil \frac{\rho_{sd}\tilde{u}}{1+\rho_{sd}} - \frac{\rho_{sd}}{q_s} \rceil, \tag{3.19}$$

where $\tilde{u} = \max\left(u, \frac{\rho_{sd}}{q_s}+\frac{1}{q_s}\right)$ and $\lceil x \rceil$ denotes the smallest integer larger than x[1].

The approximate BER and Ergodic capacity curves for hybrid cooperation technique with best SNR threshold λ are presented in Figures 3.5 and 3.6 respectively, and compared against the performance corresponding to full cooperation ($\lambda \to \infty$) and direct communication only ($\lambda = 0$). For the ease of presentation, the exact performance results are only presented for the hybrid cooperation case. It is readily observed that hybrid cooperation scheme with a carefully chosen SNR threshold results in a BER performance comparable to the full cooperation scheme while achieving the a capacity close to that of the direct communication.

[1] We limit λ to an integer to reduce the load on feedback channel in communicating λ and to account for possible errors in approximating λ as given by (3.18).

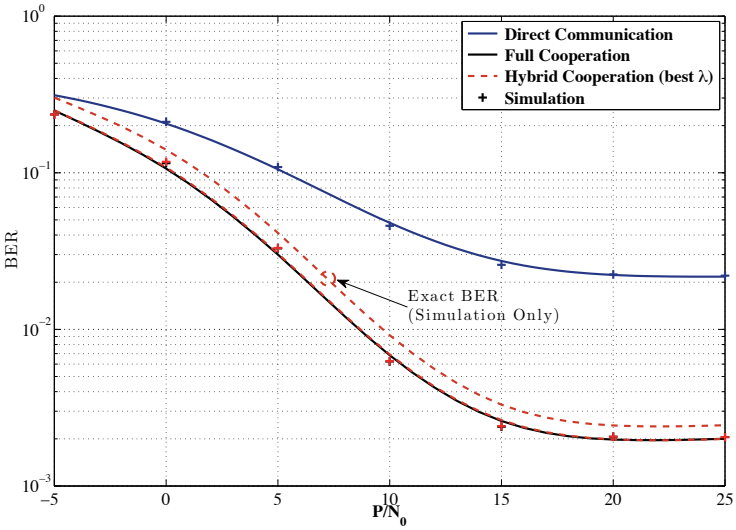

Figure 3.5: The BER curves for the proposed hybrid cooperation with one relay and best λ. $\Omega_{\phi,sd} = \Omega_{\varphi,s} = \Omega_{\varphi,l} = -3$ dB, $\Omega_{\phi,sl} = \Omega_{\phi,ld} = 0$ dB, and $Q_{th} = N_0 + 10$ dB.

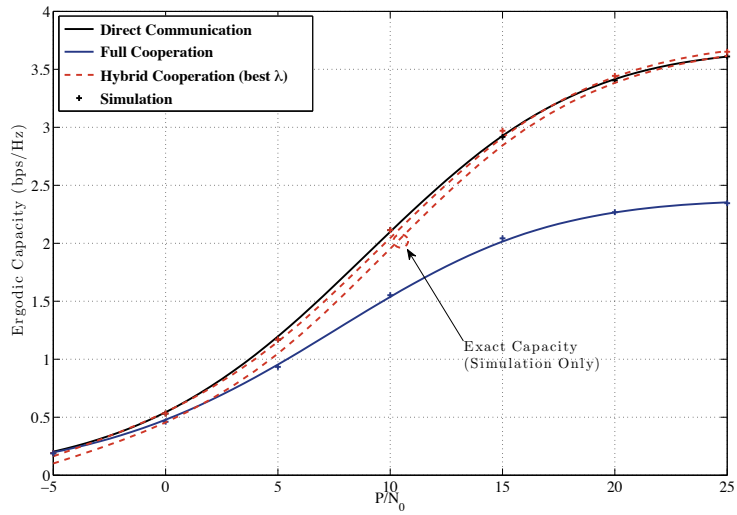

Figure 3.6: The Ergodic capacity of proposed hybrid cooperation with one relay and best λ. $\Omega_{\phi,sd} = \Omega_{\varphi,s} = \Omega_{\varphi,l} = -3$ dB, $\Omega_{\phi,sl} = \Omega_{\phi,ld} = 0$ dB, and $Q_{th} = N_0 + 10$ dB.

3.4.4 Outage Probability Calculation

Assuming the secondary communication is subject to a quality of service (QoS) constraint, which is realized by a target BER ε for a given modulation scheme; a ST is said to be in outage if the target BER at the SBS is not met even after being assisted by relays. Therefore, the outage probability for a given channel condition can be written as $P_{out} = \Pr(\zeta_{\mathrm{HC}}(\rho_{sd}, \rho_{sl}, q_s; \lambda) > \varepsilon)$. Moreover, for a specific modulation scheme, the target BER at the SBS can be translated to a corresponding target SNR ξ. For example, a target BER of 0.001 with BPSK modulation translates to a target SNR of approximately 7 dB. Considering the proposed hybrid cooperation technique, the outage probability can then be evaluated using the CDFs of the SNRs through the direct link and that through the relay as

$$P_{out}(\xi; \rho_{sd}, \rho_{sl}, q_s, \lambda) = \left(1 - F_{\gamma,sd}(\lambda)\right) F^{(\mathrm{d})}_{\gamma,sd}(\xi) H(\xi - \lambda) + F_{\gamma,sd}(\lambda) F^{(\mathrm{r})}_{\gamma,sd}(\xi), \tag{3.20}$$

which is the weighted sum of the outage probability through the direct link and that through the relay; with $H(x)$ representing the heaviside step function. The first term in (3.20) involves the CDF of $\gamma^{(\mathrm{d})}_{sd}$, which is given by $F^{(\mathrm{d})}_{\gamma,sd}(r) = 1 - \frac{1 - F_{\gamma,sd}(r)}{1 - F_{\gamma,sd}(\lambda)}$, where $F_{\gamma,sd}(r)$ is given by (3.5). The CDF of the $\gamma^{(\mathrm{r})}_{sd}$ in the second term of (3.20) is evaluated from the earlier derived MGF using the relation [10, eq. 1.6]

$$F^{(\mathrm{r})}_{\gamma,sd}(\xi) = \frac{1}{2\pi j} \oint \frac{\mathcal{M}^{(\mathrm{r})}_{\gamma,sd}(s)}{s} e^{s\xi} ds. \tag{3.21}$$

The integrals in (3.13) and (3.21) can be numerically evaluated efficiently using available mathematical softwares or different numerical techniques, for example by virtue of the Euler summation technique [17] using the procedures demonstrated in [18].

The outage probability curves for different values of the target BER are plotted in Figure 3.7, where the SNR threshold is determined as $\hat{\lambda}$ (which is around 7 dB for higher values of P/N_0). From the presented curves, we observe that when $\xi \leq \hat{\lambda}$, the outage performance of the proposed hybrid cooperation scheme is similar with that of conventional cooperative scheme. However for $\xi > \hat{\lambda}$ the former scheme demonstrates higher outage. With the proposed hybrid cooperation scheme, the final SNR is not further boosted with the help of the relays when an SNR greater than $\hat{\lambda}$ can be readily achieved through the direct link itself. This also points to the fact that the SNR variation with the proposed hybrid cooperation is less compared to the conventional cooperation scheme.

The above finding further highlights the importance of considering the target BER and other system parameters such as the modulation scheme (or more precisely, the target SNR) alongside the achieved BER in determining the best SNR threshold $\hat{\lambda}$.

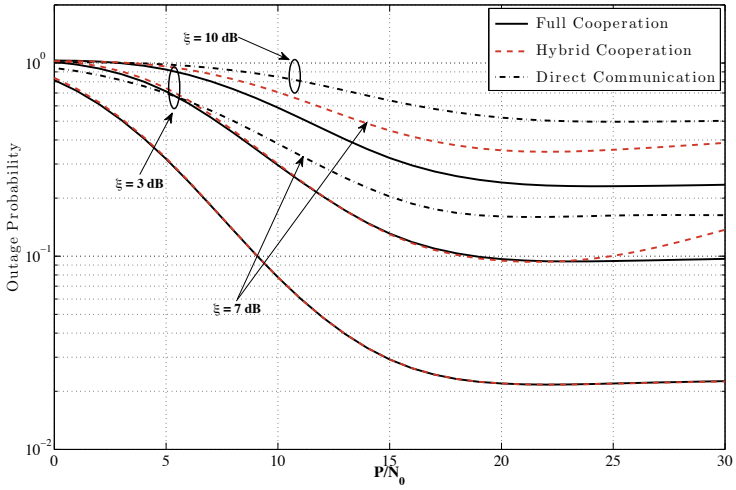

Figure 3.7: The Outage Probability for different target BER with BPSK modulation for the proposed hybrid cooperation involving a single relay. $\Omega_{\phi,sd} = \Omega_{\varphi,s} = \Omega_{\varphi,l} = -3$ dB, $\Omega_{\phi,sl} = \Omega_{\phi,ld} = 0$ dB, and $Q_{th} = N_0 + 10$ dB.

3.4.5 Impact of Interference Threshold Q_{th}

In this section we present some additional numerical results for the proposed hybrid cooperation scheme to demonstrate the impact of the interference-threshold Q_{th} on the performance of the proposed scheme. The average BER and the ergodic capacity curves for different values of the interference threshold Q_{th} are plotted against the normalized maximum transmit power in Figure 3.8 and Figure 3.9.

For the ease of presentation, curves presenting the exact BER performance are only presented for the interference threshold $Q_{th}/N_0 = 20$ dB in Figures 3.8 and 3.9. The curves for the other cases show similar trend and hence are omitted here. It is interesting to note that the approximation adopted on the SNR through the relay in this work is very tight at higher SNRs, as evident from the close match between the approximate BER curves and the exact BER curves. Moreover, we observe that the BER floor is reached at a higher and higher transmit powers with increasing interference threshold Q_{th}.

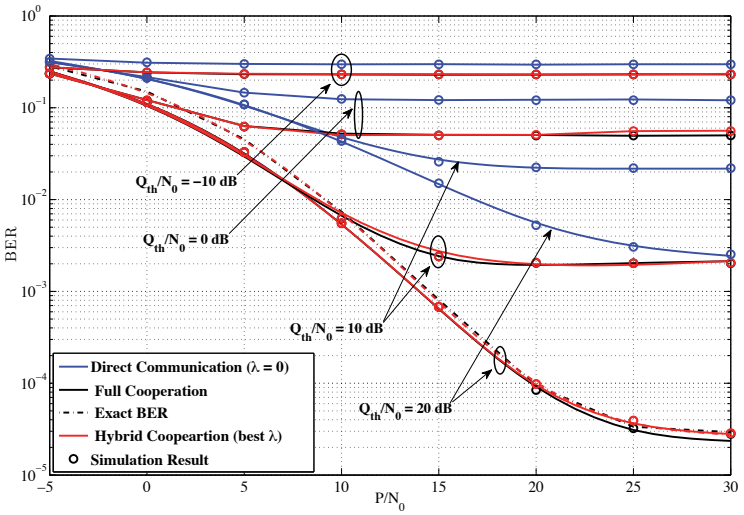

Figure 3.8: The BER curves for the proposed hybrid cooperation with one relay and best λ for different values of Q_{th}. The solid lines present the analytically derived approximate BER. $\Omega_{\phi,sd} = \Omega_{\varphi,s} = \Omega_{\varphi,l} = -3$ dB, $\Omega_{\phi,sl} = \Omega_{\phi,ld} = 0$ dB.

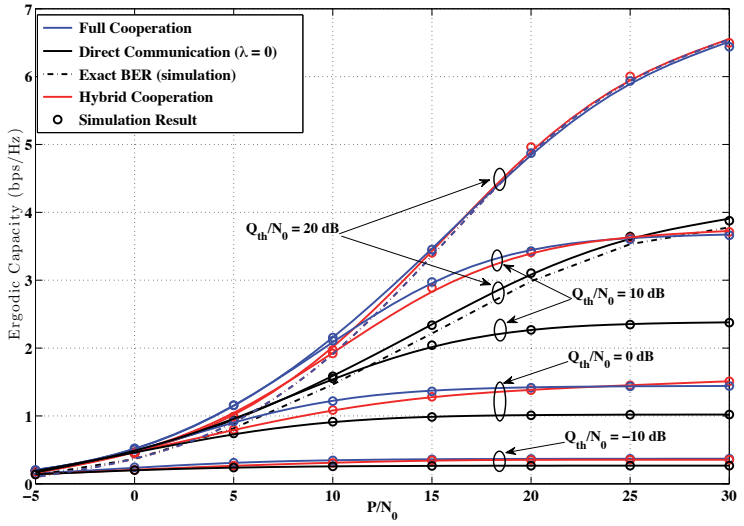

Figure 3.9: Ergodic capacity curves for the proposed hybrid cooperation with one relay and best λ for different values of Q_{th}. The solid lines present the analytically derived approximate BER. $\Omega_{\phi,sd} = \Omega_{\varphi,s} = \Omega_{\varphi,l} = -3$ dB, $\Omega_{\phi,sl} = \Omega_{\phi,ld} = 0$ dB.

3.5 Diversity-Multiplexing Tradeoff Analysis

Cooperation provides multiple and in most cases independent spatial channels between a source and its destination. The data rate of the source-destination link can be increased by transmitting independent information streams in parallel through the spatial channels. This effect is known as *spatial multiplexing*. Alternately, the multiple independent links between the source and the destination can be used to introduce *diversity* to combat channel fading [19]. Given multiple links between a source and destination, there is a fundamental tradeoff between how much *multiplexing gain* and the *diversity gain* can be extracted through cooperative communication. Furthermore higher spatial multiplexing gain comes at the price of sacrificing diversity [19, 20]. In this section, we focus on the diversity and multiplexing gain analysis of the proposed hybrid cooperation scheme.

Let us define the variable $\tilde{\rho} \triangleq \frac{P}{N_0}$. The *multiplexing gain* (MG) and the *diversity gain* (DG) for the traditional communication link (i.e. without interference constraint) as a function of the $\tilde{\rho}$ are respectively defined as $MG = \lim_{\tilde{\rho}\to+\infty} C(\tilde{\rho})/\log\tilde{\rho}$ and $DG = -\lim_{\tilde{\rho}\to\infty} \frac{\log(P_{out}(\tilde{\rho}))}{\log\tilde{\rho}}$ [20]. However, it is not appropriate to apply the traditional definitions of multiplexing and diversity gain in CRN due to the imposed interference constraint on the transmission powers of the STs [7]. Following the approach adopted in [7] and other similar works, we analogously define the multiplexing gain and the diversity gain of a relay assisted CRN under the proposed hybrid cooperation scheme as

$$\begin{aligned} MG_{\mathrm{HC}} &= \lim_{\tilde{\rho}\to+\infty} \frac{\lim\limits_{\Omega_{\varphi,I}\to 0} C_{\mathrm{HC}}(\tilde{\rho})}{\log\tilde{\rho}}, \\ DG_{\mathrm{HC}} &= -\lim_{\tilde{\rho}\to\infty} \frac{\lim\limits_{\Omega_{\varphi,I}\to 0} \log(P_{out,HC}(\tilde{\rho}))}{\log\tilde{\rho}}. \end{aligned} \tag{3.22}$$

The achievable rate of the proposed hybrid cooperation scheme as a function of the $\tilde{\rho}$ is $R_{\mathrm{HC}}(\tilde{\rho}) = \big(1 - F_{\gamma,sd}(\lambda)\big) C_{\mathrm{DC}}(\tilde{\rho}) + F_{\gamma,sd}(\lambda) C_{\mathrm{FC}}(\tilde{\rho})$. Similarly, the corresponding outage probability is $P_{out,\mathrm{HC}}(\tilde{\rho}) = \big(1 - F_{\gamma,sd}(\lambda)\big) P_{out,\mathrm{DC}}(\tilde{\rho}) + F_{\gamma,sd}(\lambda) P_{out,\mathrm{FC}}(\tilde{\rho})$. For a given $\tilde{\rho}$ and in the absence of any constraints on the received interference, the capacity through the cooperative link is half of that through the direct communication link due to the use of the double resource slots with the former scheme, i.e. $C_{\mathrm{FC}}(\tilde{\rho}) = \frac{1}{2} C_{\mathrm{DC}}(\tilde{\rho})$. Hence, the multiplexing gain of the proposed hybrid cooperation scheme is straightforwardly

obtained as

$$MG_{\mathrm{HC}}(\lambda) = \left(1 - \frac{F_{\gamma,sd}(\lambda)}{2}\right)\eta, \tag{3.23}$$

where $\eta \triangleq \lim_{\tilde{\rho}\to+\infty} R_{\mathrm{DC}}(\tilde{\rho})/\log\tilde{\rho}$ is the multiplexing gain of the direct link, which has the range $\eta \in (0,1)$.

Following well known results on the diversity-multiplexing tradeoff in traditional and cooperative channels, the optimal diversity gain of the direct communication link and that of the cooperative link are respectively given by $DG_{\mathrm{DC}}(\eta) = 1-\eta$ and $DG_{\mathrm{FC}}(\eta) = 2(1-2\eta)^{+}$, [20] where $(x)^{+} = \max(0,x)$. Therefore, the optimal diversity-multiplexing tradeoff for the proposed hybrid cooperation scheme is thereby given by

$$DG_{\mathrm{HC}}(\eta,\lambda) = \left(1 - F_{\gamma,sd}(\lambda)\right)(1-\eta) + 2F_{\gamma,sd}(\lambda)(1-2\eta)^{+}. \tag{3.24}$$

Discussion on Diversity-Multiplexing Tradeoff Analysis

It is evident from (3.24) that the proposed hybrid cooperation scheme provides a tradeoff between the multiplexing gain and diversity gain in the high SNR regimes. However, an underlay CRN is most likely to operate in the low to medium SNR regime due to the interference temperature constraint at the PRs. As we have observed from the findings presented in Section 3.4, the proposed hybrid cooperation technique delivers the diversity gain of the full cooperation scheme at the multiplexing gain of the direct link in the practical operating SNR regimes of an underlay CRN, thus highlighting the advantages of the proposed technique in CR communication.

The diversity multiplexing tradeoff for the proposed hybrid cooperation scheme is illustrated in Figure 3.10 and is compared against that of the traditional cooperation scheme and the direct communication (i.e. no relay). Moreover, the upper bound on the optimal diversity gain for the AF relaying scheme with a single relay, as given by $DG(\eta) = (1-\eta) + (1-2\eta)^{+}$ [20], is also plotted for comparison.

3.6 Relay Selection Schemes

When there are more than one potential relays to assist the source SU, it is spectrally most efficient to choose only one of those potential relays to amplify and forward the message

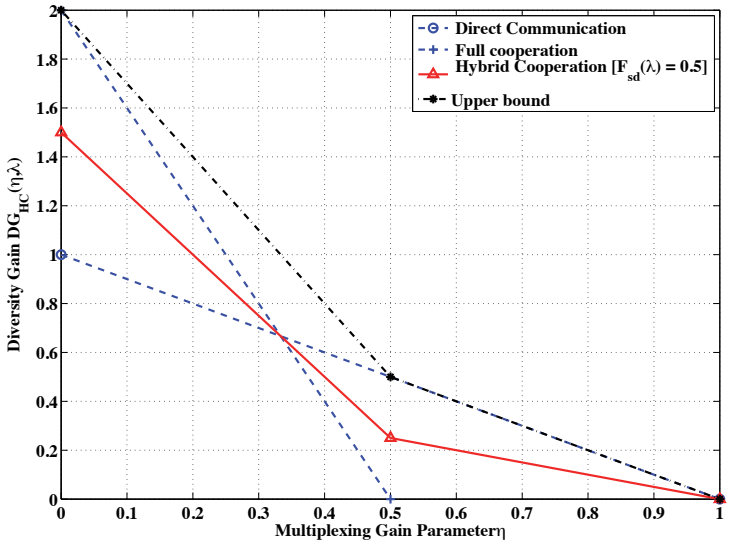

Figure 3.10: The optimal diversity-multiplexing tradeoff for the proposed hybrid cooperation scheme with a single relay.

signal of the transmitter to the SBS [21]. In this section, we present further analysis of the proposed hybrid cooperation scheme with multiple relays, wherein one relay is selected to assist the secondary transmission. In the following sequel, we assume the relay selection is performed at the SBS.

Best-Relay Selection Strategy

Let us consider the cooperative link, i.e. the link from the secondary source to the SBS through a relay. In the best relay selection strategy, the "best relay" is defined as the relay that maximizes the end-to-end SNR of the relayed link while satisfying the interference temperature constraint Q_{th}. Mathematically, the SNR of the message signal received at the SBS through the "best relay" is given by $\hat{\gamma}_l = \max_l(\gamma_l) \approx \max_l\{\min(\gamma_{sl}, \gamma_{ld})\}$.

With the given definition of the best relay, the CDF of the SNR $\hat{\gamma}_l$ is obtained as $F_{\hat{\gamma},l}(r) = \prod_{l=1}^{L}\left(F_{\gamma,l}(r)\right)$ [14]. Assuming every potential relay is equally faded, i.e. γ_l are independently and identically distributed (i.i.d.) for all l, the PDF of $\hat{\gamma}_l$ is given by [14]

$$f_{\hat{\gamma},l}(r) = L f_{\gamma,l}(r) F_{\gamma,l}(r)^{L-1}. \tag{3.25}$$

The approximate distributions of $f_{\gamma,l}(r)$ and $F_{\gamma,l}(r)$ are given earlier. Using those given distributions, the MGF $\mathcal{M}_{\hat{\gamma},l}(s)$ of $\hat{\gamma}_l$ can be subsequently approximated as $\mathcal{M}_{\hat{\gamma},l}(s) = \mathbb{E}[\exp(-s\hat{\gamma}_l)]$. The resulting MGF can be derived in closed form using any suitable mathematical software or even by hand. However, it has a long and cumbersome expression, and hence is not presented here for the ease of readability. Subsequently, the SNR $\hat{\gamma}^{(\mathrm{r})}$ of the combined signal at the SBS after the two TS communication through the relay is given $\hat{\gamma}^{(\mathrm{r})} = \gamma_{sd}^{(1)} + \hat{\gamma}_l$. Finally, the final end-to-end SNR at the SBS considering the proposed hybrid cooperation scheme is obtained as $\mathcal{M}_{\hat{\gamma}}(s) \geq \left(1 - F_{\gamma,sd}(\lambda)\right) \mathcal{M}_{\gamma,sd}^{(\mathrm{d})}(s;\lambda) + F_{\gamma,sd}(\lambda)\mathcal{M}_{\gamma,sd}^{(1)}(s;\lambda)\mathcal{M}_{\hat{\gamma},l}(s)$.

The BER and the ergodic capacity of the source ST to destination SBS communication with multiple relays under the best-relay selection strategy can be readily evaluated following the steps outlined in Section 3.4. The BER and the ergodic capacity curves with different number of relays under the best relay selection strategy are respectively presented in Figures 3.11 and 3.12. It is observed that increasing the number of relays greatly improve the BER performance. However, the gains in terms of the ergodic capacity from having more relays is not so profound, especially with the proposed hybrid cooperation scheme.

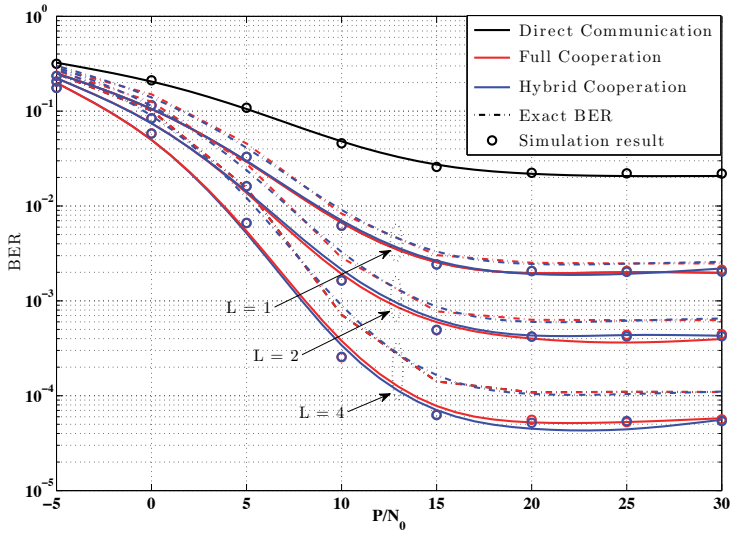

Figure 3.11: BER curves for the proposed hybrid cooperation with multiple relays and best λ. The solid lines present the analytically derived approximate BER. $\Omega_{\phi,sd} = \Omega_{\varphi,s} = \Omega_{\varphi,l} = -3$ dB, $\Omega_{\phi,sl} = \Omega_{\phi,ld} = 0$ dB.

3.7 Conclusion

Cooperative communication is known to effectively improve the performance of a wireless link by generating multiple copies of the message signal over independent channels, and hence generating diversity. In order to balance a between SNR enhancement and over-utilization of scarce opportunistic resources, we have proposed a novel hybrid cooperation technique in this contribution, and derived lower bounds on its error rate and the outage performance under the constraint of satisfying a maximum interference temperature constraint at a co-exisiting PR. The proposed scheme is found to achieve significantly higher capacity at a much lower BER compared to the conventional amplify-and-forward cooperation scheme. The performance gains observed demonstrate the benefits of the proposed technique for an underlay Cognitive Radio Network (CRN).

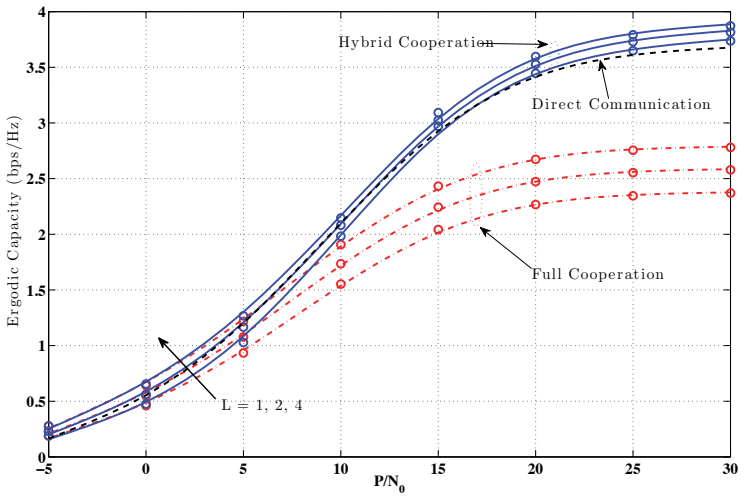

Figure 3.12: Ergodic Capacity curves for the proposed hybrid cooperation with multiple relays and best λ. The solid lines present the analytically derived approximate BER. $\Omega_{\phi,sd} = \Omega_{\varphi,s} = \Omega_{\varphi,l} = -3$ dB, $\Omega_{\phi,sl} = \Omega_{\phi,ld} = 0$ dB.

Appendix 3-A: Approximating the BER of the Direct Link

Using (3.13) and the definition of the MGF, the BER through the direct link is given by

$$\begin{aligned}
\zeta_{\mathrm{DC}}(\rho_{sd},q_s;\lambda) &= \frac{1-F_{\gamma,sd}(\lambda)}{\pi}\int_0^{\frac{\pi}{2}} \mathcal{M}^{(\mathrm{d})}_{\gamma,sd}\left(\frac{1}{\sin^2 x};\lambda\right) dx \\
&\approx \frac{1-F_{\gamma,sd}(\lambda)}{4}\mathcal{M}^{(\mathrm{d})}_{\gamma,sd}(1;\lambda) \\
&= \frac{e^{-\lambda/\rho_{sd}(1+\rho_{sd})}}{4(1+\rho_{sd})}\left\{\frac{\rho_{sd}-\lambda q_s/\rho_{sd}}{1+\lambda q_s/\rho_{sd}}e^{-1/q_s}+1\right\}+ \\
&\quad \frac{\rho_{sd}}{4q_s}e^{\rho_{sd}/q_s}\mathrm{Ei}\Big(-(1+\rho_{sd})\,(1/q_s+\lambda/\rho_{sd})\Big) \\
&\approx \frac{e^{-\lambda/\rho_{sd}(1+\rho_{sd})}}{4(1+\rho_{sd})}\left\{\frac{\rho_{sd}-\lambda q_s/\rho_{sd}}{1+\lambda q_s/\rho_{sd}}e^{-1/q_s}+1\right\}- \\
&\quad \frac{\rho_{sd}}{8q_s}e^{-1/q_s-\lambda-\lambda/\rho_{sd}}\ln\left(1+\frac{2q_s\rho_{sd}}{(1+\rho_{sd})(\rho_{sd}+\lambda q_s)}\right) \\
&\approx \frac{e^{-\lambda/\rho_{sd}(1+\rho_{sd})}}{4(1+\rho_{sd})}\left\{\frac{\rho_{sd}-\lambda q_s/\rho_{sd}}{1+\lambda q_s/\rho_{sd}}e^{-1/q_s}+1\right\}- \\
&\quad \frac{\rho_{sd}e^{-1/q_s-\lambda-\lambda/\rho_{sd}}}{4(1+\rho_{sd})(1+\lambda q_s/\rho_{sd})+4q_s} \\
&= \frac{e^{\frac{\rho_{sd}}{q_s}-u}}{4}\left\{\frac{\rho_{sd}}{uq_s}\left(\frac{1}{u+1}+\frac{1}{\rho_{sd}}\right)+\frac{1}{1+\rho_{sd}}\left(e^{1/q_s}-1\right)\right\}, \quad (3.26)
\end{aligned}$$

where $u \triangleq (1+\rho_{sd})(1/q_s+\lambda/\rho_{sd})$. The first approximation in (3.26) follows from approximating the integral by a 2-point trapezoidal sum [13, Eq. 25.4.1]. The second simplification results from approximating the exponential integral by its upper bound $\mathrm{Ei}(-x) < -\frac{1}{2}\exp(-x)\ln\left(1+\frac{2}{x}\right)$ for $x>0$ [13, Eq. 5.1.20]. The last step involves approximating the natural logarithm $\ln(x)$ by its first order area hyperbolic series expansion $\ln(x) = \frac{2(x-1)}{x+1}$ [13, Eq. 4.1.27].

It must be noted here that for some extreme operating regimes (e.g. at low or high transmit powers), some of the above approximations are not very tight. However, these approximations are used to evaluate the BER for the purpose of determining the SNR threshold λ, and not in approximating the BER itself. Hence, the above approximation for $\zeta_{\mathrm{DC}}(\rho_{sd},q_s;\lambda)$, which results in a simple expression involving λ, is suitable for the purpose in hand. Moreover, λ is rounded to the largest positive integer that satisfies $\zeta_{\mathrm{DC}}(\rho_{sd},q_s;\lambda) \ll \zeta_{\mathrm{FC}}(\rho_{sd},\rho_{sl},q_s)$ in order to account for any possible approximation errors.

Appendix 3-B: Solving (3.18) to Determine the SNR Threshold

Equation (3.18) requires

$$\frac{\rho_{sd}}{uq_s}e^{\frac{\rho_{sd}}{q_s}-u}\left(\frac{1}{u+1}+\frac{1}{\rho_{sd}}\right)+\frac{\left(e^{1/q_s}-1\right)e^{\frac{\rho_{sd}}{q_s}-u}}{1+\rho_{sd}}-\frac{\zeta_{\mathrm{FC}}(\rho_{sd},\rho_{sl},q_s)}{25}\leq 0, \tag{3.27}$$

where $u \geq (\frac{\rho_{sd}}{q_s}+\frac{1}{q_s}) > 0$. Let us define the constants $a \triangleq \frac{\rho_{sd}}{q_s}e^{\rho_{sd}/q_s}$, $b \triangleq \frac{\left(e^{1/q_s}-1\right)e^{\frac{\rho_{sd}}{q_s}}}{1+\rho_{sd}}$, and $K = \frac{\zeta_{\mathrm{FC}}(\rho_{sd},\rho_{sl},q_s)}{25}$. Using these definitions, we can express the left hand side of (3.27) as the function $f(u) = ae^{-u}/u(u+1) + ae^{-u}/u\rho_{sd} + be^{-u} - K$. By inspection, we observe that $f(u)$ is a monotonically decreasing function of u with a maximum value of $\frac{1}{1+\rho_{sd}}\left(\frac{\rho_{sd}q_s e^{-1/q_s}}{1+\rho_{sd}+q_s}+1\right)-K$ at $u = \frac{\rho_{sd}}{q_s}+\frac{1}{q_s}$ and a minimum value of $-K$ as $u \to \infty$.

The variable ρ_{sd}, which is defined as $\rho_{sd} = \frac{P\Omega_{\phi,sd}}{N_0}$, is in fact the achievable SNR on the direct link with maximum transmit power P. Similarly, the variable q_s, defined as $q_s = \frac{P\Omega_{\varphi,s}}{Q_{th}}$ is in fact the received interference power at the PR corresponding to the maximum transmit power P, normalized by the interference threshold Q_{th}. On the other hand, the constant K is a factor of the BER achieved at a particular SNR under the full cooperation scheme.

To observe the behavior of the function $f(u)$, let us consider its maximum value at high and low SNR regimes. At low SNRs $\rho_{sd} \to 0$ and $q_s \to 0$, and the associated value of the maximum of the function $f(u)$, $f(\frac{\rho_{sd}}{q_s}+\frac{1}{q_s}) \to 1-K$, which is a positive value.

On the other hand, at high SNRs, $\rho_{sd} \to \infty$ and $q_s \to \infty$. Therefore, the minimum value of u (at which $f(u)$ is maximized), $\frac{\rho_{sd}}{q_s}+\frac{1}{q_s} \to \frac{\rho_{sd}}{q_s}$. Correspondingly, the maximum value of $f(u)$ approaches $f(\frac{\rho_{sd}}{q_s}) \to \frac{q_s}{\rho_{sd}+q_s}-K$. The variable K is a factor of the BER, which approaches zero much faster than the value of $\frac{q_s}{\rho_{sd}+q_s}$ as the SNR $\to \infty$. Hence $\frac{q_s}{\rho_{sd}+q_s}-K \to \frac{q_s}{\rho_{sd}+q_s} > 0$. Therefore, we observe that the maximum of the monotonically decreasing function $f(u)$ is always greater than 0 in all SNR conditions. Hence, we can confirm that $f(u)$ has one real root, and therefore we can satisfy the condition in (3.27) by selecting any value of u greater than the root of $f(u)$.

To find the roots of $f(u)$, we write the equation $f(u) = 0$, and modify it by introducing the variable v defined as a function of u as $v = \exp(v)$. The modified equation $f(u) = 0$

then becomes

$$\begin{aligned}
\frac{ae^{-u}}{u(u+1)}+\frac{ae^{-u}}{u\rho_{sd}}+b\exp(-u)-K &= 0\\
\frac{a}{v\ln(v)\Big(\ln(v)+1\Big)}+\frac{a}{v\ln(v)\rho_{sd}}+\frac{b}{v}-K &= 0\\
\left(\frac{a}{2}-\frac{a}{2\rho_{sd}}+b\right)+\left(a+\frac{a}{\rho_{sd}}-4b-K\right)v+\left(\frac{a}{2}+\frac{3a}{2\rho_{sd}}+3b+4K\right)v^2-3Kv^3 &= 0.
\end{aligned} \tag{3.28}$$

The roots of the final cubic equation in (3.28) can be easily obtained, from which u is given by $u=\ln(v')$, where v' is the smallest positive real root of (3.28). In obtaining (3.28) above, we have approximated $\ln(v)$ by its first order area hyperbolic series expansion $\ln(x)=\frac{2(x-1)}{x+1}$ [13, Eq. 4.1.27].

Bibliography

[1] S. Haykin, "Cognitive radio: Brain-empowered wireless communications," *IEEE Journal on Selected Areas in Communication*, vol. 23, no. 2, pp. 201–220, Feb. 2005.

[2] A. Goldsmith, S. A Jafar, I. Maric, and S. Srinivasa, "Breaking spectrum gridlock with cognitive radios: An information theoretic perspective," *Proceedings of the IEEE*, vol. 97, no. 5, pp. 894–914, May 2009.

[3] M. Gastpar, "On capacity under receive and spatial spectrum-sharing constraints," *IEEE Transactions on Information Theory*, vol. 53, no. 2, pp. 471–487, Feb. 2007.

[4] A. Nosratinia, T. E Hunter, and A. Hedayat, "Cooperative communication in wireless networks," *IEEE Communications Magazine*, vol. 42, no. 10, pp. 74– 80, Oct. 2004.

[5] O. Simeone, Y. Bar-Ness, and U. Spagnolini, "Stable throughput of cognitive radios with and without relaying capability," *IEEE Transactions on Communications*, vol. 55, no. 12, pp. 2351–2360, Dec. 2007.

[6] K. Ben Letaief and W. Zhang, "Cooperative communications for cognitive radio networks," *Proceedings of the IEEE*, vol. 97, no. 5, pp. 878 –893, May 2009.

[7] Y. Zou, J. Zhu, B. Zheng, and Y.-D. Yao, "An adaptive cooperation diversity scheme with best-relay selection in cognitive radio networks," *IEEE Transactions on Signal Processing*, vol. 58, no. 10, pp. 5438–5445, Oct. 2010.

[8] S. I. Hussain, M. M. Abdallah, M.-S Alouini, M. Hasna, and K. Qaraqe, "Performance analysis of selective cooperation in underlay cognitive networks over rayleigh channels," in *Proceedings of the IEEE 12th International Workshop on Signal Processing Advances in Wireless Communications (SPAWC'11)*, San Francisco, USA, June 2011, pp. 116–120.

[9] A. Rabbachin, T. Q. S. Quek, H. Shin, and M. Z. Win, "Cognitive network interference," *IEEE Journal on Selected Areas in Communications*, vol. 29, no. 2, pp. 480–493, Feb. 2011.

[10] M. K. Simon and M.-S. Alouini, *Digital Communication over Fading Channels*, John Wiley & Sons, New Jersey, USA, 2nd edition, Dec. 2005.

[11] A.-S. Hu and S. D. Servetto, "On the scalability of cooperative time synchronization in pulse-connected networks," *IEEE Transactions on Information Theory*, vol. 52, no. 6, pp. 2725 –2748, June 2006.

[12] S. Ikki and M. H. Ahmed, "Performance analysis of cooperative diversity wireless networks over Nakagami-m fading channel," *IEEE Communications Letters*, vol. 11, no. 4, pp. 334–336, Apr. 2007.

[13] M. Abramowitz and I. Stegun, Eds., *Handbook of Mathematical Functions with Formulas, Graphs, and Mathematical Tables*, Dover Publications, New York, USA, 2nd edition, 1972.

[14] H. A. David and H. N. Nagaraja, *Order Statistics*, Wiley, New Jersey, USA, 3rd edition, Dec. 2003.

[15] T. M. Cover and J. A. Thomas, *Elements of Information Theory*, John Wiley & Sons, 2nd edition, Jul. 2006.

[16] K. A. Hamdi, "A useful lemma for capacity analysis of fading interference channels," *IEEE Transaction on Communications*, vol. 58, no. 2, pp. 411–416, Feb. 2010.

[17] J. Abate and W. Whitt, "Numerical inversion of Laplace transforms of probability distributions," *ORSA Journal on Computing*, vol. 7, no. 1, pp. 36–43, 1995.

[18] Y.-C. Ko, M.-S. Alouini, and M. K. Simon, "Outage probability of diversity systems over generalized fading channels," *IEEE Transaction on Communications*, vol. 48, no. 11, pp. 1783–1787, Nov. 2000.

[19] L. Zheng and D. N. C. Tse, "Diversity and multiplexing: a fundamental tradeoff in multiple-antenna channels," *IEEE Transactions on Information Theory*, vol. 49, no. 5, pp. 1073 – 1096, May 2003.

[20] K. Azarian, H. El Gamal, and P. Schniter, "On the achievable diversity-multiplexing tradeoff in half-duplex cooperative channels," *IEEE Transactions on Information Theory*, vol. 51, no. 12, pp. 4152 –4172, Dec. 2005.

[21] A. Bletsas, A. Khisti, D. P. Reed, and A. Lippman, "A simple cooperative diversity method based on network path selection," *IEEE Journal on Selected Areas in Communications*, vol. 24, no. 3, pp. 659– 672, Mar. 2006.

Paper C

A Relative Rate Utility based Distributed Power Allocation Algorithm for Cognitive Radio Networks

Nurul Huda Mahmood, Geir Egil Øien, Lars Lundheim and Umer Salim

In Proceedings of the 2012 International WDN Workshop on Cooperative and Heterogeneous Cellular Networks (WDN-CN2012) held in conjunction with IEEE PIMRC 2012, Sydney, Australia, September, 2012.

Chapter 4

A Relative Rate Utility based Distributed Power Allocation Algorithm for Cognitive Radio Networks

Nurul Huda Mahmood, Geir E. Øien, Lars Lundheim and Umer Salim

Abstract - In an underlay Cognitive Radio Network, multiple secondary users coexist geographically and spectrally with multiple primary users under a constraint on the maximum received interference power at the primary receivers. Given such a setting, one may ask "*how to achieve maximum utility benefit at the secondary users given the imposed interference temperature constraint*"? In an attempt at answering this question, we introduce a measure of the marginal secondary utility per unit primary interference (termed as *relative rate utility*) and propose a distributed algorithm that tries to maximize this measure. We present selected computer based Monte-Carlo simulation results, demonstrating the effectiveness of the introduced measure, and the improved performance of the proposed algorithm.

Keywords – Distributed resource allocation, cognitive radio network, interference pricing, power control.

4.1 Introduction

In multi-user communication, the interference channel (IFC) models the scenario where several transmitter-receiver pairs are active in parallel, with the data flow of each user pair influencing the others. The achievable sum-rate across the different user pairs in an IFC

is a commonly used measure of the system performance. Maximizing the sum rate across all user pairs is a well known challenging problem [1,2], and the difficulty is further exacerbated in wireless systems where transmitters are subject to a strict sum received power constraint, such as the underlay cognitive radio networks (CRN) [2]. A centralized approach to addressing this problem requires a prohibitive amount of signaling exchange and other complexities even for moderate network sizes, and therefore distributed technique are preferred [1]. However, distributed resource allocation techniques require a proper control and coordination mechanism among the competing users in order to avoid strong unwarranted interference at other nodes resulting from selfish and myopic behavior.

The use of *pricing* mechanisms as a control technique in resource allocation problems is commonly used in forcing competing users to behave more altruistically or to account for the utility of users in a more comprehensive way [1,3]. The idea of incentive and pricing as a control parameter for resource allocation among competing users operating in an IFC is well studied (see [1] for a comprehensive survey). Applying such pricing mechanisms in a CRN entails the additional task of controlling the secondary to primary interference in addition to the interference among the secondary user pairs (SU), and hence is not a straightforward extension. A non-exhaustive list of works investigating the concept of pricing as a control mechanism in CRNs include [4–7].

The works by Hong and Garcia [4] investigates the use of interference pricing in CRNs, where all SUs pay the same price for interfering at a given primary receiver (PR). In practice, different SUs, even when transmitting with the same transmit power. do not result in the same amount of interference at a particular PR, nor is the received signal-to-interference-plus-noise-ratio (SINR) at the intended secondary receiver (SR) the same. Therefore, the cost incurred by different SUs for interfering at a PR should not be the same. In [5], the authors propose a joint power/channel allocation scheme that improves the performance of an underlay CRN through a distributed pricing approach. In their work, the interference temperature constraint is implemented in the form of a power mask constraint at individual secondary transmitters (ST) instead of a sum interference power constraint, and as such the interaction among the interference signals from multiple SUs at a PR is not considered.

Another relevant work is reference [6] by Scutari et al., where the authors propose a game theoretic, totally decentralized approach to designing cognitive MIMO transceivers. In this contribution, the PRs are assumed to compute and communicate the maximum tolerable interference power for each ST, thus entailing primary-secondary cooperation. Distributed power control in a game theoretic framework is also studied in [7], where

different prices for the inter-secondary and secondary-primary interference are proposed. The secondary-primary interference price in [7] is an exponential function of the unutilized interference threshold. Computing these interference prices require each ST to have global channel state information (CSI) between all STs and all PRs, which require prohibitive signaling overhead even for networks of moderate size. Moreover, with global CSI available, the SUs can solve an optimization problem centrally to get the best decision for each SU through a simpler and more robust way.

In [8] a Distributed Interference Pricing (DIP) algorithm is presented for resource allocation over a conventional (non-cognitive) IFC. The DIP algorithm is a distributed game-theoretic resource allocation scheme for interference networks that only require local information at each node. The key idea is that each user announces an interference price, which is a measure of the relative change in its utility per unit interference perceived. With the knowledge of these 'interference prices', the transmitter then tries to maximize its net surplus which is its utility minus the total cost of interference summed over all unintended receivers.

We attempt at answering the question raised at the beginning of this paper by proposing a distributed power allocation algorithm that takes into consideration the inter-secondary interference, as well as that between the STs and PRs. The impact of the inter-secondary interference on the rate performance is quantified through an *'interference price'*, which is a measure of the marginal rate per unit secondary interference as in [8]. The main contribution of this work is a proposal to measure and then maximize the *relative achievable rate utility* of the SUs with respect to the interference it generates at the PRs. This is described using the term *'relative rate utility'*. Unlike most earlier works, this measure is unique for each ST, reflecting the facts that: i) different STs will cause different levels of interference at the PRs, even for the same amount of transmit power; and ii) the achievable rate for a given transmit power level is different for different SUs. in addition, with the proposed algorithm, the secondary system can operate independently from the primary system and still satisfy the interference temperature constraint at all PRs.

The rest of the paper is organized as follows. The general system model and the problem description are presented in Section 4.2, and the adopted interference prices are detailed in Section 4.3. The proposed algorithm is outlined in Section 4.4, and related simulation results are presented in Section 4.5. Finally concluding remarks are drawn in Section 4.6.

4.2 System Model and Problem Formulation

In the problem under investigation, a distributed multiuser secondary system with N active STs geo-spectrally coexisting with a cellular multiuser primary system with M active PRs is considered, where all the terminals are single input single output (SISO) devices. The secondary system can be a distributed ad-hoc-like peer-to-peer (P2P) multiuser network, or the multiple access channel (MAC) of a cellular system with multiple transmitters operating independently. Similarly, the considered model is general enough to include any narrowband primary system as long as there are multiple active PRs with constraints on the maximum received interference power. With multiple STs, the interference temperature constraint is on the sum interference power from all the STs and not on individual SU's interference contribution. An instance of the considered system setup is illustrated in Figure 4.1.

The interference within the primary system is assumed taken care of (e.g. through interference cancellation, or by using orthogonal transmission) and hence does not affect the interference temperature constraint at the PRs. On the other hand, such interference cancellation techniques are not assumed at the SRs, and thus, the inter-secondary interference cannot be ignored. The inter-secondary interference and the interference from the primary system at the SRs can be treated as an additional contribution to the Additive White Gaussian Noise (AWGN) by assuming that the primary system uses a random Gaussian codebook [9]. Such assumption further allows the implementation of low complexity decoders at the receivers [9] and simplifies the analysis of the secondary system in order to help reach some intelligible results and an understanding of the performance trends of the proposed technique. However, in practice, the inter-system interference may, in some scenarios, be slightly different from the Gaussian distribution [10].

At the time instant t, let $p_n(t)$ denote the SU S_n's transmission power and $h_{j,i}(t)$ denote the channel gain between the ST S_i to the SR S_j. Let $\sigma_n^2(t)$ represent the power of total AWGN plus interference from the primary transmitters at SR S_n and $g_{m,n}(t)$ represent the channel gain between the ST S_n and the PR P_m.

The complete channel matrix of the considered system is not assumed to be known at all the STs. Rather, we only consider that each node can approximately measure the channels that are associated with itself. Thus, a particular ST S_i is assumed to have measurements of $h_{j,i}$[1] $\forall\, j$, but not that of $h_{j,k}$ for any $k \neq i$. A block fading model is assumed for the channel variation, where all the transmitted symbols of the same block experience the

[1]The time index t is dropped henceforth for the sake of brevity.

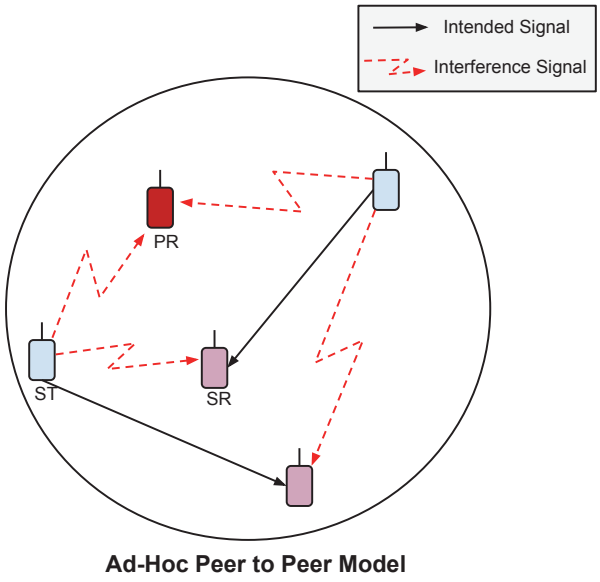

Figure 4.1: The System Model shown for the ad-hoc setup with two SUs and one PR. The SUs interfere at each other as well as at the PR.

same channel fade, but are independent across blocks and across users.

At the receiver S_n, the SINR of the message signal from the ST transmitted with power p_n is given by

$$\gamma_n = \frac{|h_{n,n}|^2 p_n}{\zeta_n + \sigma_n^2} \tag{4.1}$$

where $\zeta_n = \sum_{j \neq n} \zeta_{n,j} = \sum_{j \neq n} |h_{n,j}|^2 p_j$, is the total interference experienced at the receiver of S_n from the other STs. On the other hand, the total interference ξ_m experienced by the PR P_m from the STs is given by $\xi_m = \sum_{n=1}^{N} \xi_{m,n} = \sum_{n=1}^{N} |g_{m,n}|^2 p_n$. Under the Gaussian assumption on the interference, and considering that the corresponding Shannon capacity can be achieved at all SINRs in any resource slot, the maximum achievable rate R_n of the SU S_n is given by $R_n = \log(1+\gamma_n)$ [11].

Problem Formulation

In this contribution, we propose a distributed algorithm with the objective of maximizing the achievable sum-rate across the different user pairs in an IFC-CRN, where the following constraints are imposed on the STs

C-1 *Maximum transmit power constraint*:
$p_n \leq p_n^{max} \; \forall \; n \in \{1,2,\ldots,N\}$, and

C-2 *Sum interference constraint at PR*:
$\xi_m \leq \xi_m^{max} \; \forall \; m \in \{1,2,\ldots,M\}$.

Given the above constraints, the sum rate maximization problem can be mathematically expressed as

$$\begin{aligned} \max_{\{p_1,p_2,\ldots,p_N\}} \quad & R \triangleq \sum_{n=1}^{N} \log\left(1+\frac{|h_{n,n}|^2 p_n}{\zeta_n+\sigma_n^2}\right) \\ \text{s.t.} \quad & 0 \leq p_n \leq p_n^{\max} \quad \forall\, n \\ & \xi_m \leq \xi_m^{\max} \quad \forall\, m \end{aligned} \tag{4.2}$$

4.3 Interference Pricing as Control Mechanism

An increase in the transmitted power of an SU results in an increase in the interference experienced by the other SUs from this particular SU, subsequently resulting in a fall in their SINRs and hence their achievable rates. At the same time, this renders an additional limitation on the transmit powers of other SUs as a result of the sum interference constraint C-2 at the PRs. We use the term "*lost opportunity*" to refer to this indirect constraint on the transmit powers of other SUs due to the transmission of a given SU and redefine the utility of the SUs such that these effects are properly reflected.

In the absence of centralized control or coordination among the secondary users, SUs can act selfishly aiming at maximizing only its own utility with disregard to that of other SUs [12]. In such a situation, a penalty on the utility of an SU proportional to the 'disutility' it causes at other SUs through the use of pricing mechanisms can be imposed to restrain the selfish behavior; and instead achieve some socially beneficial objective. In this work, two types of prices are considered, one for the interference caused at other SUs (termed as '*inter-secondary interference price*', and denoted by μ), and the other for interference caused at the PRs (termed as '*relative rate utility*', and denoted by ν).

4.3.1 Inter Secondary Interference Price

The inter-secondary interference price of an SU is a reflection of the loss in its achievable rate due to the interference it experiences from the other SUs. In this work, we follow

a similar approach as in [8] and define it for the SU S_n as $\mu_n \triangleq -\frac{\partial R_n}{\partial \zeta_n}$. This reflects how the achievable rate of S_n changes with respect to the sum interference from other SUs. Using (4.1) and the expression for R_n given earlier, the inter secondary interference price is obtained as

$$\mu_n = \frac{|h_{n,n}|^2 p_n}{(\zeta_n + \sigma_n^2)\,(|h_{n,n}|^2 p_n + \zeta_n + \sigma_n^2)}. \tag{4.3}$$

With the knowledge of this inter-secondary interference price, a given SU S_n can estimate the resultant loss in the achievable rate of another SU S_j due to its own transmission with locally available CSI, which is given by $p_n \mu_j |h_{j,n}|^2$.

In order to restrain the selfish and myopic behavior of individual SUs, let us introduce the term '*rate utility*', defined as the difference between an SU's achievable rate and the estimated loss in the achievable rates of the other SUs due to the resultant interference from the SU. This rate utility reflects a more socially beneficial utility compared to the Shannon-achievable rate defined earlier, and is expressed as

$$U_n(p_n) = R_n - \sum_{j=1, j\neq n}^{N} \mu_j \zeta_{j,n}. \tag{4.4}$$

4.3.2 Relative Rate Utility

Since our objective is to maximize the secondary sum rate given the tolerable interference limit at the PRs, we are interested in measuring how the achievable rate changes with respect to the interference generated at a particular PR. Having defined the rate utility of an SU, we now introduce the term '*relative rate utility*', which is a measure of the rate utility per unit interference caused at the PRs. This relative rate utility ν_n of SU S_n is defined as the rate of change in the rate utility of S_n with respect to the interference $\xi_{m,n}$ that it generates at the PR P_m, i.e. $\nu_n = \frac{\partial U_n}{\partial \xi_{m,n}}$.

The interference price μ_n at the SRs can be calculated at and exchanged among the SRs. However, the same cannot be assumed in the case of the price of interfering at PRs, since the PRs are considered oblivious to the presence of, and thus can not cooperate with, the secondary system. Instead, we assume that each SU calculates this interference price ν_n and broadcasts it to other SUs.

With multiple PRs, the primary interference price will be different for interfering at different PRs. In that case, a particular ST should be concerned with the PR at which it

interferes the most. Let this PR be identified as the k^{th} PR, P_k. Hence, for each SU, $k_n = \arg\max_m |g_{m,n}|^2$. The interference experienced by this PR P_k from the ST S_n is $\xi_{k_n,n} = p_n |g_{k_n,n}|^2$.

Using (4.4) and the definition of the relative rate utility given above, ν_n can be expressed as

$$\nu_n = \frac{|h_{n,n}|^2}{|g_{k_n,n}|^2 (\zeta_n + \sigma_n^2) + \xi_{k_n,n} |h_{n,n}|^2} - \frac{\sum_{j \neq n} \mu_j |h_{j,n}|^2}{|g_{k_n,n}|^2}. \tag{4.5}$$

Once this is computed, each ST is assumed to broadcast it in an auction-like manner, the knowledge of which is then used to allocate resources among the SUs distributedly according to the algorithm detailed in the next section.

4.4 The Proposed Algorithm

We are now ready to present the proposed *relative rate utility based power allocation algorithm* (RUPA) in this section. RUPA is a sequential distributed algorithm that does not entail any primary-secondary cooperation and only requires minimum information exchange among the SUs. Before proceeding, let us define the *primary interference matrix* Ξ, whose element in the i^{th} row and j^{th} column is $\xi_{i,j}$. Each ST is assumed to have an updated local copy of this matrix.

Initialization

The algorithm starts with zero power at each ST. The primary interference matrix Ξ, is also initialized to zero at each ST.

Successive iterations

Each iteration of the algorithm begins with each ST computing the inter-secondary interference price μ_n and sharing it with the other STs. With $\mu_j \; \forall \; j \in \{1, 2, \ldots, N\}$ known, each ST can compute its relative rate utility ν_n and broadcast it among all the STs.

In this sequential algorithm only one ST updates its transmission power at each iteration, which is the ST with the highest relative rate utility ν_n. At each iteration, the ST with the highest ν_n increases its power by an incremental unit Δp, *provided it results in an increase in its utility*. Thereafter the ST updates the corresponding column of the primary

interference matrix Ξ and shares this column among all the STs, so that each ST can update its own copy of Ξ.

If the maximum transmit power is reached at any ST, it is removed from the list of contending STs in the successive iterations of the algorithm.

Conditions for termination of the algorithm

The above steps of the algorithm are repeated until any of the following termination conditions are reached:

- All STs transmit with maximum transmit power, i.e. $p_n = p_n^{max} \; \forall \, n \in \{1, 2, \ldots, N\}$,
- Interference at *any* PR equals the maximum Interference threshold, ξ^{max}.
- Increasing the transmit power results in a fall in the sum utility of the secondary systems, indicating that a local maxima is reached.

The algorithm pseudocode is presented in Algorithm 1.

Algorithm 1 Proposed RUPA Algorithm

```
Initialize: p_n = 0 ∀n; Continue = TRUE.
while Continue do
    Compute μ_n according to (4.3), and broadcast;
    Compute ν_n according to (4.5), and broadcast;
    ñ = arg max_n ν_n; p_ñ = p_ñ + Δp.
    while ξ_m > ξ_m^max for any PR m do
        p_ñ = (I_m^max − Σ_{j≠ñ, j=1}^{N} ξ_{m,j}) / |g_{m,ñ}|^2
    end while
    Update Ξ and broadcast
    if p_ñ = p_n^max then
        remove S_ñ from list of potential STs.
    end if
    Compute R_ñ^(l) =: Rate of ST S_ñ at this iteration (l).
    if p_n = p_n^max ∀ n OR ξ_m = ξ_m^max for any PR OR R_ñ^(l) < R_ñ^(l−1) then
        Continue = FALSE
    else
        Continue = TRUE
    end if
end while
```

4.4.1 Discussions on the algorithm

The optimality of the proposed algorithm and other related issues are briefly discussed in this section.

Performance of the algorithm

Having presented the algorithm, it is natural to ask "How well does the algorithm perform?". The problem setup constitutes an IFC, the performance of which is very difficult to analyze theoretically [2]. Instead, we attempt at answering this question by comparing the achievable rate performance of the algorithm with the maximum achievable rate obtained by *brute-force* or *exhaustive search*. Such brute-force methods have been used in the literature to compare the performance of resource allocation techniques in an IFC [1].

Comparative sum rate performance for a scenario with two PRs and two STs is presented. The maximum achievable rate is found by searching through the entire feasible region by taking very small steps at each iteration. The achievable sum rate found through this search method is presented and compared with the sum-rate performance of the algorithm in Figure 4.2. Four different cases are considered based on the relative mean power gain of the direct channel (ST to intended SR), the SU interference channel (ST to interfered SRs), and the primary interference channel (ST to PR). The different cases are presented in Table 4.1, where SNR is the mean power gain of the direct channel. A Rayleigh fading channel is assumed and an interference threshold equal to the noise power is considered for the simulations.

In all the four cases, the performance of the proposed algorithm is observed to be very close to the maximum achievable rate found through exhaustive search. The achievable rates flatten out at higher SNRs in the *interference-limited region*, as is common with IFCs [12, Ch 6]. Furthermore, the achievable rates for *Case 2* and *Case 3* are almost the same. This implies that the sum achievable rate of the secondary system is affected by the interference threshold at the PR more than the inter-secondary interference for the considered scenario. The presented comparison is an indication of the performance of this algorithm, though no claims are made about its optimality. Due to the non-convex nature of the optimization problem under consideration, an analytical investigation giving insights to optimal resource allocation techniques is not straightforward even though it would be an important and strongly desired extension of this work.

Table 4.1: Table showing the different test cases for Figure 4.2

Cases	**Description**	$\mathbb{E}[h_{i,k}^2]\,(i \neq k)$	$\mathbb{E}[g_{i,j}^2]$ (for any i, j)
Case 1	weak interference	$\mathbb{E}[h_{k,k}^2]/10$	$\mathbb{E}[h_{k,k}^2]/10$
Case 2	strong interference	$10 \times \mathbb{E}[h_{k,k}^2]$	$10 \times \mathbb{E}[h_{k,k}^2]$
Case 3	weak SU interference, strong PR interference	$\mathbb{E}[h_{k,k}^2]/10$	$10 \times \mathbb{E}[h_{k,k}^2]$
Case 4	strong SU interference, weak PR interference	$10 \times \mathbb{E}[h_{k,k}^2]$	$\mathbb{E}[h_{k,k}^2]/10$

Usefulness of the relative rate utility measure

The performance of the proposed RUPA algorithm in terms of the achievable sum rate of the secondary system is presented in Figure 4.3, and compared with the sum-rate maximizing Distributed Interference Pricing (DIP) algorithm from [8] (with an added interference temperature constraint). The convergence of the DIP algorithm is only guaranteed for certain utility measures, for example the high SINR approximation of the Shannon-rate given by $R = \log(\gamma)$. Therefore, a scenario with weak inter-secondary interference is considered when comparing the proposed RUPA with DIP algorithm. The monte-carlo simulation results presented in Figure 4.3 are for a scenario where $\mathbb{E}[|h_{k,k}|^2] = 0$ dB, $\mathbb{E}[|h_{i,k}|^2] = -15$ dB (for $i \neq k$) and $\mathbb{E}[|g_{i,j}|^2] = -5$ dB (for any i, j), where $\mathbb{E}[X]$ is the expectation operator over the statistics of the random variable X. The max transmit power $p_n^{\max} = 15$ dB and the noise power $\sigma_n^2 = \sigma^2 = 1\,\forall n$. The maximum interference threshold at the PRs is assumed $\xi_m^{max} = \sigma^2 + 10$ dB $\forall m$. Significant gain is observed in the rate performance of the proposed RUPA, demonstrating the usefulness of the proposed relative rate utility measure. It must also be noted here that, unlike the DIP algorithm, the convergence of proposed RUPA is not limited by the utility measure, though the performance is not optimal.

Sequential Gradient update vs one shot update

One may question the rationale behind proposing such a sequential gradient update algorithm, where the utility function given (4.4) is concave in p_n, and hence the optimum p_n can be solved for at each iteration. The reasons are two fold: *convergence*, and *interference constraint at PR*. Firstly, convergence of iteratively updating the power by maximizing the utility function as that given in (4.4) depends on the choice of the rate function. A sufficient condition for the convergence depending on the choice of the rate function is given in terms of the *coefficient of relative risk aversion*. This coefficient, which is used

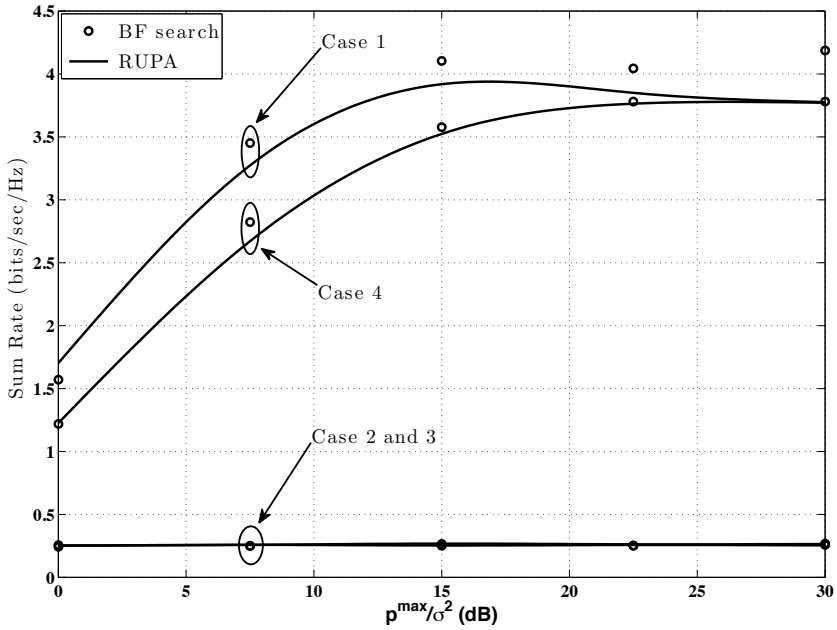

Figure 4.2: Secondary system sum rate performance of the proposed algorithm compared with maximum achievable sum rate obtained through exhaustive search across the entire feasible region. Two SU and two PRs are considered with $\xi_m^{max} = \sigma^2 \, \forall \, m$.

in economics, is a measure of the relative concavity of a rate function, and is defined by $CR_k(\gamma) = -\frac{R_n''(\gamma)\gamma}{R_n'(\gamma)}$, where $R_n'(\gamma)$ and $R_n''(\gamma)$ are respectively the first and second derivative of the rate function with respect to its argument. The sufficient condition for convergence in iterative update is that $CR_k(\gamma) \geq 1$ for all feasible SINRs, which unfortunately does not hold for the Shannon rate function considered in this problem [8].

Therefore, we opt for the sequential gradient based update of this algorithm instead of solving for p_n in order to guarantee the convergence of the algorithm. Moreover, the multiple interference-temperature constraints imposed by the PRs do not lend themselves to be easily translated to the said optimization problem.

Convergence Analysis

The rate of convergence of the above algorithm is shown in Figure 4.4 for a scenario with 5 SUs and 5 PRs under different interference scenario as described in Table 4.1 with SNR = 10 dB. The case "moderate interference" refers to a scenario where the the

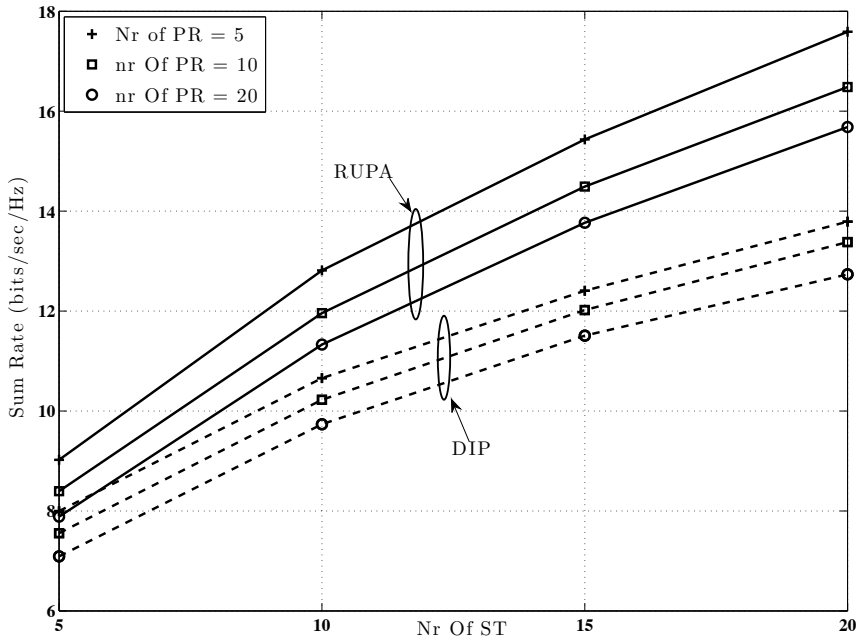

Figure 4.3: Secondary system sum rate performance with the proposed algorithm compared with modified version of DIP algorithm proposed in [8]. Results shown for different number of PRs and SUs with $\xi_m^{max} = \sigma^2 + 10$ dB $\forall m$.

SU interference channel and the primary interference channel have average power gain equal to that of the SU direct channel. The incremental power step at each iteration of the algorithm is set at $\Delta p = 0.125 p_n^{\max}$. It is observed that the algorithm converges fast to a solution, and hence is suitable for distributed implementation over slowly varying channels.

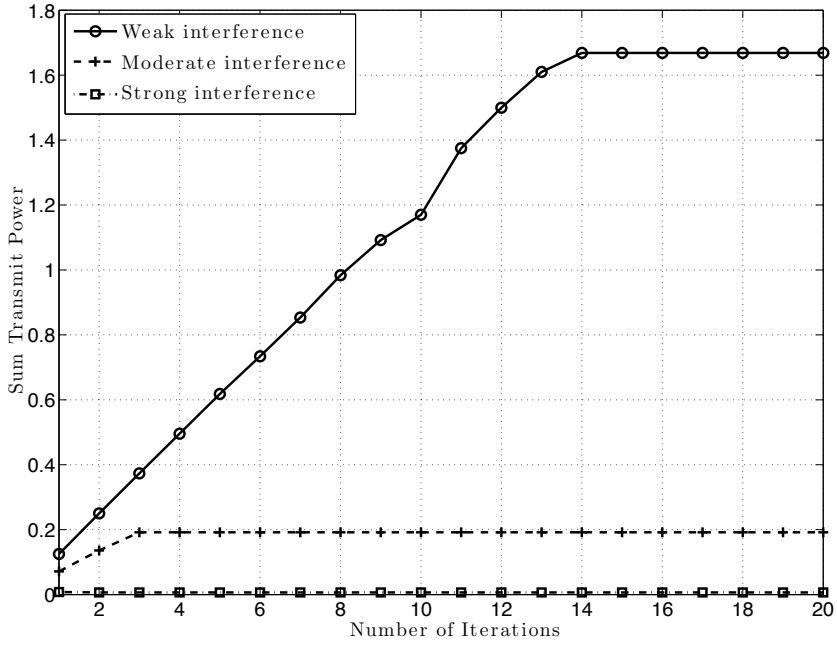

Figure 4.4: Rate of convergence of the proposed algorithm with 5 SUs and 5 PRs under different interference scenario with $\Delta p = 0.125 p_n^{\max}$ and $\frac{p^{\max}}{\sigma^2} = 10$ dB with $\mathbb{E}[h_{k,k}^2] = 1$ and $\xi_m^{max} = \sigma^2 \forall m$.

Scalability with Network Size

Scalability in the context of a wireless network can be defined as its ability to accommodate an increasing number of elements or nodes and/or spatial network size [14]. In this paper, we have considered a secondary system that coexists geo-spectrally with a primary system, where the communication between the nodes takes place over a single-hop. The spatial range of such single-hop systems is limited by the radio-coverage of the nodes, and hence, consideration for scalability with spatial size of the network is beyond the scope of this contribution. The issue of scalability with node size is discussed in the next section.

Signaling Overhead Analysis

At each iteration, each ST broadcasts μ_n and ν_n, and the selected ST, $S_{\tilde{n}}$, broadcasts $\xi_{m,\tilde{n}} \forall m$. Hence, each of the N SUs have to broadcast 2 single byte information messages, in addition to the selected ST broadcasting M-byte information message at each iteration as explained below. Thus, there are $2N+M$ byte broadcast messages in total at each iteration.

The broadcasted pricing messages are quantized scalar variables from a continuous, rather than discrete distribution. This naturally introduces some quantization noise, raising the question of accuracy of the control information. Note here that, the pricing information is used by each SU to calculate its relative rate utility. These utilities are then compared against each other to choose the 'selected SU' at each iteration, but are not directly used in the power allocation step. Hence, as long as these sets of information at the different SUs are at the same level of accuracy, the quantization error does not effect the end-performance. Thus, we have assumed that representing the pricing information by a byte length message gives reasonable accuracy.

In contrast, having full channel knowledge at all SUs would require an $(M+N)$-byte information message broadcast by each SU. This leads to $N(M+N)$ information exchanges in total, which scales quadratically with the size of the network, in comparison with the linear scaling in the proposed algorithm.

The typical size of a physical layer broadcast message symbol is around $3-6$ bytes [15] which includes header, information about sender, and the actual message. But this signaling overhead is insignificant compared to the gain in achievable rate obtained by exchanging this information as shown in Figure 4.3 and further discussed in Section 4.5.

Moreover, the broadcasting of price information can take place over a separate channel that is not subject to the interference temperature constraint so as to enhance the coverage area of the broadcast messages, as is commonly considered in underlay CRNs. For example, the signaling broadcast can be over a dedicated narrowband licensed channel or the publicly available unlicensed ISM band.

Other Issues

In this algorithm, we assume the SUs are 'honest' and cooperate fully with other SUs. Incentive issues that may occur in networks with non-cooperating users, such as users announcing wrong price information in order to increase its own utility at the expense of

the overall network utility, are ignored. There are ways to control these issues, for example, by making the algorithm fixed and inaccessible such that it cannot be manipulated. However, such a discussion is beyond the scope of this paper.

4.5 Numerical results

Matlab® based Monte-carlo simulation results evaluating the performance of the proposed algorithm in terms of the achievable sum rate under different scenarios are presented in this section. Results are obtained by averaging over many runs ($50,000 - 500,000$ depending on the scenario and required runtime) of the algorithm. A Rayleigh fading channel is assumed for all the presented cases.

4.5.1 Impact of network size

The Secondary system sum rate performance for different numbers of STs and PRs is plotted against $p^{\max}/\sigma^2$ in Figure 4.5. The same interference threshold is considered at all the PRs, and is 10 dB higher than the noise power. For this given interference threshold, we observe that at low transmit power, there is almost no impact of increasing the number of PRs on the sum rate. However, at higher SNRs, the impact of the constraint imposed by the PRs on the transmission powers of the STs become evident. This is because the interference threshold constraint becomes tighter as the number of PRs are increased. Furthermore, the impact of the inter-secondary interference on the sum rate is manifested in the flattening of the sum rate curve at higher SNRs, as also observed previously. In addition, a peak in the sum rate is observed for a large number of STs at moderate SNR values, after which the sum rate falls due to the dual effect of the increased received power constraint at the PRs and the increased inter-secondary interference from other STs.

4.5.2 Impact of interference threshold

The impact of the interference threshold for different channel scenarios is presented in Figure 4.6, where the secondary sum rate is plotted against the interference threshold (normalized by noise power) for five PUs and five SUs with $p^{\max}/\sigma^2$ set at 20 dB. The SU direct channel average power gain is varied between 0 dB and -10 dB with different combinations of the average power gain of the inter-secondary and secondary-primary interference channels.

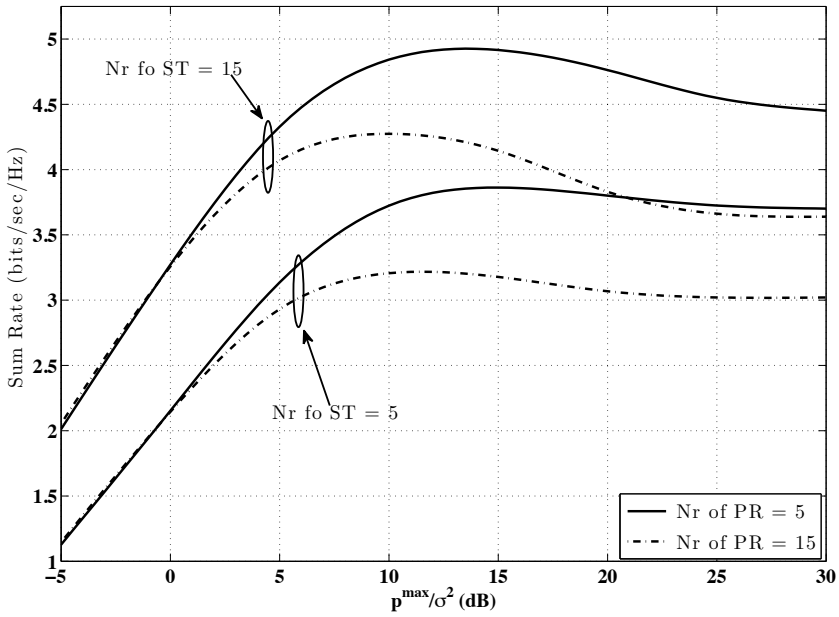

Figure 4.5: Secondary system sum rate for different number of STs and PRs plotted against $\frac{p^{\max}}{\sigma^2}$ with $\mathbb{E}[h_{k,k}^2] = \mathbb{E}[h_{i,k}^2]\,(i \neq k) = \mathbb{E}[g_{i,j}^2]$ (for any i, j) $= 1$ and $\xi_m^{max} = \sigma^2 + 10$ dB $\forall\, m$.

The most notable observation from these curves is the behavior at high and low interference thresholds. At high interference thresholds, which correspond to a relaxed received power constraint, there are virtually no impact of the interference temperature constraint on the secondary performance and the secondary system behaves like a non-cognitive network with the inter-secondary interference becoming the limiting factor in the performance. On the other hand, at very tight interference constraint, the performance is severely bottlenecked by the interference temperature constraint at the PRs.

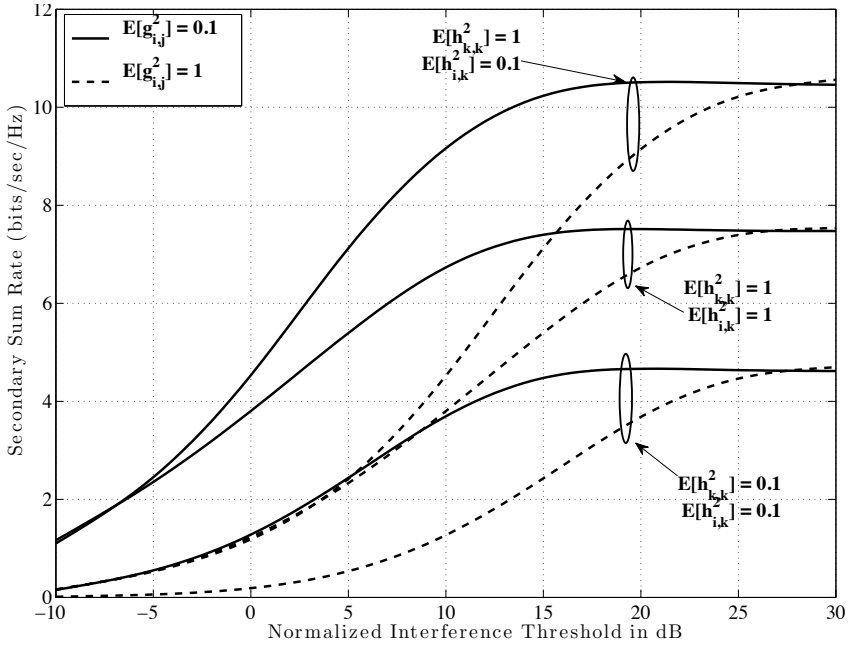

Figure 4.6: Secondary system sum rate performance for different channel conditions plotted against interference threshold at PR (normalized by noise power) with five PRs and five STs.

In order to demonstrate the interference condition at the different PRs, a bar chart representing the distribution of the interference at different PRs is illustrated in Figure 4.7 for the strong interference scenario with 5 STs and 5 PRs. It is readily observed that there are no cases of the interference constraint being violated at any of the PR, while on average the max interference is reached at each PR for about 20% of the cases. This figure shows conclusively that the interference temperature constraint indeed does protect the primary users from the interference, keeping the interference power below the pre-specified acceptable level.

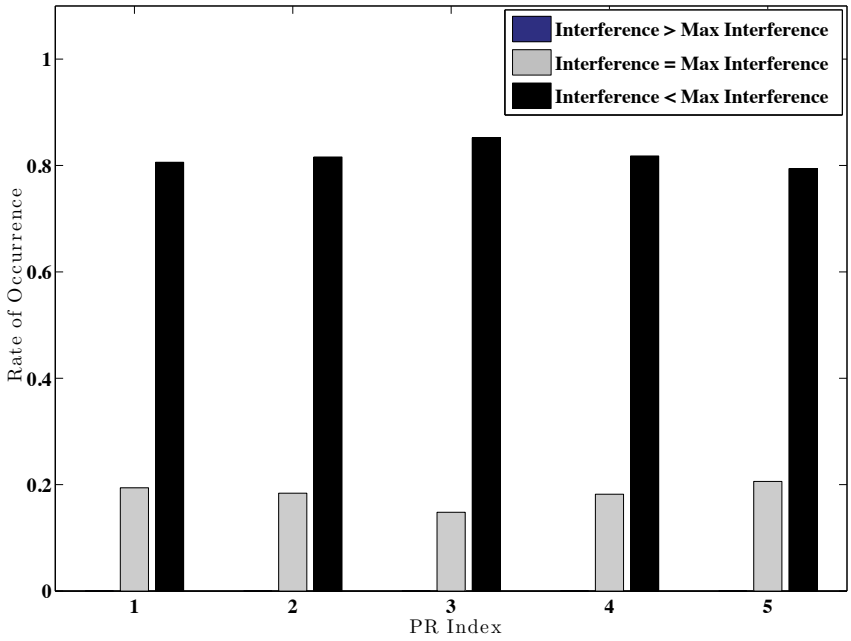

Figure 4.7: Distribution of the mean Interference at different PRs normalized by $\xi_m^{\max}$. Scenario consists of 5 STs and 5 PRs with $\mathbb{E}[h_{k,k}^2] = 0$ dB, $\mathbb{E}[g_{i,j}^2]$ (for any i, j) $= -5$ dB, $\mathbb{E}[h_{i,k}^2]$ $(i \neq k) = -10$ dB, and $\frac{p_n^{\max}}{\sigma_n^2} = 15$ db $\forall n$.

4.6 Concluding Remarks

In this contribution, we have proposed a sequential distributed power allocation algorithm for an underlay CRN that tries to maximize the secondary sum rate by maximizing the rate utility per unit primary interference for each SU. By comparing our proposed algorithm with a similar algorithm which only takes the primary interference temperature constraint into consideration, but not the relative rate utility of the SUs, we demonstrate the effectiveness of the proposed algorithm and the usefulness of the introduced *relative rate utility* measure. It is also shown that the proposed algorithm, which only requires some information exchange among the SUs, performs close to the maximum achievable rate found by exhaustive search with global channel knowledge for certain scenarios.

Bibliography

[1] D. Gesbert, S. G. Kiani, A. Gjendemsjø, and G. E. Øien, "Adaptation, coordination, and distributed resource allocation in interference-limited wireless networks," *Proceedings of the IEEE*, vol. 95, no. 12, pp. 2393–2409, Dec. 2007.

[2] M. Gastpar, "On capacity under receive and spatial spectrum-sharing constraints," *IEEE Transactions on Information Theory*, vol. 53, no. 2, Feb. 2007.

[3] E. Jorswieck, H. Boche, and S. Naik, "Energy-aware utility regions: Multiple access pareto boundary," *IEEE Transactions on Wireless Communications*, vol. 9, no. 7, pp. 2216 –2226, July 2010.

[4] M. Hong and A. Garcia, "Equilibrium pricing of interference in cognitive radio networks," *IEEE Transactions on Signal Processing*, vol. 59, no. 12, pp. 6058 –6072, Dec. 2011.

[5] F. Wang, M. Krunz, and S. Cui, "Price-based spectrum management in cognitive radio networks," *IEEE Journal on Selected Topics in Signal Processing*, vol. 2, no. 1, pp. 74–87, Feb. 2008.

[6] G. Scutari, D. P. Palomar, and S. Barbarossa, "Cognitive MIMO radio: Competitive optimality design based on subspace projections," *IEEE Signal Processing Magazine*, vol. 25, no. 6, pp. 46 – 59, Nov. 2008.

[7] W. Wang, Y. Cui, and W. Wang, "Noncooperative power control game with exponential pricing for cognitive radio network," in *Proc. 65th IEEE Vehicular Technology Conference (VTC-Spring)*, Dublin, Apr. 2007, pp. 3125–3129.

[8] D. A. Schmidt, C. Shi, R. A. Berry, M. L. Honig, and W. Utschick, "Distributed resource allocation schemes: Pricing algorithm for power control and beamformer design in interference networks," *IEEE Signal Processing Magazine, special issue on Game Theory in Signal Processing and Communications*, vol. 29, no. 5, pp. 53–63, Sep. 2009.

[9] A. Kaul and B. Woerner, "Analytic limits on performance of adaptive multistage interference cancellation for CDMA," *Electronics Letters*, vol. 30, no. 25, pp. 2093 –2095, Dec. 1994.

[10] A. Rabbachin, T. Q. S. Quek, H. Shin, and M. Z. Win, "Cognitive network interference," *IEEE Journal on Selected Areas in Communications*, vol. 29, no. 2, pp. 480–493, Feb. 2011.

[11] T. M. Cover and J. A. Thomas, *Elements of Information Theory*, 2nd ed. Wiley-Interscience, 2006.

[12] A. Ozdaglar and R. Srikant, "Incentives and pricing in communications networks," in *Algorithmic Game Theory*, N. Nisan, T. Roughgarden, E. Tardos, and V. Vazirani, Eds. New York, USA: Cambridge University Press, 2007.

[13] D. Tse and P. Viswanath, *Fundamentals of Wireless Communication*. Cambridge University Press, Cambridge, U.K., June 2005.

[14] A. B. Bondi, "Characteristics of scalability and their impact on performance," in *Proc. 2nd international workshop on Software and performance*, ser. WOSP '00. New York, NY, USA: ACM, 2000, pp. 195–203.

[15] M. Sugano, T. Kawazoe, Y. Ohta, and M. Murata, "Indoor localization system using RSSI measurement of wireless sensor network based on ZigBee standard," in *Proc. IASTED International Conference on Wireless Sensor Network (WSN 2006)*. Alberta, Canada: IASTED/ACTA Press, 2006, pp. 1–6.

Paper D

Generalized Hierarchical Spectrum Usage under Spatio-orthogonal Co-existence Policy

Nurul Huda Mahmood and Geir Egil Øien

Manuscript submitted for possible publication to the IEEE Wireless Communications and Networking Conference (IEEE-WCNC) 2013.

Partial results of this work has been presented as a poster at the third Nordic Workshop on System and Network Optimization for Wireless (SNOW 2012), Trysil, Norway, April 10-12, 2012.

Chapter 5

Generalized Hierarchical Spectrum Usage under Spatio-orthogonal Co-existence Policy

Nurul Huda Mahmood and Geir E. Øien

Abstract - Different interference management techniques for multi antenna systems under a hierarchical spectrum usage policy, where different systems access the same wireless channel under different operating conditions, are investigated in this work. More specifically, we propose an scheduling scheme for the MISO case, and study different transmit precoder design principles for the MIMO case, considering an opportunistic wireless systems accessing the spectrum of a legacy system under a strictly "*no interference*" policy. The proposed transmit precoder design techniques are evaluated using computer based Monte-Carlo simulations, and have been found to result in a considerable sum rate performance of the opportunistic system without affecting the operation of the incumbent system.

Keywords – Interference Alignment, zero forcing beamforming, interference nulling.

5.1 Introduction

The wireless channel is inherently broadcast in nature, where multiple links interfere with each other. Such broadcast nature of the wireless channel has traditionally been viewed as a disadvantage which was addressed by carefully designing systems to avoid the interference. General interference avoidance techniques involve orthogonalizing re-

sources, e.g. in time, frequency, space, or codes. Recently however, there have been a paradigm shift from interference avoidance to interference rejection in dealing with interference, where advanced receiver-based processing such as beamforming, Interference Rejection Combining (IRC), iterative decoding etc. are employed to mitigate the interference between co-existing wireless links. Interference exploitation is another emerging interference management principle through which different interfering sources coordinate their transmission to induce exploitable structure to the interference at the interfered receiver [1]. On a different but related note, hierarchical spectrum usage has recently been proposed to facilitate heterogeneous access to the spectrum by different systems, possibly with different access priorities [2]. Macro-femto coexistence [3] and Dynamic Spectrum Access (DSA) in Cognitive Radio Networks (CRNs) [4] are specific examples of such hierarchical spectrum usage.

In this work, we address the problem of mitigating the interference at a set of legacy receivers in a generalized hierarchical spectrum usage scenario, where the opportunistic users are allowed to share the legacy spectrum under a strict policy of "*no-interference at legacy receiver*". More specifically, we investigate two different interference avoidance/ coordination strategies for an opportunistic system to hierarchically utilize the spectrum of a legacy system. In the first investigation, we consider an Multiple-Input Single-Output (MISO) opportunistic system that avoids interference at the undesired receivers by employing transmit beamforming techniques to null the interference; and propose a scheduling scheme that improves the sum rate at the intended receivers by selecting mutually (semi)-orthogonal users. Secondly, we study different transmit precoder design principles for a Multiple-Input Multiple-Output (MIMO) opportunistic system whereby the transmitters cooperate to 'pack' the interference into a subspace of the received space at the interfered receiver, through IA techniques.

Transmit and/or receive beamformers provide a versatile form of spatial filtering. A beamformer applied at the transmitter shapes the transmission direction to place nulls at the interfered co-channel receivers [5], thus allowing the transmitters to coexist with the interfered receivers in the same tempo-spectral domain. Various beamforming techniques for different hierarchical spectrum usage scenarios have been investigated in [6–8] among others. The authors in [6] consider a Cognitive Radio (CR) system coexisting with a legacy system; and proposes transmit beamforming solutions for the CR user that nulls the interference at the Primary Receivers (PRs). The proposed scheme is enabled by the legacy user's sharing of its Channel State Information (CSI). Reference [7] studies a similar problem from a different approach, whereby the authors formulate the problem in a game theoretical framework, and characterize transmission strategies that results

in Pareto optimal operation points for the CR system. Interestingly, it is noted that the Pareto boundary can be achieved as the outcome of a non-cooperative game by imposing certain null shaping constraints at the transmitters. In [8], the authors present a cross-layer optimized cooperative beamforming technique to forward messages in busy time slots without causing interference to the Primary Users (PUs). The proposed cooperative scheme can achieve cooperative diversity gain and improve Quality of Service (QoS) for the Secondary Users (SUs) without consuming additional idle time slots or temporal spectrum holes.

Interference, unlike noise, can potentially be pre-shaped to give it an exploitable structure, as in IA techniques. The main idea in IA is to align the transmission of signals from different transmitters such that all the unwanted interference at a particular interfered receiver overlap in the same signal sub-space. This allows a transmitter-receiver pair to communicate interference-free over the remaining dimensions. Each user in a fully connected K user wireless interference channel can, in theory, communicate reliably at rates approaching one half of the rates the user can achieve in a single user (interference free) channel by employing IA principles [9]. Due to the natural separation of the interference and the information signal subspaces, IA naturally lends itself to systems like the CRN where SUs seek to avoid/seggregate the interference generated at the PRs.

Interference Alignment (IA) in a CR environment is studied in [10, 11] among others. The Opportunistic Interference Alignment (OIA) scheme is introduced in [10], which considers a single MIMO SU harmlessly coexisting with a single MIMO PU. The authors in this work, propose a power allocation and an IA scheme for the SU such that the interference at the PR does not spill into the PU's desired direction of communication; while simultaneously maximizing the SU rate. On the other hand, the concept of constrained interference alignment is introduced in [11], where the authors derive an outer bound on the Degree of Freedom (DoF) of the SUs in the presence of a MIMO PU that maximizes its own rate. In addition, an iterative cognitive IA algorithm achieving the derived DoF is presented.

We built on the above referred and other related works to explore efficient orthogonal coexistence strategies between an existing legacy system and an opportunistic system. In particular, we explore strategies whereby an entrant system share the time-frequency resource of the legacy system by orthogonalizing its operation in the space domain. We present our findings in the context of a CRN coexisting with a primary system. However, the proposed techniques are equally valid for other general hierarchical spectrum usage scenarios as well. More specifically, in this work we propose: i) a semi-orthogonal

scheduling scheme that improves the secondary system's opportunistic access of the primary spectrum by judiciously scheduling SUs to control the inter-secondary interference; and ii) different beamformer design principles for an 'interference aligned' cognitive radio system. The proposed schemes are found to result in secondary system performance improvement in terms of the sum rate, even under the strictly zero interference constraint at the PRs.

The remainder of this paper is organized as follows. The system model is elaborated in Section 5.2. The semi-orthogonal scheduling scheme for the null steering based coexistence strategy is proposed and evaluated in Section 5.3. In Section 5.4, different secondary beamformer design principles are investigated and analyzed for the Interference Alignment (IA)-based coexistence strategy. Finally, concluding remarks are drawn in Section 5.5.

Notations

Vectors are represented by a lower case bold face letter ($\mathbf{a}$), and matrices by the upper case bold face letter ($\mathbf{A}$). $\mathbf{I}_n$ represents the $n \times n$ identity matrix. $\det\{\mathbf{A}\}$, $\text{rank}\{\mathbf{A}\}$, $\text{sp}\{\mathbf{A}\}$, $\mathcal{N}\{\mathbf{A}\}$ and $\mathbf{A}^H$ denote the determinant, rank, range, kernel (or nullspace) and Hermitian transpose of the matrix $\mathbf{A}$ respectively. $\|\mathbf{x}\|$ denotes the L^2-norm of the vector $\mathbf{x}$, $\mathbb{E}\{\cdot\}$ denotes the mathematical expectation operation, and $(x)^+ = \max(x, 0)$. The eigenvalues of the matrix $\mathbf{A}$ corresponding to its l maximum (minimum) eigenvalues are denoted by $\nu_l^{\max(\min)}(\mathbf{A})$.

Degrees of Freedom

The term DoF is commonly used in the literature as an important capacity approximation that is accurate in the high SNR. It also represent the maximum multiplexing gain of a generalized MIMO system. Following the definition used in [9] and [11], we define the DoF as *the number of interference free signaling dimension of a user* and denote the DoF of the user k by d_k.

5.2 System Model

We consider a scenario where there is a secondary system operating in the spectrum of a primary system. Both the systems are assumed to be peer to peer networks, where each

transmitter communicates with its designated receiver. We assume there are K users in total, of which K_p are PUs and K_s are SUs. Let the set $I \triangleq \{1,2,\cdots,K_\mathrm{p}\}$, $\mathcal{J} \triangleq \{1,2,\cdots,K_\mathrm{s}\}$ and $\mathcal{K} \triangleq \{1,2,\cdots,K\}$ represent the indices of the PUs, the SUs and all the users respectively. All nodes are assumed to possibly have multiple antennas. An example of the system model is shown in Figure 5.1.

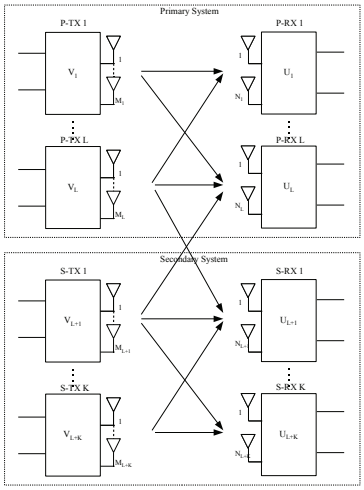

Figure 5.1: General System Model under investigation

Let the number of transmit and receive antennas at the k^{th} user pair be M_k and N_k respectively. The received signal at the k^{th} receiver at the n^{th} channel use can be written as

$$\mathbf{y}_k(n) = \sum_{i\in\mathcal{K}} \mathbf{H}_{ki}(n)\mathbf{x}_i(n) + \mathbf{z}_k(n), \tag{5.1}$$

for all $k \in \mathcal{K}$ and $n \in \mathbb{Z}$. In the above, $\mathbf{y}_k(n) \in \mathbb{C}^{N_k\times 1}$ is the output signal of the k^{th} receiver, $\mathbf{x}_k(n) \in \mathbb{C}^{M_k\times 1}$ is the input signal at the k^{th} transmitter, $\mathbf{H}_{ij}(n) \in \mathbb{C}^{N_i\times M_j}$ contains the channel fade coefficients between transmitter i and receiver j, and $\mathbf{z}_j(n) \in \mathbb{C}^{N_k\times 1}$ is the circularly symmetric Additive White Gaussian Noise (AWGN) term at the k^{th} receiver; all at the n^{th} time instant. All noise terms are assumed independent and identically distributed (i.i.d.) with zero mean and unit variance. The elements of all channel matrices $\mathbf{H}_{ij}$ are also assumed i.i.d and drawn from a continuous distribution. The transmit power of the k^{th} transmitter at the n^{th} time instance is $\mathrm{E}[\|\mathbf{x}_k(n)\|^2] = P_k(n)$. The channel use index n is omitted hereafter for the sake of brevity.

The inter-primary interference is assumed taken care of. This can be done by making

the PUs' transmission orthogonal to each other using orthogonal frequencies, orthogonal codes, or by sharing the codewords to allow each user to decode and remove any unwanted information. However the PUs are interfered by the secondary system and vice versa.

At each transmission slot, each user can communicate over d_k parallel streams of information signal where d_k is upper bounded by the minimum of its transmit and receive antennas, i.e. $d_k \leq \min(M_k, N_k)$. At each transmitter, let the d_k-dimensional information message signal to be transmitted be $\tilde{\mathbf{x}}_k$. This message is transmitted through the M_k antennas by mapping it onto an M_k-dimensional signal $\mathbf{x}_k$ using a $M_k \times d_k$-dimensional unitary transmit precoder $\mathbf{V}_k$. Thus, $\mathbf{x}_k = \mathbf{V}_k \tilde{\mathbf{x}}_k$.

At the receiver end, the N_k-dimensional message signal received through the N_k antennas is $\mathbf{y}_k$. This received message signal is post-processed using an $N_k \times d_k$-dimensional receiver post-coder $\mathbf{U}_k$ to extract the d_k-dimensional received information signal $\tilde{\mathbf{y}}_k$, yielding $\tilde{\mathbf{y}}_k = \mathbf{U}_k^H \mathbf{y}_k$. Thus, the received information signal at the k^{th} receiver is given by

$$\tilde{\mathbf{y}}_k = \mathbf{U}_k^H \mathbf{H}_{kk} \mathbf{V}_k \tilde{\mathbf{x}}_k + \sum_{j \in \mathcal{K}, j \neq k} \mathbf{U}_k^H \mathbf{H}_{kj} \mathbf{V}_j \tilde{\mathbf{x}}_j + \mathbf{U}_k^H \mathbf{z}_k. \tag{5.2}$$

With this signal model, and with the earlier made assumption about the inter-primary interference, the Signal-to-Interference-plus-Noise Ratio (SINR) γ_i at the PR i is given by [12]

$$\gamma_i = P_i \mathbf{U}_i^H \mathbf{H}_{ii} \mathbf{x}_i \left(\mathbf{I}_{d_i} + \sum_{j \in \mathcal{J}} P_j \mathbf{U}_i^H \mathbf{H}_{ij} \mathbf{V}_j \mathbf{V}_j^H \mathbf{H}_{ij}^H \mathbf{U}_i \right)^{-1} \mathbf{x}_i^H \mathbf{H}_{ii}^H \mathbf{U}_i. \tag{5.3}$$

Similarly, the SINR γ_j at the SR j is given by

$$\gamma_j = P_j \mathbf{U}_j^H \mathbf{H}_{jj} \mathbf{x}_j \left(\mathbf{I}_{d_j} + \sum_{k \in \mathcal{K}, k \neq j} P_k \mathbf{U}_j^H \mathbf{H}_{jk} \mathbf{V}_k \mathbf{V}_k^H \mathbf{H}_{jk}^H \mathbf{U}_j \right)^{-1} \mathbf{x}_j^H \mathbf{H}_{jj}^H \mathbf{U}_j. \tag{5.4}$$

Assuming a capacity-achieving code is used, and under a Gaussian assumption on the interference, the achievable rate of user k for a given SINR at a given resource slot, R_k, is given by $R_k = \log_2 \det \left[\mathbf{I}_{d_k} + \gamma_k \right]$ [13].

Channel State Information Exchange

In this work, we assume that there are some degrees of cooperation between the primary and secondary network, as materialized by the PUs' sharing of their complete CSI with

the secondary systems. Such an assumption remains valid for use cases where an operator introduces 'low-priority, low-cost' secondary service on top of the existing network in order to maximize revenues. It can also be achieved with the help of external agents, for example a *dynamic frequency broker* [14]. Moreover, the primary system may have an incentive to share its CSI in exchange of a no-interference guarantee from the opportunistic system.

5.3 Null Steering Based Solution

Let us consider a scenario where all SUs have full channel knowledge at all time instant including that of the PUs' channel gains; and the SUs are allowed to use the primary spectrum as long as the desired DoF of all the PUs are not compromised. Given this setting, we would like to investigate how the secondary system can communicate opportunistically while guaranteeing the primary systems' DoF requirement. In this section we present a solution to the above-raised problem inspired by beamforming/null steering techniques.

Let the requested DoFs of the PUs be $d_i \forall i \in I$. With "*no-interference guarantee from the STs*", and with inter-primary interference assumed taken care of, the capacity achieving transmission scheme for each PU is to choose the preprocessing matrix at the transmitter $\mathbf{V}_i$, and postprocessing matrix at the receiver $\mathbf{U}_i$, such that the primary channel matrix $\mathbf{H}_{ii}$ is diagonalized [12, Ch. 7]. Hence the columns of $\mathbf{V}_i$ and $\mathbf{U}_i$ are respectively given by the right and left singular vectors of the channel matrix $\mathbf{H}_{ii}$ corresponding to its largest d_i singular values. Thus, the received signal after post-processing at PU_i is given by

$$\tilde{\mathbf{y}}_i = \mathbf{U}_i^H \mathbf{H}_{ii} \mathbf{V}_i \tilde{\mathbf{x}}_i + \underbrace{\sum_{j=\mathcal{J}} \mathbf{U}_i^H \mathbf{H}_{ij} \mathbf{V}_j \tilde{\mathbf{x}}_j}_{\text{secondary interference}} + \mathbf{U}_i^H \mathbf{Z}_i. \tag{5.5}$$

Transmit Pre-coder design at Secondary Transmitters

Given the above, the transmit pre-coders design problem at each ST SU_j can be stated as

$$\text{Choose} \quad \mathbf{V}_j \ \text{ s.t. } \ \mathbf{U}_i^H \mathbf{H}_{ij} \mathbf{V}_j = 0, \forall\, i \in I. \tag{5.6}$$

Recall that for any given matrix $\mathbf{A}$, $\mathbf{AX} = \mathbf{0} \forall \mathbf{X} \in \mathcal{N}(\mathbf{A})$ [15]. Therefore, to fulfill the condition in (5.6), the transmit precoder at each ST should lie in the nullspace of $\mathbf{U}_i^H \mathbf{H}_{ij} \forall i$.

Equivalently, this implies that for each ST S_j,

$$\mathbf{V}_j \in \mathcal{N}\left(\mathbf{U}_1^H \mathbf{H}_{1j}\right) \cap \mathcal{N}\left(\mathbf{U}_2^H \mathbf{H}_{2j}\right) \cap \ldots \cap \mathcal{N}\left(\mathbf{U}_{K_p}^H \mathbf{H}_{K_p j}\right).$$

Using the principle that $\mathcal{N}(\mathbf{A}) \cap \mathcal{N}(\mathbf{B}) = \mathcal{N}(\mathbf{C})$, where $\mathbf{C} = [\mathbf{A}^H \ \ \mathbf{B}^H]^H$ [15], and the assumption that $\mathbf{U}_i^H \mathbf{H}_{ij} \forall i$ is known at each ST, the transmit precoder at each ST fulfilling the condition in (5.6) is given by

$$\mathbf{V}_j \ \in \ \mathcal{N}\left(\tilde{\mathbf{H}}_j\right), \forall \ j \in \mathcal{J}, \tag{5.7}$$

where the matrix $\tilde{\mathbf{H}}_j$ is defined as

$$\tilde{\mathbf{H}}_j = \left[\left(\mathbf{U}_1^H \mathbf{H}_{1j}\right)^H \left(\mathbf{U}_2^H \mathbf{H}_{2j}\right)^H \ldots \left(\mathbf{U}_{K_p}^H \mathbf{H}_{K_p j}\right)^H\right]^H.$$

Receive Post-processor design at the SRs

The receive post-processor matrix at the SRs can readily be designed with different objectives such as maximizing the SINR or minimizing the mean squared error (MSE) at the receiver [16]. In this work, we have implemented the max-SINR receiver, which maximizes the SINR at the intended receiver, as given by [16]

$$\mathbf{U}_k' = \frac{\mathbf{C}_{R_k}^{-1} \mathbf{H}_{kk} \mathbf{V}_k}{\|\mathbf{C}_{R_k}^{-1} \mathbf{H}_{kk} \mathbf{V}_k\|}, \tag{5.8}$$

where $\mathbf{C}_{R_k}$ is the received interference covariance matrix defined as

$$\mathbf{C}_{R_k} \triangleq \left(\sum_{i \neq k} \mathbf{H}_{ki} \mathbf{V}_i \mathbf{V}_i^H \mathbf{H}_{ki}^H P_i + \mathbf{I}_{M_s}\right)$$

.

Feasibility of Transmit Pre-coder design

The matrix $\tilde{\mathbf{H}}_j$ at a given ST has dimension $(\sum_{i \in I} d_i) \times M_j$. Its rows are complex weighted row-sum of the channel matrix between that ST and the corresponding PR. Under the continuous distribution assumption for the channel fading gains, the matrix $\tilde{\mathbf{H}}_j$ has linearly independent rows for each ST, and hence the nullity of the matrix $\tilde{\mathbf{H}}_j$ is given by $(M_j - \sum_{i \in I} d_i)^+$. Thus, it can be stated that for a given ST to have a non-zero transmit

precoder matrix (which implies the matrix $\tilde{\mathbf{H}}_j$ has non-zero nullity) it is required that $M_j > \sum_{i \in I} d_i$. This can be expressed by the following Proposition:

Proposition 5.1 *A ST can communicate without creating any interference in the received direction at any PRs iff it has more antennas than the sum of the requested DoFs of all PUs.*

When the nullity of $\tilde{\mathbf{H}}_j$ is greater than 1, the STs have greater flexibility in the pre-coder design and can fulfill additional objectives, as discussed next.

5.3.1 Semi-Orthogonal User Selection Algorithm

Wireless transceiver optimization in MIMO communication has been extensively studied under the non-CR setup with different design criteria (see e.g. [12, 13, 17], and references therein). The capacity of MIMO Broadcast Channels (BCs) can be achieved by Dirty Paper Coding (DPC) [18], although it is difficult to implement in a practical system. For an asymptotically large number of users, similar performance can be achieved with the much simpler zero-forcing beamforming strategy by judiciously scheduling the group of users that are (semi)-orthogonal to one another for concurrent transmissions [19].

In this section, we adopt and modify the semi-orthogonal user selection algorithm presented in [19] for application to our considered scenario. Let the secondary system constitute a MISO BC with the K_s SUs served by a SBS. Let the number of transmit antennas at the SBS be M, with $M > K_p$, and let all the receivers be single antenna terminals. The columns of the matrix $\mathbf{V}$ give the set of possible transmit precoders that will ensure zero interference at the PRs, where $\mathbf{V} = \mathcal{N}\left(\tilde{\mathbf{H}}_j\right)$.

Semi-Orthogonal User Groups

The considered algorithm groups users into semi-orthogonal sets so as to reduce the mutual interference among the SUs. A particular beam vector (say, $\mathbf{v}_j$) is considered orthogonal to a given user (say, with channel vector $\mathbf{h}_i$ with the assigned beam vector $\mathbf{v}_i$) if the interference power from unintended beam is a fraction α (or less) of its power gain with the assigned beam vector, i.e.

$$\frac{|v_i^H h_i|^2}{|v_j^H h_i|^2} \leq \alpha,$$

where $\alpha \in (0,1)$ is a design parameter; and $\alpha = 0$ implies perfect orthogonality.

For the proposed algorithm, the set of semi-orthogonal users offering the highest sum of the log of their respective gains on the assigned beam vectors are selected via combinatorial search through the space of all feasible semi-orthogonal user groups. Once a set of users are selected, the traditional water-filling algorithm is used to allocate the transmit powers across the different users.

Numerical Results

Secondary system sum rate curves with the above semi-orthogonal user selection algorithm with $\alpha = 0.01$ is presented in Figure 5.2. Simulation results are presented for i.i.d. Rayleigh fading environment with all channels having the same mean power gain (denoted by SNR). Different numbers of primary and secondary users are considered, all with $d_k = 1$. A SBS with four transmit antennas are considered. Performance results are also presented for the case when the maximum number of SUs (which is $M - K_p$) with the best gains are assigned to each of the available beam vectors without any consideration for orthogonality. Moreover, results are also presented for the case when only a single user with the best gain is scheduled with full power. Note that, only one SU can operate for the scenario when $K_p = 3$, which is simply the user with the strongest channel gain.

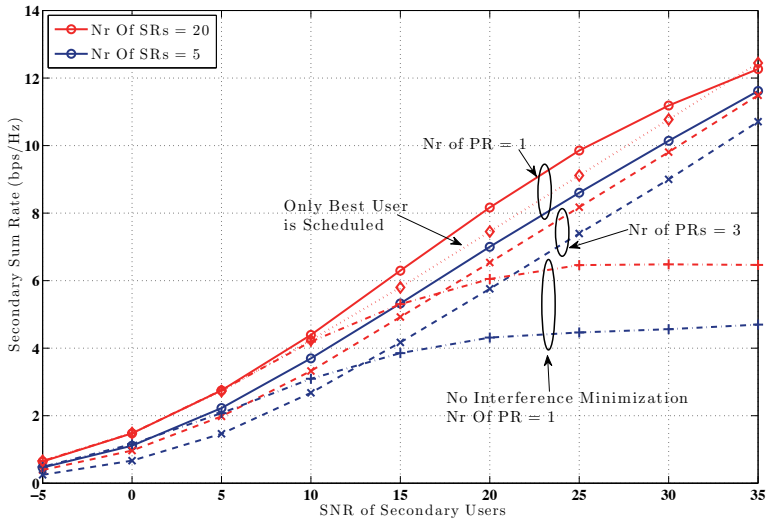

Figure 5.2: Secondary Sum Rate with Semi-Orthogonal User Selection Algorithm. $\alpha = 0.01$ and $M = 4$.

General Discussions

The feasibility of the proposed IA scheme does not depend on the number of primary antennas, and is applicable even when the PUs are single antenna devices. Cooperation among the SUs is not required too. In the proposed scheme, each SU independently null-steers the interference at all PRs' receive directions. However, the STs may cooperate to bring more benefit to the secondary system, such as forming a large virtual MIMO transmitter. Moreover, the proposed scheme can also be used in a cellular CRN with the base station having multiple antennas. The main drawback of this proposed beamforming based solution is that it requires a large number of transmit antennas be available at the STs. To overcome this problem, we proposed Interference Alignment based solutions in Section 5.4.

The presented algorithm relies on the inherent diversity in the independent channel gains of different users in order to determine the set of "semi-orthogonal" user groups. Therefore the sum rate performance improves with increasing number of SRs. Due to the zero-forcing beam vector design at the SBSs, the possible number of active SRs is upper bounded by the nullity of the secondary-primary channel matrix. Therefore, for meaningful secondary operation, the transmit antennas at the SBSs has to be more than than the number of interfered PRs, i.e. $M > K_p$. However, such consideration is not unrealistic for the assumed underlay CR system due to its limited interference range. Moreover, when $M \leq K_p$, a subset $K'_p$of the PRs that are most harmed by the SBS can be considered as active PRs such that $M > K'_p$. Such a consideration can provide a tradeoff between interference suppression at the PRs and meaningful opportunistic access of the secondary system.

Lastly, the algorithm design parameter α provides a tradeoff between the number of active SRs and the mutual interference among them. The impact of the choice of α on the secondary sum rate is presented in Figure 5.3. It is observed that at lower SNRs (i.e. in the power limited regime), a larger value α is preferred as it accommodates more users, thereby leading to a better sum rate. On the other hand, at higher SNRs (i.e. in the interference limited regime), a smaller value of α results in better performance by ensuring interference minimization among the SUs.

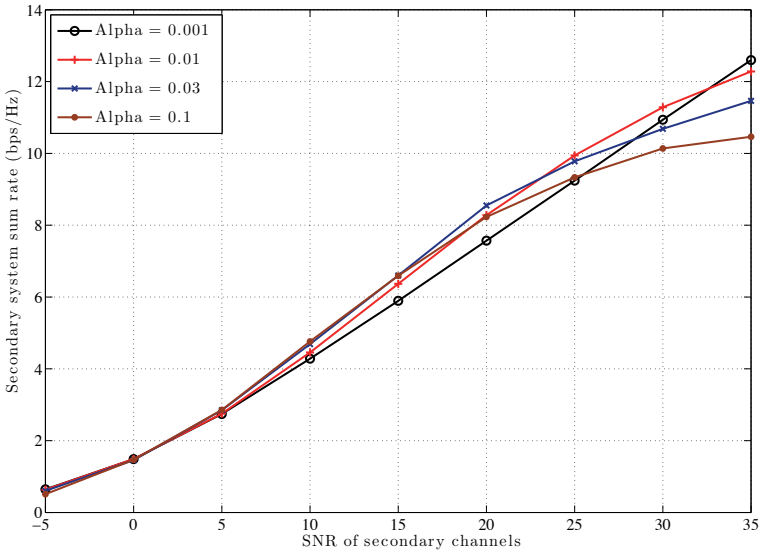

Figure 5.3: Impact of the choice of α on the secondary sum rate. $M = 4$, $K_p = 1, K_s = 5$.

5.4 Interference Alignment Based Secondary System Design

In this section, we would like to investigate applications of IA techniques in a CRN with multiple primary and multiple secondary users under different design considerations. For the sake of tractability, let us consider two symmetric PUs with M_p transmit and receive antennas and one requested DoFs per PU; and two symmetric SUs with M_s transmit and receive antennas and one requested DoFs per SU. Let the indices $1,2$ denote the PUs, while the indices $3,4$ denote the SUs.

The received signal after post-processing at the PR i , $\mathbf{y}_i$, is given by

$$\mathbf{y}_i = \mathbf{u}_i^H \mathbf{H}_{ii} \mathbf{v}_i \tilde{\mathbf{x}}_i + \sum_{j \in \mathcal{J}} \mathbf{u}_i^H \mathbf{H}_{ij} \mathbf{v}_j \tilde{\mathbf{x}}_j + \mathbf{u}_i^H \mathbf{z}_i. \tag{5.9}$$

The IA condition at the PRs require the transmit precoders at the STs be designed such that the interference signal from the two STs overlap at each of the PRs. Then each PR will be able to cancel the interference signal, and hence receive its information signal interference free over the remaining dimensions. Mathematically, the IA condition can be

written as

$$\text{Choose } \mathbf{v}_3, \mathbf{v}_4 \text{ such that: } \; \text{sp}\left(\mathbf{H}_{i3}\mathbf{v}_3\right) = \text{sp}\left(\mathbf{H}_{i4}\mathbf{v}_4\right), \forall \, \text{i} \in \{1,2\}. \tag{5.10}$$

5.4.1 Transmit Precoder design at Secondary Transmitters

The condition in (5.10) states

$$\text{Choose } \mathbf{v}_3, \mathbf{v}_4 \text{ such that: } \quad \mathbf{H}_{13}\mathbf{v}_3 = c_1\mathbf{H}_{14}\mathbf{v}_4 \quad \text{and} \quad \mathbf{H}_{23}\mathbf{v}_3 = c_2\mathbf{H}_{24}\mathbf{v}_4,$$

for any arbitrary constants c_1 and c_2. After some simple algebraic manipulation, we find that the above conditions can be met by first designing the transmit precoder $\mathbf{v}_j$ to be any arbitrary vector of unit L^2-norm; and then choosing the other transmit precoder, $\mathbf{v}_i$, to satisfy

$$\mathbf{v}_i = \frac{\left(\hat{\mathbf{H}}_i\right)^{-1}\hat{\mathbf{H}}_j\mathbf{v}_j}{\left\|\left(\hat{\mathbf{H}}_i\right)^{-1}\hat{\mathbf{H}}_j\mathbf{v}_j\right\|}, \tag{5.11}$$

for $\{i, j\} \in \{3,4\}, i \neq j$, and where the matrix $\hat{\mathbf{H}}_i$ is defined as $\hat{\mathbf{H}}_i = \begin{bmatrix}\mathbf{H}_{1i} \\ \mathbf{H}_{2i}\end{bmatrix}$.

The relation between the transmit precoders of the two secondary users are given by (5.11). Thus the IA condition stipulated in (5.10) can be met by arbitrarily designing one of the transmit precoders, and then choosing the other precoder according to (5.11).

5.4.2 Considerations for Transmit Pre-coder design

The fact that one of the transmit precoders can be arbitrarily chosen provides some flexibility in its design; and hence this precoder can be designed to fulfill some additional design objective. In this section, we lay out three such design principles.

pro-primary transmission

The secondary transmit precoder that can be arbitrarily chosen is designed to minimize the overlap of the secondary interference signal with the primary signal of interest at all the PRs.

competitive transmission

Competitive transmission illustrates the PRs' choice of precoder design to maximize its own rate after complying by the IA condition of (5.10). Thus, the first ST

precoder is designed to maximize the received information signal at the intended receiver.

cooperative transmission

In contrast to the principle above, the arbitrary precoder can also be designed to minimize the interference signal power at the unintended receiver. The term 'cooperative transmission' is used to illustrate this design principle.

The implementation of the above presented principles are discussed below.

Pro Primary Transmission

IA technique shapes the transmission direction to result in overlapping interference signals at an unintended receiver. However, this condition does not guarantee that part of the signal of interest will not overlap with the interference signal. In fact, because of this reason, at low or moderate SNRs, IA does not generally maximize utility [20].

To mitigate this problem, we propose to design the arbitrary transmit precoders at the STs such that the overlap of the secondary interference signal with the primary signal of interest is minimized at all the PRs. Without loss of generality, let $\mathbf{v}_3$ be the secondary transmit precoder to be arbitrarily designed. The power, $P^{(\mathrm{i})}_{\mathrm{overlap}}$, of the primary signal overlapping with the interference signal at the PR i from this ST is readily given by

$$P^{(\mathrm{i})}_{\mathrm{overlap}} = \left((\mathbf{H}_{ii}\mathbf{v}_i)^H \mathbf{H}_{i3}\mathbf{v}_3\right)^H \left((\mathbf{H}_{ii}\mathbf{v}_i)^H \mathbf{H}_{i3}\mathbf{v}_3\right). \tag{5.12}$$

Let $\mathbf{g}_i = \mathbf{H}^H_{i3}\mathbf{H}_{ii}\mathbf{v}_i$(hence $P^{(\mathrm{i})}_{\mathrm{overlap}} = \mathbf{v}_3^H \mathbf{g}_i \mathbf{g}_i^H \mathbf{v}_3$). Since this power has to be minimized at both PRs, the problem of minimizing the overlap power can be formulated as

$$\mathbf{v}_3 = \arg\min_{\mathbf{v}_j} \mathbf{v}_j^H \mathbf{G} \mathbf{v}_j, \tag{5.13}$$

where $\mathbf{G} = \sum_{i\in I} \mathbf{g}_i \mathbf{g}_i^H$. This can be solved using *Rayleigh's principle* [15], and the corresponding transmit precoders are given by

$$\begin{aligned} \mathbf{v}_3^{(\mathrm{pro})} &= \nu_1^{\min}(\mathbf{G}), \text{and} \\ \mathbf{v}_4^{(\mathrm{pro})} &= \frac{\left(\hat{\mathbf{H}}_4\right)^{-1} \hat{\mathbf{H}}_3 \mathbf{v}_3^{(\mathrm{pro})}}{\| \left(\hat{\mathbf{H}}_4\right)^{-1} \hat{\mathbf{H}}_3 \mathbf{v}_3^{(\mathrm{pro})} \|}. \end{aligned} \tag{5.14}$$

Competitive Transmission

It is well known that the received signal power at the intended receiver will be maximized when the transmit precoder corresponds to the maximum right singular vector of the direct channel matrix, which in this case is $\mathbf{H}_{33}$ [17]. The two secondary transmit precoders are therefore straightforwardly given by

$$\begin{aligned} \mathbf{v}_3^{(\mathrm{cmp})} &= \nu_1^{\max}\left(\mathbf{H}_{33}^H\mathbf{H}_{33}\right), \\ \mathbf{v}_4^{(\mathrm{cmp})} &= \frac{\left(\hat{\mathbf{H}}_4\right)^{-1}\hat{\mathbf{H}}_3\mathbf{v}_3^{(\mathrm{cmp})}}{\|\left(\hat{\mathbf{H}}_4\right)^{-1}\hat{\mathbf{H}}_3\mathbf{v}_3^{(\mathrm{cmp})}\|}. \end{aligned} \tag{5.15}$$

Transmit Precoder design - Cooperative Transmission

In contrast to the principle above, the objective of the arbitrary precoder design can instead be to minimize the interference signal power at the unintended SR. It is easy to note that the received secondary interference power at the unintended SR is given by

$$P_{\mathrm{SU-int}}^{(4)} = P_3\mathbf{v}_3\left(\mathbf{H}_{43}^H\mathbf{u}_4\mathbf{u}_4^H\mathbf{H}_{43}\right)\mathbf{v}_3. \tag{5.16}$$

On a first look, one may consider that $\mathbf{v}_3$ minimizing $P_{\mathrm{SU-int}}^{(4)}$ is straightforwardly given by the least dominant eigenvector of the interference covariance matrix $\mathbf{H}_{43}^H\mathbf{u}_4\mathbf{u}_4^H\mathbf{H}_{43}$. However, a close look at (5.16) reveals that the knowledge of the receive precoder at the unintended secondary receiver, $\mathbf{u}_4$, is required to solve for $\mathbf{v}_3$ in this way. Some receiver precoder design principles are function of the transmit precoder, including that of the interfering transmitters, such as the max-SINR precoder considered in this investigation. Such a receive precoder makes the problem of choosing $\mathbf{v}_3$ to minimize $P_{\mathrm{SU-int}}^{(4)}$ much more complex than it may seem in hind sight.

Iterative updating of the transmit and receive precoder until convergence is one possible way of overcoming this difficulty. However, it takes time and requires to and fro information exchange between the transmitter and the receiver, resulting information overhead. Note that, since full information is assumed available at each terminal, the transmitter can solve for the receive precoder and estimate it at the transmitter itself, if the receive precoder design principle is known. This will overcome the need for information exchange, though the time and processing overhead for iterative update will remain.

In this problem, we have taken at alternative approach, which solves for $\mathbf{v}_3$ in a single step and does not require information exchange among the transmitters and the receivers. The

approach involves '*assuming*' the receive precoder to be designed according to any of the well known design principles that does not require knowledge of transmit precoder. In that case, the transmit precoder can be solved for using the Rayleigh's principle, and is given by the least dominant eigenvector of the corresponding interference covariance matrix. In this particular example, $\mathbf{u}_4$, $\tilde{\mathbf{u}}_4$ is considered to be the Equal Gain Combining (EGC); which is given by $\tilde{\mathbf{u}}_4 = \frac{1}{\sqrt{M_s}}[1, 1, \cdots, 1]^H$. This particular receive precoder choice is motivated by the fact that it is the optimum precoder in the absence of channel information when the channel fading distribution follows the zero mean spatially white (ZMSW) channel gain model [13, Ch. 10].

With this assumption on the receive precoder, the transmit precoders at the STs are given by

$$\begin{aligned} \mathbf{v}_3^{(\mathrm{cpr})} &= \mathbf{v}_1^{\min}\left(\mathbf{H}_{43}^H \tilde{\mathbf{u}}_4 \tilde{\mathbf{u}}_4^H \mathbf{H}_{43}\right), \\ \mathbf{v}_4^{(\mathrm{cpr})} &= \frac{\left(\hat{\mathbf{H}}_4\right)^{-1} \hat{\mathbf{H}}_3 \mathbf{v}_3^{(\mathrm{cpr})}}{\| \left(\hat{\mathbf{H}}_4\right)^{-1} \hat{\mathbf{H}}_3 \mathbf{v}_3^{(\mathrm{cpr})} \|}. \end{aligned} \tag{5.17}$$

5.4.3 Numerical Results

In this section, we present some numerical results for the performance of the secondary and as well as primary system where the ST precoders follow the different design principles outlined in the preceding sections. The secondary terminals are all equipped with four antennas, while the primary terminals are all two-antenna devices; i.e. $M_p = 2$ and $M_s = 4$. The receiver precoder at the PRs are assumed to be zero-forcing precoders that nulls the the received interference signal from the STs. All channel fades are modeled by the Rayleigh fading distribution, and all presented results are averaged over at least $10,000$ realizations to ensure statistical accuracy.

Simulation results for the weak interference scenario (mean interference channel SNRs are 10 dB less than the direct channel mean SNR) is presented in Figure 5.4 followed by the strong interference scenario (mean interference channel SNRs are 10 dB higher than the direct channel mean SNR) in Figure 5.5. The power of the sum interference power from the SUs at the PRs are also presented in the figure. It is found to be zero, which shows that interferences from the STs are perfectly aligned and zero forced at the PRs.

Each user has a requested DoF of one, which results in comparable primary and secondary system sum rate. Within the primary system, the pro-primary design of the STs result in a higher sum-rate. In one sense, this can be seen as an example of the overlay CR model,

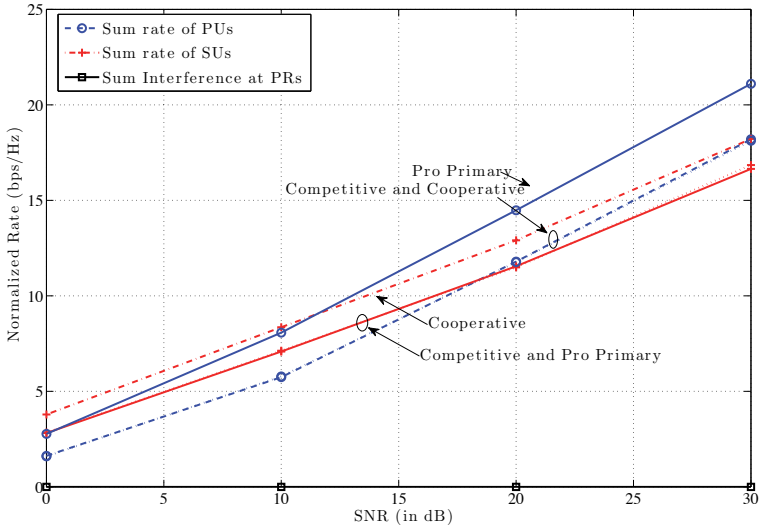

Figure 5.4: Performance of Interference Alignment technique in Cognitive Radio Network with different design considerations under weak interference scenario

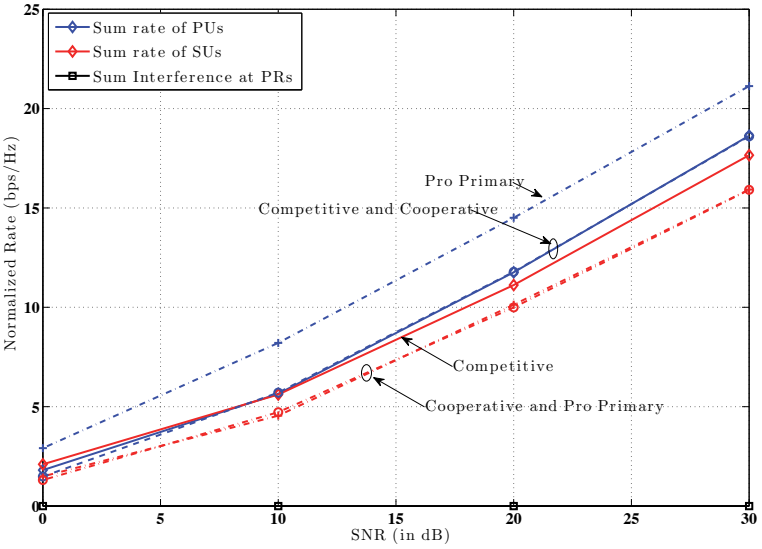

Figure 5.5: Performance of Interference Alignment technique in Cognitive Radio Network with different design considerations under weak interference scenario

where the PTs share message side information with the coexisting STs in order to benefit from cooperation with the STs [21].

When it comes to the secondary sum rate, the competitive transmission outperforms the cooperative strategy for the strong interference scenario, and vice versa. Thanks to the generous available degrees of freedom at the STs, the max-SINR receive beam-former can readily cancel the interference signal from the signal of interest, thereby enabling the high sum rate even in the presence of strong interference. Therefore, it can be observed that it is more beneficial for SUs with multiple antennas to use part of the available DoF to mitigate the inter-secondary as well as secondary-primary interference.

5.4.4 Discussions on the Proposed Interference Alignment Schemes

The proposed IA based beamforming technique requires each PU to have at least d_i transmit antennas. At the receiver end, each PU requires at least $d_i + \max_{j \in \mathcal{J}} d_j$, so as to accommodate aligning and subsequent zero-forcing of the secondary signals. On the other hand, the requirement on the SU terminals is not straightforwardly derived. The presented IA solution involves a matrix inversion, and hence we have chosen the secondary terminal size to be such that the matrices to be inverted are square matrix. Investigation of the general case, with non-square matrix inversions is left as a future extension of this work.

5.5 Conclusion and Future Works

We have presented two interference mitigation techniques for the generalized hierarchical spectrum usage between an opportunistic system and a legacy system. The proposed techniques are presented in the context of an underlay CR system coexisting with a primary system under a strict interference temperature constraint, and are inspired by interference nulling schemes, and IA techniques. The proposed schemes rely on utilizing the multiple antennas at the STs to "steer" the secondary transmission away from the PRs. Both of the proposed schemes represents various design tradeoffs.

The different investigated interference coordination schemes are generally found to facilitate satisfactory secondary sum-rate performance in addition to ensuring interference-free communication of the PUs. However, accurate and instantaneous knowledge of the secondary-primary as well and secondary-secondary channel gains are assumed known in most of the considered cases. It would be interesting to investigate robust interference

coordination techniques that are more CSI-insensitive than those presented in this work. Furthermore, generalized interference coordination techniques for random network density with random terminal sizes is a natural topic for extension of this preliminary investigation.

Bibliography

[1] D. Gesbert, S. Hanly, H. Huang, S. S. Shitz, O. Simeone, and W. Yu, "Multi-cell MIMO cooperative networks: A new look at interference," *IEEE Journal on Selected Areas in Communications*, vol. 28, no. 9, pp. 1380 –1408, Dec. 2010.

[2] M. Buddhikot, "Understanding dynamic spectrum access: Models,Taxonomy and challenges," in *Proceedings of the 2nd IEEE International Symposium on New Frontiers in Dynamic Spectrum Access Networks, 2007. DySPAN 2007*, Apr. 2007, pp. 649 –663.

[3] V. Chandrasekhar, J. G. Andrews, and A. Gatherer, "Femtocell networks: A survey," *IEEE Communications Magazine*, vol. 46, no. 9, pp. 59 –67, Sep. 2008.

[4] Q. Zhao and B. Sadler, "A survey of dynamic spectrum access," *Signal Processing Magazine, IEEE*, vol. 24, no. 3, pp. 79 –89, May 2007.

[5] F. Rashid-Farrokhi, K. Liu, and L. Tassiulas, "Transmit beamforming and power control for cellular wireless systems," *IEEE Journal on Selected Areas in Communications*, vol. 16, no. 8, pp. 1437 –1450, oct 1998.

[6] O. Bakr, M. Johnson, B. Wild, and K. Ramchandran, "A Multi-Antenna framework for spectrum reuse based on Primary-Secondary cooperation," in *Proceedings of the 3rd IEEE International Symposium on New Frontiers in Dynamic Spectrum Access Networks (DySPAN)*, Oct. 2008, pp. 1 –5.

[7] E. Jorswieck and R. Mochaourab, "Beamforming in underlay cognitive radio: Null-shaping design for efficient nash equilibrium," in *Proceedings of the International Workshop on Cognitive Information Processing (CIP)*, Tuscany, Italy, Jun. 2010, pp. 476–481.

[8] J. Liu, W. Chen, Z. Cao, and Y. Zhang, "Cooperative beamforming for cognitive radio networks: A Cross-Layer design," *IEEE Transactions on Communications*, vol. 60, no. 5, pp. 1420 –1431, May 2012.

[9] V. Cadambe and S. Jafar, "Interference alignment and degrees of freedom of the K-user interference channel," *IEEE Transactions on Information Theory*, vol. 54, no. 8, pp. 3425 –3441, Aug. 2008.

[10] S. Perlaza, N. Fawaz, S. Lasaulce, and M. Debbah, "From spectrum pooling to space pooling: Opportunistic interference alignment in MIMO cognitive networks," *IEEE Transactions on Signal Processing*, vol. 58, no. 7, pp. 3728 –3741, July 2010.

[11] M. Amir, A. El-Keyi, and M. Nafie, "Constrained interference alignment and the spatial degrees of freedom of mimo cognitive networks." *IEEE Transactions on Information Theory*, vol. 57, no. 5, pp. 2994–3004, 2011.

[12] D. Tse and P. Viswanath, *Fundamentals of Wireless Communication*. Cambridge University Press, Cambridge, U.K., June 2005.

[13] A. Goldsmith, *Wireless Communications*, 1st ed. New York, NY, USA: Cambridge University Press, 2005.

[14] T. Maseng and T. Ulversøy, "Dynamic frequency broker and cognitive radio," in *The IET Seminar on Cognitive Radio and Software Defined Radios: Technologies and Techniques*, London, UK, Sep. 2008.

[15] G. Strang, *Linear Algebra and Its Applications*, 3rd ed. USA: Brooks/Cole, Feb. 1988.

[16] A. Paulraj, R. Nabar, and D. Gore, *Introduction to Space-Time Wireless Communications*, 1st ed. Cambridge, UK: Cambridge University Press, 2003.

[17] Z. Ho and D. Gesbert, "Balancing egoism and altruism on interference channel: The mimo case," in *Proceedings of the IEEE International Conference on Communications (ICC)*, Cape Town, South Africa, May 2010, pp. 1 –5.

[18] H. Weingarten, T. Liu, S. Shamai, Y. Steinberg, and P. Viswanath, "The capacity region of the degraded multiple-input multiple-output compound broadcast channel," *IEEE Transaction on Information Theory*, vol. 55, no. 11, pp. 5011–5023, Nov. 2009. [Online]. Available: http://dx.doi.org/10.1109/TIT.2009.2030458

[19] T. Yoo and A. Goldsmith, "On the optimality of multiantenna broadcast scheduling using zero-forcing beamforming," *IEEE Journal on Selected Areas in Communication*, vol. 24, pp. 528–541, 2006.

[20] D. Schmidt, C. Shi, R. Berry, M. Honig, and W. Utschick, "Minimum mean squared error interference alignment," in *Conference Record of the Forty-Third Asilomar Conference on Signals, Systems and Computers (ACSSC '09)*, Pacific Grove, CA, USA, Nov. 2009, pp. 1106 –1110.

[21] S. Srinivasa and S. Jafar, "The throughput potential of cognitive radio: A theoretical perspective," in *Conference Record of the fortieth Asilomar Conference on Signals, Systems and Computers (ACSSC '06)*, Pacific Grove, CA, USA, Nov. 2006, pp. 221–225.